Dynamics of Poisson-Nernst-Planck systems and applications to ionic channels

By

Mingji Zhang

Submitted to the graduate degree program in the Department of Mathematics and the Graduate Faculty of the University of Kansas in partial fulfillment of the requirements for the degree of Doctor of Philosophy.

Doctor of Philosophy

Committee members

Dr Weishi Liu, Chairperson

Dr Milena Stanislavova

Dr Xuemin Tu

Dr Erik Van Vleck

Dr Jack Shi, Physics and Astronomy

Date Defended: July 8, 2013

The Dissertation Committee for Mingji Zhang certifies
that this is the approved version of the following dissertation:

Dynamics of Poisson-Nernst-Planck systems and applications to ionic channels

---

Dr Weishi Liu, Chairperson

Date approved: July 8, 2013

Abstract

Dynamics of Poisson-Nernst-Planck systems and its applications to ion channels are studied in this dissertation.

The Poisson-Nernst-Planck systems serve as basic electro-diffusion equations modeling, for example, ion flow through membrane channels and transport of holes and electrons in semiconductors. The model can be derived from the more fundamental models of the Langevin-Poisson system and the Maxwell-Boltzmann equations, and from the energy variational analysis EnVarA. A brief description of the model is given in Chapter 2 including the physical meaning of each equation involved.

Ion channels are cylindrical, hollow proteins that regulate the movement of ions (mainly Na^+, K^+, Ca^{++} and Cl^-) through nearly all the membrane channels. When an initial potential is applied at one end of the channel, it will drive the ions through the channel, and the movement of these ions will produce the current which can be measured. Different initial potentials will result in different currents, and the collection of all those data will provide a relation, the so-called I-V (current-voltage) relation, which is an important characterization of two most relevant properties of a channel: permeation and selectivity.

In Chapter 3, a classical Poisson-Nernst-Planck system is studied both analytically and numerically to investigate the *cubic-like* feature of the I-V relation. For the case of zero permanent charge, under electroneutrality boundary conditions at both ends of the channel, our result concerning the I-V relation for two oppositely charged ion species

is that the third order correction is *cubic* in the potential V , and furthermore, up to the third order, the cubic I-V relation has *three distinct real roots* (except for a very degenerate case) which corresponds to the bi-stable structure in the FitzHugh-Nagumo simplification of the Hodgkin-Huxley model. Numerical simulations are performed and and they are consistent with our analytical results.

In Chapter 4, we consider a one-dimensional steady-state Poisson-Nernst-Planck type model for ionic flow through membrane channels including ionic interaction modeled by a *nonlocal* hard-sphere potential from the Density Functional Theory. The resulting problem is a singularly perturbed boundary value problem of an integro-differential system. Ion size effect on the I-V relations is investigated numerically. Two numerical tasks are conducted. The first one is a numerical approach of solving the boundary value problem and obtaining I-V curves. This is accomplished through a numerical implement of the analytical strategy introduced in [46]. The second task is to numerically detect two critical potential values V_c and V^c. Our numerical detections are based on the defining properties of V_c and V^c and are designed to use the numerical I-V curves directly. For the setting in the above mentioned reference, our numerical results agree well with the analytical predictions.

In Chapter 5, a one-dimensional steady-state Poisson-Nernst-Planck type model for ionic flow through a membrane channel is analyzed, which includes a *local* hard-sphere potential that depends pointwise on ion concentrations to account for ion size effects on the ionic flow. The model problem is treated as a boundary value problem of a singularly perturbed differential system. Based on the geometric singular perturbation theory, especially, on specific structures of this concrete model, the existence of solutions to the boundary value problem for small ion sizes is established and, treating the ion sizes as small parameters, we also derive an approximation of the I-V relation and identify two critical potentials or voltages for ion size effects. Under electroneutrality (zero net

charge) boundary conditions, each of these two critical potentials separates the potential into two regions over which the ion size effects are qualitatively opposite to each other. On the other hand, without electroneutrality boundary conditions, the qualitative effects of ion sizes will depend not only on the critical potentials but also on boundary concentrations. Important scaling laws of I-V relations and critical potentials in boundary concentrations are obtained. Similar results about ion size effects on the flow of matter are also discussed. Under electroneutrality boundary conditions, the results on the first order approximation in ion diameters of solutions, I-V relations and critical potentials agree with those with a *nonlocal* hard-sphere potential examined in [46].

Acknowledgements

I owe my gratitude to all those people who have made this dissertation possible and because of whom my graduate experience has been one that I will cherish for my whole life.

My deepest gratitude is to my academic advisor Dr Weishi Liu. He patiently teaches me how to do research and helps me develop a career plan. It is his guidance, encouragement and support that make my accomplishments possible.

I am grateful to Dr Milena Stanislavova, Dr Xuemin Tu and Dr Erik Van Vleck for their help and suggestions in the past years. I would like to thank Dr Jack Shi for serving on my committee.

I gratefully acknowledge Dr Ralph Bayers, Dr Robert Brown, Dr Yaozhong Hu, Dr Weizhang Huang, Dr Craig Huneke, Dr Jeffrey Lang, Dr Albert Sheu, Dr Milena Stanislavova, Dr Atanas Stefanov, Dr Xuemin Tu and Dr Hongguo Xu for their teaching and valuable advice. Many thanks are also due to Dr Margaret Bayer, Dr Mat Johnson and Dr Erik Van Vleck for their supervision on my teaching.

This dissertation can not be made easily without the efforts of many staffs in the department of mathematics. Especially, great thanks are given to Kerrie Brecheisen, Debbie Garcia, Gloria Prothe and Lori Springs for their help in many ways.

I would like to thank all my friends for their great help and encouragement. In particular, I would like to thank Nicole Abaid, Tim Dorn, Pedro Lei, Xi Li, Xianping Li, Fei

Lu, Jian Song and Xiaoming Song for numerous mathematical discussions and lectures on related topics that helped me improve my knowledge.

Great thanks to Min Hu and Jun Fu who take care of my wife Qingqing and me like parents, especially when my daughters were born.

Finally, I would like to thank my family, especially my wife Qingqing Cui and my two lovely daughters Sophia Zhang and Bonnie Zhang, for their love, encouragement and support.

Contents

Chapter 1

Introduction

In this dissertation, we study the dynamics of Poisson-Nernst-Planck (PNP) systems and its applications to ionic channels. It is a collection of my work and some joint works with Dr. Guojian Lin (from Renmin University of China), Dr. Xuemin Tu (from University of Kansas), Dr. Yingfei Yi (from Georgia Institute of Technology), and my advisor Dr. Weishi Liu.

1.1 Ion channels and Poisson-Nernst-Planck systems

Ion channels are cylindrical and hollow proteins, as stated in [30], which regulate the movement of ions (mainly Na^{+}, K^{+}, Ca^{++}, and Cl^{-}) across nearly all biological membranes. A major way for ions to cross the membrane is through the pore that runs down the long axis of a channel due to the impermeability of the membranes to charged particles. This property has been exploited by evolution to produce many varied and complicated phenomena necessary for life: channels are responsible for the initiation and continuation of the electric signals in the nervous system; in the kidneys, lungs, and intestines, channels coordinate changes in ionic concentration gradients that result in the absorption or release of water; in muscle cells, a group of channels is responsible for the timely delivery of the Ca^{++} ions that initiate a contraction. Furthermore, a large number of drugs (including valium and PCP) act directly or indirectly on channels.

To produce such phenomena, channels act in group, opening and closing at the same time and letting only specific ion species get through the membrane (for example, some channels prefer Na^+ over K^+ while some ones prefer K^+ over Na^+). In spite of the complicated results, the individual channels only do the following two things: they open and close (the so-called *gating* phenomenon), when open, they conduct ions. A single channel could be possibly removed from the biological system and studied as an isolated physical system. To do this, one can place the single channel into a phospholipid membrane which separates two baths with known ionic concentration. Far away from the channel, applying a voltage to the system by electrodes in the baths, one can measure the amount of current that passed through the channel, and this is the so-called I-V relation, which is an important characterization of two most relevant properties of a channel: permeation and selectivity (for more detailed description, see [30]). One of our interest in this dissertation is to study the I-V relations, in particular, to study the ion size effect on the I-V relations.

The PNP systems serve as basic electro-diffusion equations modeling, for example, ion flow through membrane channels, transport of holes and electrons in semiconductors (see, for example [4, 5, 6, 24, 65, 81]). In the context of ion flow through a membrane channel, the flow of ions is driven by their concentration gradients and by the electric field modeled together by the Nernst-Planck continuity equations, and the electric field is in turn determined by the concentrations through the Poisson equation.

Each equation has its physical meaning just as stated in [30]. The Poisson equation is the differential form of the Maxwell's First Law which states that the flux of the electric field across any closed surface is equal to the total amount of charge inside the surface. The Nernst-Planck equations state that the flux of a specific species has two components:

simple diffusion and drift along the electric field. The continuity equations state that, for the flux of each species, there are no sinks or sources.

Under various reasonable conditions, it can be derived from the more fundamental models of the Langevin-Poisson system (see, for example, [2, 8, 9, 13, 31, 43, 64, 67, 77, 78, 85, 90]) and the Maxwell-Boltzmann equations (see, for example, [4, 42, 43, 77, 90]), and from the energy variational analysis *EnVarA* ([23, 38, 39, 40, 41, 55, 56]).

1.2 Outline of thesis

In Chapter 2, a brief description of PNP systems and some basic elements of dynamical system theory of differential equations are provided. In particular, the method of asymptotic expansions and a modern dynamical theory, the so-called geometric singular perturbation theory that are the main tools for the research in this dissertation, are introduced.

In Chapter 3, a classical PNP model which treats ions as point-charges and ignores the ion-to-ion interaction is studied. Our main interest is the I-V relation of the ion channels, in particular, the *cubic-like* feature of the I-V relation. Numerical simulations are performed and the numerical results are consistent with our analytical ones.

In chapter 4, we focus on the ion size effect on the I-V relation by considering a one-dimensional steady-state PNP type model for ionic flow through membrane channels including ionic interaction modeled by nonlocal hard-sphere potentials from the Density Functional Theory. The ion size effect on I-V relations is investigated numerically, focusing on the case where only the hard-sphere components are included. Two numerical tasks are conducted. The first one is a numerical approach of solving the boundary value problem and obtaining I-V curves. The second task is to numerically detect two critical potential values V_c and V^c first obtained in [46].

In Chapter 5, we analyze a one-dimensional steady-state PNP model including a local hard-sphere potential that depends pointwise on ion concentrations to account for ion size effects on the ionic flow. Under the framework of geometric singular perturbation theory and the specific structures of this concrete model, we are able to establish the existence of solutions to the problem for small ion sizes. An approximation of the I-V relation is derived and two critical potentials for ion size effects are identified. Important scaling laws of I-V relations and critical potentials in boundary concentrations are obtained. Similar results about ion size effects on the flow of matter are also discussed.

In Chapter 6, a brief summary of our previous work is given and our future plan is discussed.

Chapter 2

Preliminaries

We give a brief description of PNP system and review some basic elements of dynamical system theory of differential equations, for which we refer to [1, 19, 20, 21, 23, 24, 28, 30, 37, 39, 41, 46, 47, 49, 57, 58, 59, 61, 62, 65, 70, 85, 87, 93, 94], *etc.* for further details.

2.1 Possion-Nernst-Planck system

2.1.1 A one-dimensional steady-state Poisson-Nernst-Planck system

We start with a brief description of a three-dimensional PNP type model for ion flows. As an approximation, we consider an ion channel Ω, whose longitudinal length has been normalized to one,

$$\Omega = \{X = (x,y,z) : 0 < x < 1,\ y^2 + z^2 < g^2(x)\},$$

where g is a smooth function. The boundary $\partial\Omega$ of Ω consists of three portions:

$$\mathscr{L} = \{X \in \Omega : x = 0\},\ \mathscr{R} = \{X \in \Omega : x = 1\},$$

$$\mathscr{M} = \{X \in \Omega : y^2 + z^2 = g^2(x)\}.$$

Here, $\mathscr{L}$ and $\mathscr{R}$ are viewed as the two ends (inside and outside of the cell) and $\mathscr{M}$ the wall of the channel.

The basic electrodiffusion model of PNP type systems for ion flow through the channel is (see, for example, [31, 33])

$$\begin{aligned} -\nabla \cdot (\varepsilon_r(X)\varepsilon_0 \nabla \Phi) =& e\Big(\sum_{j=1}^{n} z_j c_j + Q(X)\Big), \\ -\mathscr{J}_i =& \frac{1}{kT} D_i(X) c_i \nabla \mu_i, \\ \frac{\partial c_i}{\partial t} + \nabla \cdot \mathscr{J}_i =& 0, \quad i = 1, 2, \cdots, n, \end{aligned} \tag{2.1}$$

where e is the elementary charge, k is the Boltzmann constant, T is the absolute temperature; Φ is the electric potential, $Q(X)$ is the permanent charge of the channel, $\varepsilon_r(X)$ is the relative dielectric coefficient, ε_0 is the vacuum permittivity; for the ith ion species, c_i is the concentration, z_i is the valence (the number of charges per particle), μ_i is the electrochemical potential, $\mathscr{J}_i$ is the flux density, and $D_i(X)$ is the diffusion coefficient.

Depending on specific biological settings of ion channel problems, one may impose different boundary conditions. We will consider the situation that the concentration of charges and electrical potentials on $\mathscr{L} \cup \mathscr{R}$ are constants. An argument is that the inside and the outside of cells are macroscopic regions in which the concentration of charges and electrical potentials remain nearly constants. The wall of the channel will be assumed to be perfectly insulated. We thus assume the following boundary conditions

$$\Phi|_{\mathscr{L}} = V,\ c_i|_{\mathscr{L}} = L_i, \quad \Phi|_{\mathscr{R}} = 0,\ c_i|_{\mathscr{R}} = R_i, \quad \frac{\partial \Phi}{\partial \mathbf{n}}|_{\mathscr{M}} = \frac{\partial c_i}{\partial \mathbf{n}}|_{\mathscr{M}} = 0, \tag{2.2}$$

where V, $L_i > 0$ and $R_i > 0$ are constants, and $\mathbf{n}$ is a unit normal vector to $\mathscr{M}$.

We assume the channel is narrow so that it can be effectively viewed as a one-dimensional channel and normalize it as the interval $[0,1]$ that connects the interior and the exterior of the channel. A natural one-dimensional steady-state PNP type model for ion flows of n ion species is (see [62, 65])

$$\begin{aligned}
&\frac{1}{h(x)}\frac{\partial}{\partial x}\left(\varepsilon_r(x)\varepsilon_0 h(x)\frac{\partial \Phi}{\partial x}\right) = -e\left(\sum_{j=1}^{n} z_j c_j + Q(x)\right),\\
&\frac{\partial \mathscr{J}_i}{\partial x} = 0, \quad -\mathscr{J}_i = \frac{1}{kT} D_i(x) h(x) c_i \frac{\partial \mu_i}{\partial x}, \quad i = 1, 2, \cdots, n.
\end{aligned} \tag{2.3}$$

The boundary conditions are, for $i = 1, 2, \cdots, n$,

$$\Phi(0) = V,\ \ c_i(0) = L_i > 0; \quad \Phi(1) = 0,\ \ c_i(1) = R_i > 0, \tag{2.4}$$

where $h(x) = \pi g^2(x)$ is the cross-section area of the channel over the longitudinal location x. The above one-dimensional version PNP system was suggested in [65] and it differs from the traditional one-dimensional PNP system in that the cross-section area function $h(x)$ is contained, which captures the main geometric property of a non-uniform channel.

Remark 2.1. *For the one-dimensional case, the permanent charge $Q(x)$ will be modeled by a piecewise constant function; that is, we assume, for a partition $x_0 = 0 < x_1 < \cdots < x_{m-1} < x_m = 1$ of $[0,1]$ into m sub-intervals, $Q(x) = Q_j$ for $x \in (x_{j-1}, x_j)$ where Q_j's are constants with $Q_1 = Q_m = 0$ (the intervals $[x_0, x_1]$ and $[x_{m-1}, x_m]$ are viewed as the reservoirs where there is no permanent charge).*

The simplest PNP system is the classical Poisson-Nernst-Planck (cPNP) system. It has been simulated ([10, 11, 12, 14, 16, 31, 34, 36, 37, 43, 44, 45, 51, 65, 82, 95, 96]) and analyzed ([1, 5, 6, 24, 30, 57, 58, 63, 69, 80, 81, 86, 87, 88, 89, 94]) to a great extent. However, a major weak point of the cPNP is that ions are treated as *point-charges*, which is reasonable only in near infinite dilute situation. Many extremely important properties of ion channels, such as *selectivity*, rely on ion sizes critically. For example, Na^+ (sodium) and K^+ (potassium), having the *same* valence, are mainly different by their ionic sizes. It is the difference in their ionic sizes that allows certain channels to prefer Na^+ over K^+ and some channels to prefer K^+ over Na^+.

2.1.2 Hard-sphere potential

To study the ion size effects on ionic flows, one has to consider the ion specific components of the electrochemical potential in the PNP models. A first step toward a better modeling is to include hard-sphere potentials of the excess electrochemical potential, which is also necessary to account for ion size effects in the physiology of ion flows. For hard-sphere potentials, there are two types of models, *local* and *nonlocal*. Local models for hard-sphere potentials depend *pointwise* on ion concentrations, while nonlocal models are proposed as *functionals* of ion concentrations.

The electrochemical potential μ_i for the ith ion species consists of the ideal component $\mu_i^{id}(x)$, the excess component $\mu_i^{ex}(x)$ and the concentration-independent component $\mu_i^0(x)$ (e.g. a hard-well potential):

$$\mu_i(x) = \mu_i^0(x) + \mu_i^{id}(x) + \mu_i^{ex}(x).$$

where

$$\mu_i^{id}(x) = z_i e\phi(x) + kT \ln \frac{c_i(x)}{c_0} \tag{2.5}$$

with some characteristic number density c_0 which will be normalized to one in the sequel.

The excess electrochemical potential $\mu_i^{ex}(x)$ accounting for the finite size effect of charges is the most intriguing component which consists of two components: the hard-sphere component μ_i^{HS} and the electrostatic component μ_i^{ES} for screening effects, etc. of finite sizes of charges ([3, 25, 26, 29, 74, 75, 91, 92], etc.); that is,

$$\mu_i^{ex} = \mu_i^{HS} + \mu_i^{ES}.$$

As mentioned above, as a first step, we will only include the hard-sphere component μ_i^{HS}. The hard-sphere component $\mu_i^{HS}(x)$ is naturally defined as a functional of the *probability distributions*, $\{f_j(x,v)\}$, where $f_j(x,v)dxdv$ is the number of jth ions at the location in $(x, x+dx)$ with the velocity in $(v, v+dv)$. There are different proposals for the specifics of $\mu_i^{HS}(x)$. The most successful one comes from the celebrated Density Functional Theory (DFT) ([25, 26], etc.) which states that $\mu_i^{HS}(x)$ is actually a functional of the *concentrations*, $\{c_j(x)\}$, where the concentration c_j and the probability distribution are related by $c_j(x) = \int f_j(x,v)dv$.

However, a practical difficulty is that an exact formula for the functional dependence of $\mu_i^{HS}(x)$ on $\{c_j(x)\}$ cannot be expected. A major breakthrough was made by Rosenfeld ([74, 75]). He treated ions as charged spheres and introduced novel ideas for an approximation of $\mu_i^{HS}(x)$ based on the geometry of spheres. An outcome of Rosenfeld's theory is an explicit approximation of $\mu_i^{HS}(x)$ depending *non-locally* on the concentrations $\{c_j\}$. (See also the recent review article [76] on hard-sphere mixtures and the references therein.) Accuracy of Rosenfeld's model and its further refinements has been demonstrated by a number of applications ([32, 84, 91, 92], etc.); in particular, applications to ion channel problems have been conducted numerically in [9, 31, 33], etc. and they have shown a great improvement.

On the other hand, *local-* or *pointwise-dependent* models for hard sphere potentials $\mu_i^{HS}(x)$ had been proposed and tested for a long time. One of earliest local models for hard-sphere potentials was proposed by Bikerman ([7]), which contains ion size effect of mixtures but is not ion specific (i.e., the hard-sphere potential is assumed to be the same for different ion species). Local models have evolved through several stages and become very reliable; for example, the Boublík-Mansoori-Carnahan-Starling-Leland local model is ion specific and has been shown to be accurate ([75, 76], etc.).

To end this section, we review a well-known non-local hard-sphere model used in [46], and derive a local model based on it which is studied in Chapter 5.

Recall that, for one-dimensional space case, one has ([29, 71, 72, 73, 74, 75]) the following formula for the hard-sphere (hard-rod) potential

$$\mu_i^{HS} = \frac{\delta\Omega(\{c_j\})}{\delta c_i}, \tag{2.6}$$

where

$$\begin{aligned} &\Omega(\{c_j\}) = -\int n_0(x;\{c_j\})\ln[1-n_1(x;\{c_j\})]dx, \\ &n_l(x,\{c_j\}) = \sum_{j=1}^{n}\int c_j(x')\omega_l^j(x-x')dx', \quad (l=0,1), \\ &\omega_0^j(x) = \frac{\delta(x-r_j)+\delta(x+r_j)}{2}, \quad \omega_l^j(x) = \Theta(r_j-|x|), \end{aligned} \tag{2.7}$$

where δ is the Dirac function, Θ is the Heaviside function, and $r_j = d_j/2$ is the radius of jth ion species.

The *nonlocal* hard-sphere model derived from (2.6) and (2.7) in [46] is

$$\begin{aligned} \mu_i^{HS}(x) = &-\frac{kT}{2}\ln\left(\left(1-\sum_j\int_{x-r_i-r_j}^{x-r_i+r_j}c_j(x')dx'\right)\left(1-\sum_j\int_{x+r_i-r_j}^{x+r_i+r_j}c_j(x')dx'\right)\right) \\ &+\frac{kT}{2}\int_{x-r_i}^{x+r_i}\frac{\sum_j(c_j(x'-r_j)+c_j(x'+r_j))}{1-\sum_j\int_{x'-r_j}^{x'+r_j}c_j(x'')dx''}dx'. \end{aligned} \tag{2.8}$$

Now we derive the *local* model

$$\frac{1}{kT}\mu_i^{LHS}(x) = -\ln\left(1-\sum_{j=1}^{n}d_jc_j(x)\right)+\frac{d_i\sum_{j=1}^{n}c_j(x)}{1-\sum_{j=1}^{n}d_jc_j(x)}, \tag{2.9}$$

where d_j is the diameter of the jth ion species. This local model is studied in Chapter 5.

For the first term in (2.8),

$$\ln\left(\left(1-\sum_j\int_{x-r_i-r_j}^{x-r_i+r_j}c_j(x')dx'\right)\left(1-\sum_j\int_{x+r_i-r_j}^{x+r_i+r_j}c_j(x')dx'\right)\right),$$

we expand $c_j(x')$ at $x'=x$

$$c_j(x')=c_j(x)+c_j'(x)(x'-x)+O((x'-x)^2).$$

This gives

$$\begin{aligned}\sum_j\int_{x-r_i-r_j}^{x-r_i+r_j}c_j(x')dx' &=\sum_j\int_{x-r_i-r_j}^{x-r_i+r_j}\left(c_j(x)+c_j'(x)(x'-x)+O((x'-x)^2)\right)dx'\\ &=\sum_j\left(2r_jc_j(x)-2r_ir_jc_j'(x)+O\left(2r_jr_i^2+\frac{2}{3}r_j^3\right)\right)\\ &=\sum_j 2r_jc_j(x)+O(r^2),\end{aligned}$$

where $r=\min\{r_1,r_2\}$. Similarly, one has

$$\sum_j\int_{x+r_i-r_j}^{x+r_i+r_j}c_j(x')dx'=\sum_j 2r_jc_j(x)+O(r^2).$$

Therefore, the first term in $\mu_i^{HS}(x)$ becomes

$$\begin{aligned}&-\frac{kT}{2}\ln\left(\left(1-\sum_j\int_{x-r_i-r_j}^{x-r_i+r_j}c_j(x')dx'\right)\left(1-\sum_j\int_{x+r_i-r_j}^{x+r_i+r_j}c_j(x')dx'\right)\right)\\ =&-\frac{kT}{2}\ln\left(\left(1-\sum_j 2r_jc_j(x)+O(r^2)\right)\left(1-\sum_j 2r_jc_j(x)+O(r^2)\right)\right)\\ =&-kT\ln\left(1-\sum_j 2r_jc_j(x)+O(r^2)\right).\end{aligned}\tag{2.10}$$

For the second term in (2.8)

$$\frac{kT}{2}\int_{x-r_i}^{x+r_i}\frac{\sum_j(c_j(x'-r_j)+c_j(x'+r_j))}{1-\sum_j\int_{x'-r_j}^{x'+r_j}c_j(x'')dx''}dx',$$

we first expand the numerator of the integrand at x to get

$$\sum_j(c_j(x'-r_j)+c_j(x'+r_j))=2\sum_j(c_j(x)+c_j'(x)(x'-x)+O((x-x')^2)).$$

Expanding the summation term in the denominator first at x' and then at x, we have

$$\begin{aligned}\sum_j\int_{x'-r_j}^{x'+r_j}c_j(x'')dx'' =&\sum_j\int_{x'-r_j}^{x'+r_j}\left(c_j(x')+c_j'(x')(x''-x')+O((x''-x')^2)\right)dx'',\\ =&\sum_j\left(2r_jc_j(x')+O(r^3)\right)\\ =&\sum_j 2r_j\left(c_j(x)+c_j'(x)(x'-x)+O((x'-x)^2)+O(r^3)\right).\end{aligned}$$

Hence,

$$\frac{kT}{2}\int_{x-r_i}^{x+r_i}\frac{\sum_j(c_j(x'-r_j)+c_j(x'+r_j))}{1-\sum_j\int_{x'-r_j}^{x'+r_j}c_j(x'')dx''}dx'=kT\frac{2r_i\sum_j c_j(x)}{1-\sum_j 2r_jc_j(x)}+O(r^2). \qquad (2.11)$$

Ignoring the higher order terms, the nonlocal hard sphere model $\mu_i^{HS}(x)$ in (2.8) with (2.10) and (2.11) gives the local hard sphere model $\mu_i^{LHS}(x)$.

2.2 Dynamical system theory of differential equations

In this section, some basic concepts, definitions and terminologies which are closely related to the work that has been done in this dissertation are listed (for morel details, see [70]). Tow main methods, matched asymptotic expansions, a classical method, and geometric singular perturbation theory, a modern dynamical theory, used to study the singularly perturbed boundary value problem (2.3) and (2.4) for my research are briefly described.

2.2.1 Basic concepts

Consider the following nonlinear *autonomous* systems of differential equations

$$\dot{x} = f(x), \tag{2.12}$$

where $f : E \to \mathbb{R}^n$ and E is an open set subset of $\mathbb{R}^n$. Together with an initial condition $x(0) = x_0$ (2.12) is called an initial value problem (IVP).

The following definitions and theorems used many times in the thesis are all from [70].

Definition 2.2. *For $x_0 \in E$, let $\phi(t, x_0)$ be the solution of the initial valuable problem* (2.12) *defined on its maximal interval of existence $I(x_0)$. Then for $t \in I(x_0)$, the set of mappings ϕ_t defined by*

$$\phi_t(x_0) = \phi(t, x_0)$$

is called the flow of differential equation (2.12)*; ϕ_t is also referred to as the flow of the vector field $f(x)$.*

Definition 2.3. *A point $x_0 \in \mathbb{R}^n$ is called an equilibrium point or critical point of* (2.12) *if $f(x_0) = 0$. An equilibrium is called a hyperbolic equilibrium point of* (2.12) *if none of the eigenvalues of the matrix $A = Df(x_0)$ has zero real part. The linear system*

$$\dot{x} = Ax \tag{2.13}$$

with the matrix $A = Df(x_0)$ is called the linearization of (2.12) *at x_0.*

Definition 2.4. *A point $p \in E$ is an $\omega-$limit point of the trajectory $\phi(\cdot,x)$, a map from $\mathbb{R}$ to E of system* (2.12) *if there is a sequence $t_n \to \infty$ such that*

$$\lim_{n\to\infty} \phi(t_n,x) = p.$$

Similarly, if there is a sequence $t_n \to -\infty$ such that

$$\lim_{n\to\infty} \phi(t_n,x) = q,$$

and the point $q \in E$, then the point q is an $\alpha-$limt point of system (2.12)*. The set of all $\omega-$limt points of a trajectory Γ (defined through the map $\phi(\cdot,x)$) is called the $\omega-$limit set of Γ and it is denoted by $\omega(\Gamma)$. The set of all $\alpha-$limit points of a trajectory Γ is called the $\alpha-$limit set of Γ and it is denoted by $\alpha(\Gamma)$.*

2.2.2 Method of matched asymptotic expansions

Matched asymptotic expansion is a classical method to study singularly perturbed problems. In particular, it is best suited for layer-type problems. To illustrate the idea, for simplicity, we consider the following singularly perturbed initial value problem

$$\varepsilon \dot{x} = f(x;\varepsilon), \quad t > 0, (\varepsilon > 0, \text{ but small}) \tag{2.14}$$

with the initial condition

$$x(0) = x_0.$$

For system (2.14), we assume that there is a layer occurring at the boundary $t = 0$ where rapid change is expected, in other words, in the limit $\varepsilon \to 0$, the layer is expected to become discontinuity. For convenience, we formulate the concept of rapid change by introducing scaled variables $\xi = t/\varepsilon$ at $t = 0$. In this context, we call ξ the *inner variable* and t the *outer variable*. Correspondingly, the system deals with the boundary layers is called *inner system* while the one deals with (2.14) for $t > 0$ is called *outer system*.

To solve the singularly perturbed problem (2.14) and obtain an approximation solution, the following three steps are taken.

- Step1: Study the outer systems for each order in ε, that is, we look for outer expansions of the form

$$x(t;\varepsilon) = x_0(t) + \varepsilon x_1(t) + \varepsilon^2 x_2(t) + \cdots . \tag{2.15}$$

  Substitute (2.15) into (2.14), and expand $f(x,\varepsilon)$ in the form of

$$f(x;\varepsilon) = f_0(x) + \varepsilon f_1(x) + \varepsilon^2 f_2(x) + \cdots ,$$

  we obtain the outer systems for each order, $j = 1, 2, \ldots$

$$0 = f_0, \quad \varepsilon^j \dot{x}_{j-1} = f_j. \tag{2.16}$$

- Step2: Consider the inner systems for each order at $t = 0$. At $t = 0$, in terms of the inner variable $\xi = t/\varepsilon$, let $X(\xi;\varepsilon) = x(\varepsilon\xi;\varepsilon)$ and $F(\xi;\varepsilon) = f(\varepsilon\xi;\varepsilon)$, system (2.14) becomes

$$\frac{dX}{d\xi} = F(\xi;\varepsilon). \tag{2.17}$$

We then look for inner expansions of the form

$$X(\xi;\varepsilon) = X_0(\xi) + \varepsilon X_1(\xi) + \varepsilon^2 X_2(\xi) + \cdots. \tag{2.18}$$

Substitute (2.18) into (2.17) and expand $F(\xi;\varepsilon)$ as

$$F(\xi;\varepsilon) = F_0(\xi) + \varepsilon F_1(\xi) + \varepsilon^2 F_2(\xi) + \cdots,$$

one has the inner systems for each order, $j = 0, 1, \ldots,$

$$\frac{dX_j}{d\xi} = F_j(\xi). \tag{2.19}$$

- Step3: After solving the resulting outer and inner systems for each order obtained from step 1 and step 2, we do the matching. The piecing of the inner solution and outer solution is achieved by matching principles. There are two mainstreams in matching. One is the *intermediate matching* of Kaplun-Lagerstrom and the other is the *asymptotic matching* of Van Dyke (see [17, 18, 53]). We will use the asymptotic matching principle for our matching purpose. For the above problem, the k-th order outer and inner expansions are denoted by, respectively,

$$E_x^k(x(t;\varepsilon)) = \sum_{j=0}^{k} \varepsilon^j x_j(t), \quad E_\xi^k(X(\xi;\varepsilon)) = \sum_{j=0}^{k} \varepsilon^j X_j(\xi).$$

The kth order matching principle to be applied is $E_t^k E_\xi^k(X) = E_\xi^k E_t^k(x)$ in terms of either the outer variable t or the inner variable ξ.

2.2.3 Geometric singular perturbation theory

Another basic nonlinear dynamical framework for my research on Poisson-Nernst-Planck systems is the *geometric singular perturbation theory*. We give a brief description of the general procedure.

Consider a singularly perturbed problem

$$\begin{aligned} \varepsilon\dot{x} =& f(x,y,\varepsilon), \\ \dot{y} =& g(x,y,\varepsilon), \end{aligned} \tag{2.20}$$

where overdot denotes the derivative with respect to the variable t, $x \in \mathbb{R}^n$, $y \in \mathbb{R}^l$, the functions f and g are both assumed to be C^∞ on a set $U \times [0,\varepsilon_0)$ where $U \subset \mathbb{R}^N$ is open, with $N = n+l$, and ε is a real parameter. System (2.20) is called *slow* system.

For $\varepsilon > 0$, the rescaling $t = \varepsilon\xi$ of the independent variable t gives rise an equivalent system, the *fast* system

$$\begin{aligned} x' =& f(x,y,\varepsilon), \\ y' =& \varepsilon g(x,y,\varepsilon), \end{aligned} \tag{2.21}$$

where prime denotes the derivative with respect to the variable ξ.

For $\varepsilon > 0$, system (2.20) and (2.21) have exactly the same phase portrait. But their limits at $\varepsilon = 0$ are different and, very often, the two limiting systems provide complementary information on state variables. Therefore, the main task of singularly perturbed problems is to patch the limiting information together to form an solution for the entire $\varepsilon > 0$ system.

To solve the singularly perturbed problem, we take the following key steps

- Step1: Study the *limiting fast system* (the limit of system (2.21) at $\varepsilon = 0$), that is,

$$\begin{aligned} x' =& f(x, y; 0), \\ y' =& 0 \end{aligned} \tag{2.22}$$

  which allows us to completely understand boundary or internal layers and characterize landing points of boundary layers on the so-called *slow* manifold $\mathscr{Z}_0$ which is obtained by setting $\varepsilon = 0$ in (2.20);

- Step 2: Construct a solution of the *limiting slow system* (the limit of system (2.20) at $\varepsilon = 0$), that is,

$$\begin{aligned} 0 &= f(x, y; 0), \\ \dot{y} &= g(x, y; 0) \end{aligned} \tag{2.23}$$

  on the slow manifold which connects the landing points obtained from step 1;

- Step 3: Based on the study in step 1 and step 2, one can construct a singular orbit which is a union of the solutions of limiting fast and slow systems. Then, one can apply the geometric singular perturbation theory, such as Exchange Lemma, to show that, for $\varepsilon > 0$ small, there is a unique solution that is close to the singular orbit.

To end this section, we review two theorems that are crucial for our research.

Suppose $y = H(x)$ solves $f(x, y; 0) = 0$, in other words,

$$\mathscr{Z}_0 = \{(x, y) : y = H(x), x \in \mathbb{R}\}.$$

Observe that $\mathscr{Z}_0$ is a set of equilibria of (2.22). The linearization of (2.22) at points in $\mathscr{Z}_0$ is

$$\begin{pmatrix} D_x f(x,y;0)_{m\times m} & D_y f(x,y;0)_{m\times n} \\ 0_{n\times m} & 0_{n\times n} \end{pmatrix}.$$

Definition 2.5. *$\mathscr{Z}_0$ is normally hyperbolic if no eigenvalues of $D_x f(x,y;0)$ has zero real part for all $(x,y) \in \mathscr{Z}_0$.*

For convenience, we assume that For $D_x f(x,y;0)$, there are k eigenvalues β_j with positive real parts, and l eigenvalues α_j with negative real parts, where $k+l=m$.

The first theorem is (see [27, 35])

Theorem 2.6. *Suppose $\mathscr{Z}_0$ is normally hyperbolic, then for $\varepsilon > 0$ small*

- *There is an invariant manifold $\mathscr{Z}_\varepsilon$, which is C^1 $o(\varepsilon)-$close to $\mathscr{Z}_0$; that is, there exists a function $y = H(x;\varepsilon)$ with $H(x;\varepsilon)$ C^1 $o(\varepsilon)-$close to $y = H(x)$ such that*

$$\mathscr{Z}_\varepsilon = \{(x,y) : y = H(x;\varepsilon)\}.$$

- *There are stable and unstable manifolds $W^s_\varepsilon(\mathscr{Z}_\varepsilon)$ and $W^u_\varepsilon(\mathscr{Z}_\varepsilon)$ of $\mathscr{Z}_\varepsilon$ such that*
  - *$W^{s,u}_\varepsilon(\mathscr{Z}_\varepsilon) = \cup_{z_\varepsilon \in \mathscr{Z}_\varepsilon} W^{s,u}_\varepsilon(z_\varepsilon)$, and $W^{s,u}_\varepsilon(z_\varepsilon)$ is C^1 $o(\varepsilon)-$close to $W^{s,u}_{\varepsilon=0}(z_{\varepsilon=0})$.*
  - *$\forall z_\varepsilon, \quad \phi^t_\varepsilon(W^s_\varepsilon(z_\varepsilon)) = W^s_\varepsilon(\phi^t_\varepsilon(z_\varepsilon)), \quad \phi^t_\varepsilon(W^u_\varepsilon(z_\varepsilon)) = W^u_\varepsilon(\phi^t_\varepsilon(z_\varepsilon))$.*
  - *$\forall z_1, z_2 \in W^s_\varepsilon(z_\varepsilon)$,*

$$|\phi^t_\varepsilon(z_2) - \phi^t_\varepsilon(z_1)| \le K e^{-\alpha t}|z_2 - z_1|,$$

where $\alpha > 0$ *is determined by* $\alpha > \min_j |\Re\alpha_j|$ *for* $t > 0$.

Similarly, $\forall z_1, z_2 \in W^u_\varepsilon(z_\varepsilon)$,

$$|\phi^t_\varepsilon(z_2) - \phi^t_\varepsilon(z_1)| \leq Ke^{\beta t}|z_2 - z_1|,$$

where $\beta > 0$ *is determined by* $\beta < \min_j |\Re\beta_j|$ *for* $t < 0$.

Let M^ε be a $(k+\sigma)-$dimensional invariant manifold with $1 \leq \sigma \leq m$. Let $\mathscr{B}$ be a neighborhood of $\mathscr{Z}_0$ with boundary $\partial\mathscr{B}$. We assume that

(A1) M^0 intersect $W^s(\mathscr{Z}_0)$ transversally.

(A2) The ω limit set $\omega(N_0) \subset \mathscr{Z}_0$ is of dimension $\sigma - 1$, where N_0 is the intersection of M^0 and $W^s(\mathscr{Z}_0)$.

(A3) On $\mathscr{Z}_0$, the reduced vector field is not tangent to $\omega(N_0)$.

With the above assumption, let us state the so-called *Exchange Lemma* (see [47, 59]).

Theorem 2.7. *For any* $\tau_0 > 0$ *and* $0 < \rho < \tau_0$, *for* $\varepsilon > 0$ *small, a portion of* $M^\varepsilon \cap \mathscr{B}$ *is* C^1 $o(\varepsilon)-$*close to* $W^u(\omega(N_0)\cdot(\tau_0-\rho, \tau_0+\rho)) \cap \mathscr{B}$. *That is, for each point* $p \in W^u(\omega(N_0)\cdot(\tau_0-\rho, \tau_0+\rho)) \cap \mathscr{B}$, *a portion of* M^ε *is close to* p, *and the tangent space of* M^ε *is close to that of* $W^u(\omega(N_0)\cdot(\tau_0-\rho, \tau_0+\rho))$.

2.3 Boundary value problem solvers

We use "bvp4c" in Matlab ([52]) as the solver for our boundary value problem (BVP) (2.3) and (2.4). It solves first order systems of ordinary differential equations with two-point boundary conditions of this form:

$$\begin{cases} y' = f(x,y), & a < x < b, \\ g(y(a), y(b)) = 0. \end{cases} \tag{2.24}$$

Given a mesh partition $a = x_0 < x_1 < \cdots < x_N = b$, the numerical solution of (2.24) is approximated by a piecewise cubic polynomial function $S(x)$. The approximated solution $S(x)$ satisfies the boundary conditions and it is a cubic Hermite interpolation polynomial for each subinterval $[x_i, x_{i+1}]$.

For $i = 0, 1, 2, \cdots, N-1$, let $y_i = S(x_i)$ and let $h_i = x_{i+1} - x_i$. The y_i's are evaluated by solving the algebraic equations

$$\Phi(X,Y) = (\phi_0(X,Y), \phi_1(X,Y), \cdots, \phi_N(X,Y)) = 0, \tag{2.25}$$

where

$$\begin{aligned} X &= [x_0, x_1, \cdots, x_N]^T, \\ Y &= [y_0, y_1, \cdots, y_N]^T, \\ \phi_0(X,Y) &= g(y_0, y_N), \\ \phi_i(X,Y) &= y_i - y_{i-1} - \tfrac{1}{6} h_{i-1}(f_{i-1} + 4f_i^* + f_i), \quad i = 1, 2, \cdots, N, \end{aligned}$$

and

$$\begin{aligned} f_i &= f(x_i, y_i), \\ f_i^* &= f\left(\tfrac{1}{2}(x_{i-1} + x_i), \tfrac{1}{2}(y_{i-1} + y_i) - \tfrac{1}{8} h_{i-1}(f_i - f_{i-1})\right). \end{aligned}$$

The algebraic system (2.25) is solved by simplified Newton's method with a weak line search. The global Jacobian $\frac{\partial \Phi}{\partial Y}$ (using finite difference approximation by default) is required and the structure of the Jacobian is important for the linear solver in each Newton's iteration. The residual of $S(x)$ is calculated by $r(x) = S(x) - f(x, S(x))$ and the residual in the boundary conditions is $g(S(a),S(b))$. The adaptive mesh strategy has been used to control the residual in "bvp4c", for details, see [52].

2.4 Problem setups

To end this section, we set up our problems with the following assumptions:

(A1). We consider two ion species ($n=2$) with $z_1>0$ and $z_2<0$.

(A2). For the electrochemical potential μ_i, in addition to the ideal component μ_i^{id}, we also include the hard-sphere potential μ_i^{HS}, where it is either *local* or *non-local* .

(A3). The relative dielectric coefficient and the diffusion coefficient are constants, that is, $\varepsilon_r(x)=\varepsilon_r$ and $D_i(x)=D_i$.

Under the assumptions (A1)–(A3), the steady-state system of (2.3) is

$$\begin{aligned}&\frac{1}{h(x)}\frac{d}{dx}\left(\varepsilon_r\varepsilon_0 h(x)\frac{d\Phi}{dx}\right)=-e\left(z_1c_1+z_2c_2+Q(x)\right),\\&\frac{d\mathscr{J}_i}{dx}=0,\quad -\mathscr{J}_i=\frac{1}{kT}D_ih(x)c_i\frac{d\mu_i}{dx},\quad i=1,2.\end{aligned}\tag{2.26}$$

We now make the dimensionless re-scaling in (2.26),

$$\phi=\frac{e}{kT}\Phi,\quad \bar{V}=\frac{e}{kT}V,\quad \varepsilon^2=\frac{\varepsilon_r\varepsilon_0 kT}{e^2},\quad J_i=\frac{\mathscr{J}_i}{D_i}.$$

Using the expression (2.5) for the ideal component $\mu_i^{id}(x)$, we have, for $i=1,2$,

$$\begin{aligned}-J_i=-\frac{\mathscr{J}_i}{D_i}&=\frac{1}{kT}h(x)c_i\frac{d\mu_i^{id}}{dx}+\frac{1}{kT}h(x)c_i\frac{d\mu_i^{HS}}{dx}\\&=\frac{e}{kT}z_ih(x)c_i\frac{d\Phi}{dx}+h(x)\frac{dc_i}{dx}+\frac{h(x)c_i}{kT}\frac{d\mu_i^{HS}}{dx}\\&=z_ih(x)c_i\frac{d\phi}{dx}+h(x)\frac{dc_i}{dx}+\frac{h(x)c_i}{kT}\frac{d\mu_i^{HS}}{dx}.\end{aligned}$$

Note also that,

$$\varepsilon_r\varepsilon_0\frac{d\Phi}{dx} = \varepsilon^2\frac{e^2}{kT}\frac{d\Phi}{dx} = \varepsilon^2\frac{e^2}{kT}\frac{kT}{e}\frac{d\phi}{dx} = \varepsilon^2 e\frac{d\phi}{dx}.$$

Therefore, the boundary value problem (2.26) and (2.4) becomes

$$\begin{aligned}
&\frac{\varepsilon^2}{h(x)}\frac{d}{dx}\left(h(x)\frac{d}{dx}\phi\right) = -z_1c_1 - z_2c_2 - Q(x),\ \frac{dJ_1}{dx} = \frac{dJ_2}{dx} = 0,\\
&h(x)\frac{dc_1}{dx} + h(x)z_1c_1\frac{d\phi}{dx} + \frac{h(x)c_1}{kT}\frac{d}{dx}\mu_1^{HS}(x) = -J_1,\\
&h(x)\frac{dc_2}{dx} + h(x)z_2c_2\frac{d\phi}{dx} + \frac{h(x)c_2}{kT}\frac{d}{dx}\mu_2^{HS}(x) = -J_2,
\end{aligned} \tag{2.27}$$

with the boundary conditions, for $i = 1,2$,

$$\phi(0) = \bar{V},\ c_i(0) = L_i > 0; \quad \phi(1) = 0,\ c_i(1) = R_i > 0. \tag{2.28}$$

For ion channels, an important characteristic is the so-called *I-V relation*. For a solution of the *steady-state* boundary value problem of (2.27) and (2.28), the *rate of flow of charge through a cross-section* or *current* $\mathscr{I}$ is

$$\mathscr{I} = z_1\mathscr{J}_1 + z_2\mathscr{J}_2. \tag{2.29}$$

For fixed boundary concentrations L_i's and R_i's, $\mathscr{J}_j$'s depend on V only and formula (2.29) provides a relation of the current $\mathscr{I}$ on the voltage V. This relation is the *I-V relation*. We will also examine ion size effects on the *flow rate of matter* through a cross-section, $\mathscr{T}$, given by

$$\mathscr{T} = \mathscr{J}_1 + \mathscr{J}_2. \tag{2.30}$$

Chapter 3

Asymptotic expansions and numerical simulations on I-V relations via a steady-state Poisson-Nernst-Planck system

In this chapter, system (2.27) with the boundary condition (2.28) is studied both analytically and numerically with particular attention on I-V relations of ion channels including only the ideal component of the electrochemical potential. Assuming ε is small, the PNP system can be viewed as a singularly perturbed system. Due to the special structures of the zeroth order inner and outer systems, one is able to derive more explicit expressions of higher order terms in asymptotic expansions. For the case of zero permanent charge, under the assumption of electro-neutrality at both ends of the channel, our result concerning the I-V relation for two oppositely charged ion species is that the third order correction is cubic in V , and furthermore (Theorem 4.1), up to the third order, the cubic I-V relation has three distinct real roots (except for a very degenerate case) which corresponds to the bi-stable structure in the FitzHugh-Nagumo simplification of the Hodgkin-Huxley model. Three numerical experiments are conducted to check the cubic-like feature of the I-V curve, study the boundary value effect on the I-V relation, and investigate the permanent charge effect on the I-V curve respectively.

3.1 Introduction

Ion channels are cylindrical, hollow proteins that regulate the movement of ions across almost all biological membranes (see [30]). The most relevant properties of a channel are the permeation and selectivity, and an important characterization is the I-V relation. The I-V relation adopted in the FitzHugh-Nagumo simplification of the famous Hodgkin-Huxley systems which describe the propagation of action potential of *an ensemble of channels* in a biological membrane is *cubic-like*. A natural question arising here is whether this cubic-like feature can be obtained from a *single channel* ?

With the assumption that the channel is narrow, it can be effectively viewed as a one-dimensional channel and normalized as the interval $[0,1]$. The natural one-dimensional steady-state PNP type model (2.27) for ion flows of 2 ion species with the boundary condition (2.28) is studied. Note that, in this chapter, we study the classical PNP system, therefore, in system (2.27), $\frac{d}{dx}\mu_i^{HS} = 0$ for $i = 1,2$.

In this work, we mainly focus on the I-V relation (2.29), more precisely, our main interest in the I-V relation is to derive the asymptotic expansion

$$\mathscr{I} = I_0 + \varepsilon I_1 + \varepsilon^2 I_2 + \varepsilon^3 I_3 + \cdots . \tag{3.1}$$

For consistence, we also write

$$\mathscr{T} = T_0 + \varepsilon T_1 + \varepsilon^2 T_2 + \varepsilon^3 T_3 + \cdots . \tag{3.2}$$

It is known that, in general, the I-V relation is *not* unique (see [24, 63, 80, 81, 88, 89] for $Q \neq 0$ and see [58] even for $Q = 0$ when more ion species are involved). In Section 3.3, we will consider a special case where the I-V relation is indeed unique. For simplicity, in this work, we assume that $Q(x) = 0$ over the whole interval $[0,1]$.

With the assumption that ε is small, viewing it as the singular parameter, system (2.27) together with the boundary condition (2.28) will be treated as a singular boundary value problem. The general framework of the classical singular perturbation theory and the newly developed geometrical singular perturbation theory suggest one to study asymptotic expansion of the I-V relation.

In [1], a one-dimensional steady-state PNP system has been studied using asymptotic expansion approach with particular attention to the I-V relations. The result shows that

- The first order correction to the zeroth order linear I-V relation is generally *quadratic* in V;
- When the electro-neutrality condition is enforced at both ends of the channel, there is NO first order correction;
- The second order correction is *cubic* in V. Moreover, under electro-neutrality condition, up to the second order (in ε), the I-V relation is a cubic function with three distinct real roots.

A natural question arising here is whether the higher order corrections follow this pattern? More precisely, is the third order correction *quartic* in V? What about the fourth order correction?

Our goal in this chapter is to further examine higher order asymptotic expansions of the I-V relation following the idea in [1] and to provide answers to these interesting questions. For the special case mentioned above, the third order correction turns out to be *cubic* with the electro-neutrality condition (see formula (3.18)) even though a *quartic* function is expected, which gives us the *first surprise*. Immediately, we get another interesting question: *are the other higher order corrections also keeping this feature*? This leads to the study of the fourth order correction. However, to our surprise, the fourth order correction is *quintic* (see formula (3.30)) instead of being cubic. Furthermore, for the third order correction, the coefficient of the cubic term is always *negative* except for a highly degenerate case (see Theorem 3.7, Lemma 3.9 and Lemma 3.10). An importance of this negative sign is that, up to the third order, the cubic I-V function has three *distinct* real roots – this agrees qualitatively with I-V relation adopted in the FitzHugh-Nagumo simplification of the Hodgkin-Huxley systems. The existence of three distinct real roots of the I-V relation is responsible for the *bi-stable* structure in the FitzHugh-Nagumo system.

Numerical simulations are performed for both the cases with zero permanent charge and nonzero one respectively. For the case with zero permanent charge, it allows us to make a comparison between the analytical results and our numerical results. And meanwhile, one can investigate the effect of the boundary conditions on the I-V relations. For the one with nonzero permanent charge defined by

$$Q(x) = \begin{cases} 0, \ \text{for } 0 < x \leq a, \\ Q, \ \text{for } a < x < b, \\ 0, \ \text{for } b \leq x \leq 1, \end{cases}$$

where Q is a nonzero constant, we mainly focus on the cubic-like feature of the I-V relation and the effect of the permanent charge.

A thorough study of higher order asymptotic expansion of ϕ and c_i's is necessary to obtain higher order asymptotic expansions of the I-V relation. Both the geometric singular perturbation method and the classical matched asymptotic expansion method work well for the zeroth order term (see [1, 6, 30, 46, 54, 61]) at least for the special case mentioned above (see [24, 58] for a treatment of general situations). For higher order terms, the classical matched asymptotic expansion approach are applied since it seems that a direct application of the geometric singular perturbation theory does not work – a research direction worthwhile to explore. It's well-known that higher order terms satisfy linear but non-autonomous and non-homogeneous systems. The homogeneous parts of the linear systems are the same and are nothing but the linearizations of the zeroth order nonlinear system along the zeroth order (inner and outer) solutions. While in general, it is impossible to get explicit solutions of a linear non-autonomous system, a special feature of the problem at hand that the zeroth order nonlinear system possesses a complete set of integrals and each integral provides an integral for the linearization (see Propositions 3.2 and 3.3) allows us to carry out a detailed asymptotic analysis.

This chapter is organized as follows. In Section 3.2, we briefly restate the outer and inner systems for each order in the asymptotic expansions from [1], and the matching principle. Starting in Section 3.3, we restrict ourselves to the special case and examine the outer, inner expansions and matching. Previous results for lower order systems from [1] are briefly restated for completeness, and the third order expansions and matching are detailed under the electro-neutrality condition. In section 3.4, under the electro-neutrality condition, we focus on the I-V relation up to the third order in ε, and obtain our main result. In section 3.5, numerical simulations are performed to system (2.27) with boundary condition (2.28) for both $Q(x) = 0$ and $Q(x) \neq 0$, and corresponding I-V relation curves are obtained. Interesting phenomena are investigated.

3.2 Systems for asymptotic expansions

In this section, we apply the method of asymptotic expansions for both outer and inner systems to study the I-V relations of the PNP model discussed above. In current context, the outer systems "determine" the dynamics of ion flows within the channel, and the inner systems "govern" the potential boundary layers that represents the effects of boundary conditions from the bath conditions. The matching principle then provides the intersection between the internal dynamics and the boundary conditions.

3.2.1 Outer systems for each order

We assume Q is constant and look for outer expansion of the form, for $i = 1, 2$,

$$\begin{aligned} \phi(x;\varepsilon) &= \phi_0(x) + \varepsilon\phi_1(x) + \varepsilon^2\phi_2(x) + \cdots, \\ c_i(x;\varepsilon) &= c_{i0}(x) + \varepsilon c_{i1}(x) + \varepsilon^2 c_{i2}(x) + \cdots, \\ J_i &= J_{i0} + \varepsilon J_{i1} + \varepsilon^2 J_{i2} + \cdots. \end{aligned} \tag{3.3}$$

Substituting (3.3) into (2.27) and denoting the derivatives with respect to x by overdots, with the convention that $\phi_{-1} = \phi_{-2} = 0, \delta_0 = 1$,and $\delta_j = 0$ for $j \neq 0$, upon introducing $u_j = \dot{\phi}_j$, the $j-$th order system in ε is, for $i = 1, 2$,

$$\begin{aligned} \dot{\phi}_{j-2} &= u_{j-2}, \quad \dot{u}_{j-2} = -(\alpha c_{1j} - \beta c_{2j} + \delta_j Q), \\ \dot{c}_{ij} &= -\sum_{p+q=j} (\alpha c_{1p} - \beta c_{2p}) u_q - J_{ij}. \end{aligned} \tag{3.4}$$

Remark 3.1. *An observation is that the homogeneous part for c_{ij}'s is*

$$\begin{pmatrix} c'_{1j} \\ c'_{2j} \end{pmatrix} = -u_0(x) \begin{pmatrix} \alpha & 0 \\ 0 & -\beta \end{pmatrix} \begin{pmatrix} c_{1j} \\ c_{2j} \end{pmatrix}.$$

Once $u_0(x)$ is found, this system can be simply integrated. And hence, system (3.4) *can be solved.*

3.2.2 Inner systems for each order

Inner systems at the left boundary $x = 0$

At the boundary $x = 0$, in terms of the inner variable $\xi = x/\varepsilon$, let $\Phi(\xi;\varepsilon) = \phi(\varepsilon\xi;\varepsilon)$, $C_i(\xi;\varepsilon) = c_i(\varepsilon\xi;\varepsilon)$. System (2.27) becomes, for $i = 1,2$,

$$\begin{aligned} &\frac{d^2}{d\xi^2}\Phi = -(\alpha C_1 - \beta C_2 + Q), \quad \frac{dJ_1}{dx} = \frac{dJ_2}{dx} = 0, \\ &\frac{dC_1}{d\xi} + \alpha C_1 \frac{d\Phi}{d\xi} = -\varepsilon J_1, \quad \frac{dC_2}{d\xi} - \beta C_2 \frac{d\Phi}{d\xi} = -\varepsilon J_2. \end{aligned} \tag{3.5}$$

We look for the inner expansion of the form:

$$\begin{aligned} \Phi(\xi;\varepsilon) =& \Phi_0(\xi) + \varepsilon\Phi_1(\xi) + \varepsilon^2\Phi_2(\xi) + \cdots, \\ C_i(\xi;\varepsilon) =& C_{i0}(\xi) + \varepsilon C_{i1}(\xi) + \varepsilon^2 C_{i2}(\xi) + \cdots, \\ J_i =& J_{i0} + \varepsilon J_{i1} + \varepsilon^2 J_{i2} + \cdots. \end{aligned} \tag{3.6}$$

We have, by introducing $U_j = \Phi_j'$,

$$\begin{aligned} &\Phi_j' = U_j, \quad U_j' = -(\alpha C_{1j} - \beta C_{2j}) - \delta_j Q, \\ &C_{1j}' = -\sum_{p+q=j} \alpha C_{1p} U_q - J_{1(j-1)}, \\ &C_{2j}' = \sum_{p+q=j} \beta C_{2p} U_q - J_{2(j-1)}. \end{aligned} \tag{3.7}$$

For $j = 0$, the system is

$$\begin{aligned} \Phi_0' =& U_0, \quad U_0' = -(\alpha C_{10} - \beta C_{20}) - Q, \\ C_{10}' =& -\alpha C_{10} U_0, \quad C_{20}' = \beta C_{20} U_0. \end{aligned} \tag{3.8}$$

and, for all $j \geq 1$, the homogeneous part of (3.7) is the same and it is the linearization of the zeroth order system (3.8).

There is a specific structure of system (3.8) that together with an abstract result allows one to get a closed form for solutions of (3.7). The specific structure is

Proposition 3.2. *The zeroth order inner system* (3.8) *has a complete set of (3) first integrals given by,*

$$H_1 = C_{10}e^{\alpha\Phi_0}, \quad H_2 = C_{20}e^{-\beta\Phi_0}, \quad H_3 = \frac{1}{2}U_0^2 - C_{10} - C_{20} + Q\Phi_0.$$

Proof. This can be verified directly (see also [58]). □

A crucial result whose proof is provided in [1] is given below.

Proposition 3.3. *Consider an autonomous system*

$$z' = f(z), \quad z \in \mathbb{R}^m. \tag{3.9}$$

For a solution $z_0(t)$ of (3.9)*, consider the linearzation along $z_0(t)$:*

$$Z' = Df(z_0(t))Z, \quad Z \in \mathbb{R}^m. \tag{3.10}$$

If a C^2 function $H : \mathbb{R}^m \to \mathbb{R}$ is an integral of system (3.9) *(that is, $H(z(t))$ is independent of t for any solution $z(t)$ of* (3.9)*), then $G(Z,t) = \langle \nabla H(z_0(t)), Z \rangle$ is an integral of the linear system* (3.10) *(that is, $G(Z(t),t)$ is independent of t for any solution $Z(t)$ of* (3.10)*).*

Noticing that the homogeneous part of (3.7) for $j \geq 1$ is the linearization of the zeroth order system (3.8), a complete set of integrals for the homogeneous part of (3.7) can be derived from Propositions 3.2 and 3.3. An application of variation of parameters allows one to get a closed form for the solutions of (3.7).

Inner systems at the right boundary $x = 1$

In the similar way, at the right boundary $x = 1$ in terms of the inner variable $\xi = (-1 + x)/\varepsilon$ and let $\Psi(\xi;\varepsilon) = \phi(1+\varepsilon\xi;\varepsilon)$, $D_k(\xi;\varepsilon) = c_k(1+\varepsilon\xi;\varepsilon)$, by introducing $V_j = \Psi'_j$, we get

$$\begin{aligned}
&\Psi'_j = V_j, \quad V'_j = -(\alpha D_{1j} - \beta D_{2j}) - \delta_j Q,\\
&D'_{1j} = -\sum_{p+q=j} \alpha D_{1p} V_q - J_{1(j-1)},\\
&D'_{2j} = -\sum_{p+q=j} \beta D_{2p} V_q - J_{2(j-1)}.
\end{aligned} \tag{3.11}$$

Same observation for inner systems at $x = 0$ applies here.

Remark 3.4. *For a more general derivation of the outer and inner systems, one can read [1].*

Then, following the third step in section 2.2.2, one can apply the matching principle to $(\phi(x;\varepsilon), c_k(x;\varepsilon))$ and $(\Phi(\xi;\varepsilon), C_k(\xi;\varepsilon))$ at the left boundary $x = 0$ and, at the right boundary $x = 1$, to $(\phi(x;\varepsilon), c_k(x;\varepsilon))$ and $(\Psi(\xi;\varepsilon), D_k(\xi;\varepsilon))$.

3.3 Third order matching under electroneutrality conditions

With $\alpha = \beta = 1$, under the electroneutrality assumption $L_1 = L_2 = L$ and $R_1 = R_2 = R$, we will derive the matched asymptotic expansions for the third order over the interval $[0,1]$, and through matching, we establish the third order correction.

For completeness, we summarize the results for lower order asymptotic expansions from [1] as follows:

Theorem 3.5. *If $L \neq R$, under the electroneutrality condition, with $I_k = J_{1k} - J_{2k}$ and $T_k = J_{1k} + J_{2k},\ k = 0,1,2,$ for the outer system, we have,*

- *For the zeroth order outer system, one has*

$$\phi_0(x) = b_0 + \frac{I_0}{T_0}\ln|a_0 - T_0 x|, \quad c_{10}(x) = c_{20}(x) = \frac{a_0 - T_0 x}{2}.$$

- *For the first order outer system, one has*

$$\phi_1(x) = c_{11}(x) = c_{21}(x) = 0.$$

- *For the second order outer system, one has*

$$\begin{aligned} c_{12}(x) =& \frac{a_2 - T_2 x}{2} + \frac{I_0^2 + 2I_0T_0}{4(a_0 - T_0x)^2}, \quad c_{22}(x) = \frac{a_2 - T_2 x}{2} + \frac{I_0^2 - 2I_0T_0}{4(a_0 - T_0x)^2}, \\ \phi_2(x) =& b_2 + \frac{I_2T_0 - I_0T_2}{T_0^2}\ln|a_0 - T_0x| + \frac{I_0(a_2T_0 - a_0T_2)}{T_0^2(a_0 - T_0x)} + \frac{I_0(I_0^2 - 4T_0^2)}{6T_0(a_0 - T_0x)^3}. \end{aligned}$$

For the inner system, we have,

- *At the boundary $x = 0$ with $x = \varepsilon\xi$,*
  - *For the zeroth order inner system, we have*

$$\Phi_0(\xi) = \bar{V} \quad U_0(\xi) = 0, \quad C_{10}(\xi) = C_{20}(\xi) = L.$$

  - *For the first order inner system, we have:*

$$\Phi_1(\xi) = -\frac{I_0}{2L}\xi, \quad C_{11}(\xi) = C_{21}(\xi) = -\frac{T_0}{2}\xi.$$

– *For the second order inner system, we have*

$$
\begin{aligned}
C_{12}(\xi) =& \frac{I_0T_0}{8L^2}\left(1-e^{-\sqrt{2L}\xi}\right), \quad C_{22}(\xi) = \frac{I_0T_0}{8L^2}\left(e^{-\sqrt{2L}\xi}-1\right),\\
\Phi_2(\xi) =& \frac{I_0T_0}{8L^3}\left(e^{-\sqrt{2L}\xi}-1\right) - \frac{I_0T_0}{8L^2}\xi^2.
\end{aligned}
$$

- *At the boundary $x=1$ with $x-1=\varepsilon\xi$,*

  – *For the zeroth order inner system, one has*

$$
\Psi_0(\xi)=0 \quad V_0(\xi)=0 \quad D_{10}(\xi)=D_{20}(\xi)=R.
$$

  – *For the first order inner system, one has*

$$
\Psi_1(\xi) = -\frac{I_0}{2R}\xi, \quad D_{11}(\xi)=D_{21}(\xi) = -\frac{T_0}{2}\xi.
$$

  – *For the second order inner system, one has*

$$
\begin{aligned}
D_{12}(\xi) =& -\frac{I_0T_0}{8R^2}\left(e^{\sqrt{2R}\xi}-1\right), \quad D_{22}(\xi) = \frac{I_0T_0}{8R^2}\left(e^{\sqrt{2R}\xi}-1\right),\\
\Psi_2(\xi) =& \frac{I_0T_0}{8R^3}\left(e^{\sqrt{2R}\xi}-1\right) - \frac{I_0T_0}{8R^2}\xi^2.
\end{aligned}
$$

Here,

$$
\begin{aligned}
a_0 =& 2L, \quad T_0 = 2(L-R), \quad I_0 = \frac{2(L-R)}{\ln L - \ln R}\bar{V}, \quad b_0 = \bar{V} - \frac{I_0}{T_0}\ln 2L;\\
a_1 =& I_1 = T_1 = b_1 = 0; \quad a_2 = -\frac{I_0^2}{8L^2}, \quad T_2 = \frac{(L-R)^3(L+R)}{2L^2R^2(\ln L - \ln R)^2}\bar{V}^2,\\
I_2 =& \frac{(L-R)^3(L^3-R^3)\bar{V}}{3L^3R^3(\ln L - \ln R)^2} + \frac{(L-R)^3}{L^2R^2(\ln L - \ln R)^3}\left(\frac{L+R}{2} - \frac{L^3-R^3}{3LR(\ln L - \ln R)}\right)\bar{V}^3,\\
b_2 =& \frac{I_0(4T_0^2-I_0^2)}{6a_0^3T_0} - \frac{I_0(a_2T_0-a_0T_2)}{a_0T_0^2} - \frac{I_2T_0-I_0T_2}{T_0^2}\ln|a_0| - \frac{I_0T_0}{8L^3}.
\end{aligned}
$$

Now we carry out the analysis for the third order asymptotic expansions and matchings in detail.

3.3.1 Third order outer expansion

The third order outer system, from (3.4), is

$$\begin{aligned}\ddot{\phi}_1 =& -c_{13}+c_{23},\\ \dot{c}_{13} =& -(c_{13}\dot{\phi}_0+c_{12}\dot{\phi}_1+c_{11}\dot{\phi}_2+c_{10}\dot{\phi}_3)-J_{13},\\ \dot{c}_{23} =&(c_{23}\dot{\phi}_0+c_{22}\dot{\phi}_1+c_{21}\dot{\phi}_2+c_{20}\dot{\phi}_3)-J_{23}.\end{aligned} \tag{3.12}$$

Solving (3.12), together with Theorem 3.5, we have

$$\begin{aligned}c_{13}(x) =& c_{23}(x)=\frac{a_3-T_3x}{2},\\ \phi_3(x) =& b_3+\left(\frac{a_3I_0}{T_0}-\frac{a_0I_0T_3}{T_0^2}\right)\frac{1}{a_0-T_0x}+\left(\frac{I_3}{T_0}-\frac{I_0T_3}{T_0^2}\right)\ln|a_0-T_0x|,\end{aligned} \tag{3.13}$$

for some constants a_3 and b_3 to be determined through matching. Here $I_3=J_{13}-J_{23}$ and $T_3=J_{13}+J_{23}$.

3.3.2 Third order inner expansion

At the boundary $x=0$, from (3.7), the third order inner system is

$$\begin{aligned}\Phi_3' =& U_3, \quad U_3'=-(C_{13}-C_{23}),\\ C_{13}' =& -(C_{10}U_3+C_{11}U_2+C_{12}U_1+C_{13}U_0)-J_{12},\\ C_{23}' =&(C_{20}U_3+C_{21}U_2+C_{22}U_1+C_{23}U_0)-J_{22}.\end{aligned} \tag{3.14}$$

As an application of Proposition 2.1 for zeroth, first and second order cases (see Proposition 3.1, 3.2 and 3.3 in [1]) and Proposition 2.2, we have the next result.

Proposition 3.6. *System* (3.14) *has the following integrals:*

$$
\begin{aligned}
G_1 =& C_{13}e^{\Phi_0} + C_{10}e^{\Phi_0}\Phi_3 + J_{12}F_1 + F_{131} + F_{132},\\
G_2 =& C_{23}e^{-\Phi_0} - C_{20}e^{-\Phi_0}\Phi_3 + J_{22}F_2 - F_{231} - F_{232},\\
G_3 =& U_0U_3 + U_1U_2 - C_{13} - C_{23} - T_2\xi,
\end{aligned}
$$

where

$$
\begin{aligned}
F_1(\xi) &= \int_0^\xi e^{\Phi_0(s)}ds, \quad F_2(\xi) = \int_0^\xi e^{-\Phi_0(s)}ds,\\
F_{131}(\xi) &= \int_0^\xi C_{11}(s)U_2(s)e^{\Phi_0(s)}ds, \quad F_{132}(\xi) = \int_0^\xi C_{12}(s)U_1(s)e^{\Phi_0(s)}ds,\\
F_{231}(\xi) &= \int_0^\xi C_{21}(s)U_2(s)e^{-\Phi_0(s)}ds, \quad F_{232}(\xi) = \int_0^\xi C_{22}(s)U_1(s)e^{-\Phi_0(s)}ds.
\end{aligned}
$$

Proof. This can be verified directly. □

Applying the integrals in Proposition 3.6, we can solve (3.14) with $\Phi_3(0) = C_{13}(0) = C_{23}(0) = 0$ to get

$$
\begin{aligned}
\Phi_3(\xi) = &\left[\frac{I_0T_0^2}{2(2L)^{\frac{7}{2}}}\left(\frac{1}{2}\xi^2 + \frac{3}{2\sqrt{2L}}\xi + \frac{1}{L}\right) - \gamma_1\right]e^{-\sqrt{2L}\xi} + \gamma_1 e^{\sqrt{2L}\xi} - \frac{I_0T_0^2}{(2L)^{\frac{9}{2}}}\\
&- \left(\frac{I_2}{2L} + \frac{2I_0T_0^2}{(2L)^4}\right)\xi - \frac{I_0T_0^2}{3(2L)^3}\xi^3.
\end{aligned}
$$

The matching will force $\gamma_1 = 0$. For convenience, we define the following functions.

$$
\begin{aligned}
k_1(x) =& \frac{I_0T_0^2}{2(2x)^{\frac{7}{2}}}\left(\frac{1}{2}\xi^2 + \frac{3}{2\sqrt{2x}}\xi + \frac{1}{x}\right),\\
k_2(x) =& \frac{I_0T_0}{4(2x)^{\frac{5}{2}}}\left(\frac{I_0}{x} - \frac{T_0}{2\sqrt{2x}}\xi - \frac{T_0}{2}\xi^2\right),\\
k_3(x) =& \frac{I_0T_0}{4(2x)^{\frac{5}{2}}}\left(\frac{I_0}{x} + \frac{T_0}{2\sqrt{2x}}\xi + \frac{T_0}{2}\xi^2\right).
\end{aligned}
$$

Then, for $\xi \geq 0$,

$$
\begin{aligned}
\Phi_3(\xi) =& k_1(L)e^{-\sqrt{2L}\xi} - \frac{I_0T_0^2}{(2L)^{\frac{9}{2}}} - \left(\frac{I_2}{2L} + \frac{2I_0T_0^2}{(2L)^4}\right)\xi - \frac{I_0T_0^2}{3(2L)^3}\xi^3, \\
C_{13}(\xi) =& k_2(L)e^{-\sqrt{2L}\xi} + \left(\frac{I_0T_0(I_0+2T_0)}{16L^3} - \frac{T_2}{2}\right)\xi - \frac{I_0^2T_0}{2(2L)^{\frac{7}{2}}}, \\
C_{23}(\xi) =& k_3(L)e^{-\sqrt{2L}\xi} + \left(\frac{I_0T_0(I_0-2T_0)}{16L^3} - \frac{T_2}{2}\right)\xi - \frac{I_0^2T_0}{2(2L)^{\frac{7}{2}}}.
\end{aligned}
\tag{3.15}
$$

Similarly, at $x = 1$, the third order inner solution is, for $\xi \leq 0$,

$$
\begin{aligned}
\Psi_3(\xi) =& -k_1(R)e^{\sqrt{2R}\xi} + \frac{I_0T_0^2}{(2R)^{\frac{9}{2}}} - \left(\frac{I_2}{2R} + \frac{2I_0T_0^2}{(2R)^4}\right)\xi - \frac{I_0T_0^2}{3(2R)^3}\xi^3, \\
D_{13}(\xi) =& -k_2(R)e^{\sqrt{2R}\xi} + \left(\frac{I_0T_0(I_0+2T_0)}{16R^3} - \frac{T_2}{2}\right)\xi + \frac{I_0^2T_0}{2(2R)^{\frac{7}{2}}}, \\
D_{23}(\xi) =& -k_3(R)e^{\sqrt{2R}\xi} + \left(\frac{I_0T_0(I_0-2T_0)}{16R^3} - \frac{T_2}{2}\right)\xi + \frac{I_0^2T_0}{2(2R)^{\frac{7}{2}}}.
\end{aligned}
\tag{3.16}
$$

3.3.3 Third order matching

For convenience, we define

$$
\begin{aligned}
\rho_1(x) =& b_2 - \frac{I_0T_0}{2(a_0-x)^2}\xi^2 + \frac{I_2T_0 - I_0T_2}{T_0^2}\ln|a_0-x| + \frac{I_0(a_2T_0-a_0T_2)}{T_0^2(a_0-x)} \\
& - \frac{I_0(4T_0^2-I_0^2)}{6T_0(a_0-x)^3}, \\
\rho_2(x) =& b_3 + \left(\frac{I_0(I_0^2-4T_0^2)}{2(a_0-x)^4} + \frac{(a_2-T_2)I_0}{(a_0-x)^2} - \frac{I_2}{a_0-x}\right)\xi - \frac{I_0T_0^2}{3(a_0-x)^3}\xi^3 \\
& + \frac{a_3I_0T_0 - a_0I_0T_3}{T_0^2(a_0-x)} + \frac{I_3T_0 - I_0T_3}{T_0^2}\ln|a_0-x|, \\
\rho_3(x,y) =& \frac{a_3-y}{2} + \left(\frac{I_0^2T_0}{2(a_0-x)^3} + \frac{I_0T_0^2}{(a_0-x)^3} - \frac{T_2}{2}\right)\xi, \\
\rho_4(x,y) =& \frac{a_3-y}{2} + \left(\frac{I_0^2T_0}{2(a_0-x)^3} - \frac{I_0T_0^2}{(a_0-x)^3} - \frac{T_2}{2}\right)\xi.
\end{aligned}
\tag{3.17}
$$

From (3.13) and (3.17), in terms of $\xi = x/\varepsilon$, the outer expansion at $x=0$ is

$$\begin{aligned}
E_\xi^3 E_x^3(\phi) =& b_0 + \frac{I_0}{T_0}\ln a_0 - \varepsilon\frac{I_0}{a_0}\xi + \varepsilon^2\rho_1(0) + \varepsilon^3\rho_2(0),\\
E_\xi^3 E_x^3(c_1) =& \frac{a_0}{2} - \varepsilon\frac{T_0}{2}\xi + \varepsilon^2\left(\frac{a_2}{2} + \frac{I_0^2 + 2I_0T_0}{4a_0}\right) + \varepsilon^3\rho_3(0,0),\\
E_\xi^3 E_x^3(c_2) =& \frac{a_0}{2} - \varepsilon\frac{T_0}{2}\xi + \varepsilon^2\left(\frac{a_2}{2} + \frac{I_0^2 - 2I_0T_0}{4a_0}\right) + \varepsilon^3\rho_4(0,0),
\end{aligned}$$

and in terms of $\xi = (x-1)/\varepsilon$, the outer expansion at $x=1$ is

$$\begin{aligned}
E_\xi^3 E_x^3(\phi) =& b_0 + \frac{I_0}{T_0}\ln|a_0 - T_0| - \varepsilon\frac{I_0}{a_0 - T_0}\xi + \varepsilon^2\rho_1(T_0) + \varepsilon^3\rho_2(T_0),\\
E_\xi^3 E_x^3(c_1) =& \frac{a_0 - T_0}{2} - \varepsilon\frac{T_0}{2}\xi + \varepsilon^2\left(\frac{a_2 - T_2}{2} + \frac{I_0^2 + 2I_0T_0}{4(a_0 - T_0)^2}\right) + \varepsilon^3\rho_3(T_0, T_3),\\
E_\xi^3 E_x^3(c_2) =& \frac{a_0 - T_0}{2} - \varepsilon\frac{T_0}{2}\xi + \varepsilon^2\left(\frac{a_2 - T_2}{2} + \frac{I_0^2 - 2I_0T_0}{4(a_0 - T_0)^2}\right) + \varepsilon^3\rho_4(T_0, T_3).
\end{aligned}$$

From (3.15) and (3.16), the inner expansion at $x=0$ is

$$\begin{aligned}
E_x^3 E_\xi^3(\Phi) =& \bar{V} - \varepsilon\frac{I_0}{2L}\xi - \varepsilon^2\left(\frac{I_0T_0}{8L^3} + \frac{I_0T_0}{8L^2}\xi^2\right) - \varepsilon^3\left(\frac{I_0T_0^2}{(2L)^{\frac{9}{2}}} + \left(\frac{I_2}{2L} + \frac{2I_0T_0^2}{(2L)^4}\right)\xi\right.\\
&\left.+\frac{I_0T_0^2}{3(2L)^3}\xi^3\right),\\
E_x^3 E_\xi^3(C_1) =& L - \varepsilon\frac{T_0}{2}\xi + \varepsilon^2\frac{I_0T_0}{8L^2} - \varepsilon^3\left(\frac{I_0^2T_0}{2(2L)^{\frac{7}{2}}} - \left(\frac{I_0T_0^2}{8L^3} + \frac{I_0^2T_0}{16L^3} - \frac{T_2}{2}\right)\xi\right),\\
E_x^3 E_\xi^3(C_2) =& L - \varepsilon\frac{T_0}{2}\xi - \varepsilon^2\frac{I_0T_0}{8L^2} - \varepsilon^3\left(\frac{I_0^2T_0}{2(2L)^{\frac{7}{2}}} - \left(\frac{I_0^2T_0}{16L^3} - \frac{I_0T_0^2}{8L^3} - \frac{T_2}{2}\right)\xi\right),
\end{aligned}$$

and the inner expansion at $x=1$ is

$$\begin{aligned}
E_x^3 E_\xi^3(\Psi) =& \bar{V} - \varepsilon\frac{I_0}{2R}\xi - \varepsilon^2\left(\frac{I_0T_0}{8R^3} + \frac{I_0T_0}{8R^2}\xi^2\right) - \varepsilon^3\left(-\frac{I_0T_0^2}{(2R)^{\frac{9}{2}}} + \left(\frac{I_2}{2R} + \frac{2I_0T_0^2}{(2R)^4}\right)\xi\right.\\
&\left.+\frac{I_0T_0^2}{3(2R)^3}\xi^3\right),
\end{aligned}$$

$$
\begin{aligned}
E_x^3E_\xi^3(D_1) =& R-\varepsilon\frac{T_0}{2}\xi+\varepsilon^2\frac{I_0T_0}{8R^2}+\varepsilon^3\left(\frac{I_0^2T_0}{2(2R)^{\frac{7}{2}}}+\left(\frac{I_0^2T_0}{16R^3}+\frac{I_0T_0^2}{8R^3}-\frac{T_2}{2}\right)\xi\right),\\
E_x^3E_\xi^3(D_2) =& R-\varepsilon\frac{T_0}{2}\xi-\varepsilon^2\frac{I_0T_0}{8R^2}+\varepsilon^3\left(\frac{I_0^2T_0}{2(2R)^{\frac{7}{2}}}+\left(\frac{I_0^2T_0}{16R^3}-\frac{I_0T_0^2}{8R^3}-\frac{T_2}{2}\right)\xi\right).
\end{aligned}
$$

Together with Theorem 3.5, the matchings $E_\xi^3E_x^3(\phi)=E_x^3E_\xi^3(\Phi), E_\xi^3E_x^3(c_i)=E_x^3E_\xi^3(C_i)$, at $x=0$ and $E_\xi^3E_x^3(\phi)=E_x^3E_\xi^3(\Psi), E_\xi^3E_x^3(c_i)=E_x^3E_\xi^3(D_i)$ at $x=1$ for $i=1,2$, then give

$$
\begin{aligned}
a_3 =& -\frac{I_0^2T_0}{(2L)^{\frac{7}{2}}}, \quad T_3=-\frac{(L-R)^3}{\sqrt{2}(\ln L-\ln R)^2}\left(\frac{1}{R^{\frac{7}{2}}}+\frac{1}{L^{\frac{7}{2}}}\right)\bar{V}^2,\\
I_3 =& -\frac{(L-R)^4}{\sqrt{2}(\ln L-\ln R)^2}\left(\frac{1}{R^{\frac{9}{2}}}+\frac{1}{L^{\frac{9}{2}}}\right)\bar{V}\\
&-\frac{(L-R)^3}{\sqrt{2}\left(\ln L-\ln R\right)^3}\left[\frac{1}{R^{\frac{7}{2}}}+\frac{1}{L^{\frac{7}{2}}}-\frac{L-R}{RL(\ln L-\ln R)}\left(\frac{L}{R^{\frac{7}{2}}}+\frac{R}{L^{\frac{7}{2}}}\right)\right]\bar{V}^3,\\
b_3 =& \frac{I_0T_3-I_3T_0}{T_0^2}\ln|a_0|-\frac{I_0(a_3T_0-a_0T_3)}{a_0T_0^2}-\frac{I_0T_0^2}{(2L)^{\frac{9}{2}}}.
\end{aligned}
\tag{3.18}
$$

3.4 I-V relations under electroneutrality conditions

Recall from (3.1) that, our main interest is to derive the asymptotic expansion of the I-V relation in the following form

$$
\mathscr{I}=I_0+\varepsilon I_1+\varepsilon^2I_2+\varepsilon^3I_3+\cdots.
$$

3.4.1 Main results

In this section, we will study the I-V relation under the electroneutrality condition up to third order in ε in detail, and state our main result.

From Theorem 3.5, and (3.18), under the assumption of electro-neutrality, up to the third order in ε, we have

$$\begin{aligned}\mathscr{I} =& I_0+\varepsilon I_1+\varepsilon^2 I_2+\varepsilon^3 I_3\\ =& f(L,R,\varepsilon)\bar{V}-\varepsilon^2 g(L,R,\varepsilon)\bar{V}^3\\ =& \frac{e}{kT}\left(f(L,R,\varepsilon)V-\varepsilon^2\left(\frac{e}{kT}\right)^2 g(L,R,\varepsilon)V^3\right),\end{aligned} \tag{3.19}$$

where

$$\begin{aligned} f(L,R,\varepsilon) =& \frac{2(L-R)}{\ln L-\ln R}+\varepsilon^2\frac{(L-R)^4}{3(\ln L-\ln R)^2}\left(\frac{L^2+R^2+LR}{L^3R^3}-\frac{3\varepsilon}{\sqrt{2}}\left(\frac{1}{L^{\frac{9}{2}}}+\frac{1}{R^{\frac{9}{2}}}\right)\right),\\ g(L,R,\varepsilon) =& \frac{(L-R)^3(L^3-R^3)}{3L^3R^3(\ln L-\ln R)^4}-\frac{(L-R)^2(L^2-R^2)}{2L^2R^2(\ln L-\ln R)^3}\\ &+\varepsilon\frac{(L-R)^3}{\sqrt{2}(\ln L-\ln R)^3}\left[\frac{1}{R^{\frac{7}{2}}}+\frac{1}{L^{\frac{7}{2}}}-\frac{L-R}{RL(\ln L-\ln R)}\left(\frac{L}{R^{\frac{7}{2}}}+\frac{R}{L^{\frac{7}{2}}}\right)\right].\end{aligned}$$

Theorem 3.7. *If $L\neq R$, for $\varepsilon>0$ small, then, up to the order of ε^3, the I-V relation $\mathscr{I}=\mathscr{I}(V)$ is a cubic function with three distinct real roots.*

Proof. From (3.19), it suffices to show that both $f(L,R,\varepsilon)$ and $g(L,R,\varepsilon)$ are positive. Note that $(L-R)/(\ln L-\ln R)>0$, for $L\neq R$, our proof follows directly from the next three lemmas.

□

Lemma 3.8. *For $L\neq R$, and $\varepsilon>0$ small,*

$$h_1(L,R,\varepsilon)=\frac{L^2+R^2+LR}{L^3R^3}-\frac{3\varepsilon}{\sqrt{2}}\left(\frac{1}{L^{\frac{9}{2}}}+\frac{1}{R^{\frac{9}{2}}}\right)>0.$$

Proof. Treat $h_1(\varepsilon)=h_1(L,R,\varepsilon)$, for fixed $L\neq R$, one has

$$h_1(\varepsilon^*)=0,\ \text{and}\ h_1'(\varepsilon)=-\frac{3}{\sqrt{2}}\left(\frac{1}{R^{\frac{9}{2}}}+\frac{1}{L^{\frac{9}{2}}}\right)<0,\ \text{for all}\ \varepsilon>0,$$

where

$$\varepsilon^* = \frac{\sqrt{2}L^{\frac{3}{2}}R^{\frac{3}{2}}(L^2+LR+R^2)}{3\left(L^{\frac{3}{2}}+R^{\frac{3}{2}}\right)\left(L^3+R^{\frac{3}{2}}L^{\frac{3}{2}}+R^3\right)}.$$

It is clear that $h_1(\varepsilon) > 0$ for $0 < \varepsilon < \varepsilon^*$. Note that $\varepsilon \ll 1$, and $\varepsilon^* = O(1)$, we have $h_1(L,R,\varepsilon) > 0$ for $\varepsilon > 0$ small. $\square$

Lemma 3.9. *For $L \neq R$,*

$$h_2(L,R) = \frac{(L-R)^3(L^3-R^3)}{3L^3R^3(\ln L - \ln R)^4} - \frac{(L-R)^2(L^2-R^2)}{2L^2R^2(\ln L - \ln R)^3} > 0.$$

Proof. Notice that $h_2(L,R) = h_2(R,L)$, it suffices to show that $h_2(L,R) > 0$ for $L > R$. Rewrite $h_2(L,R)$ as

$$h_2(L,R) = \frac{(L-R)^3}{L^2R^2(\ln L - \ln R)^3}\tilde{h}_2(L,R),$$

where

$$\tilde{h}_2(L,R) = \frac{L^3-R^3}{3LR(\ln L - \ln R)} - \frac{L+R}{2}.$$

Then,

$$h_2(L,R) > 0 \Longleftrightarrow \tilde{h}_2(L,R) > 0, \ \text{ for } L > R.$$

Fixing R, we treat $\tilde{h}_2(L) = \tilde{h}_2(L,R)$ as a function of L. A direct calculation shows $\tilde{h}_2(R) = \tilde{h}_2'(R) = 0$, but $\tilde{h}_2''(L) > 0$ for all L. Therefore, we have $\tilde{h}_2(L,R) > 0$ for all $L > R$.

$\square$

Lemma 3.10. *For $L \neq R$,*

$$h_3(L,R,\varepsilon) = \frac{1}{R^{\frac{7}{2}}} + \frac{1}{L^{\frac{7}{2}}} - \frac{L-R}{RL(\ln L - \ln R)}\left(\frac{L}{R^{\frac{7}{2}}} + \frac{R}{L^{\frac{7}{2}}}\right) > 0.$$

Proof. Rewrite $h_3(L,R)$ as $h_3(L,R) = p(L,R)/(LR)^{\frac{9}{2}}(\ln L - \ln R)$, where

$$p(L,R) = LR(\ln L - \ln R)\left(L^{\frac{7}{2}} + R^{\frac{7}{2}}\right) - (L-R)\left(L^{\frac{9}{2}} + R^{\frac{9}{2}}\right).$$

Note that $h_3(L,R) = h_3(R,L)$. It suffices to show $h_3(L,R) > 0$ for $L > R$, which is equivalent to showing that $p(L,R) > 0$ for $L > R$. To do so, we fix R, and treat $p(L) = p(L,R)$ as a function of L. Then, a direct computation gives $p(R) = p'(R) = p''(R) = 0$, but $p'''(L) > 0$ for $L > R$. Therefore, $p(L) > 0$ for $L > R$. □

3.4.2 Remarks

For the third order terms, we only treated the electro-neutrality case mainly because this is a natural biological assumption. Under this assumption, up to the order of ε^3, even though a quartic function is expected, the I-V relation $\mathscr{I}(V)$ is still a cubic function with three distinct real roots, which is potentially related to the cubic-like feature of the average I-V relation of a population of channels in the Fitzhugh-Nagumo simplification of the Hodgkin-Huxley model. The existence of three distinct real roots of the I-V relation is responsible for the bi-stable structure in the FitzHugh-Nagumo system.

Recall from [1], that the first order correction to the zeroth order linear I-V relation is quadratic without electro-neutrality condition, and we believe that the analysis for the first order terms in [1] can be applied to third order terms in this work without the electro-neutrality assumption.

For the fourth order correction to zeroth order I-V relation under electro-neutrality condition, we have

Theorem 3.11. *Under electroneutrality condition, we have*

$$
\begin{aligned}
T_4 =& \frac{3(L-R)^4\left(L^5-R^5\right)}{4L^5R^5(\ln L-\ln R)}V + \frac{(L-R)^4}{2L^5R^5(\ln L-\ln R)^2}\left(\frac{\left(L^2-R^2\right)\left(L^3-R^3\right)}{3(\ln L-\ln R)}\right. \\
&\left.+\frac{7\left(L^5-R^5\right)}{2}\right)V^2 - \frac{(L-R)^4\left(L^5-R^5\right)}{4L^5R^5(\ln L-\ln R)^3}V^3 + \frac{(L-R)^5(L+R)}{2L^4R^4(\ln L-\ln R)^4} \\
&\times\left(\frac{(L+R)}{2} - \frac{L^3-R^3}{3LR(\ln L-\ln R)}\right)V^4, \\
I_4 =& \frac{(L-R)^4}{L^4R^4(\ln L-\ln R)^2}\left(\frac{(L-R)\left(L^3-R^3\right)Q_1(L,R)}{6L^2R^2}V + \frac{3Q_3(L,R)}{4LR}V^2\right. \\
&\left.+\frac{Q_2(L,R)}{\ln L-\ln R}V^3 - \frac{Q_3(L,R)}{4LR(\ln L-\ln R)^2}V^4 + \frac{(L-R)Q_4(L,R)}{2(\ln L-\ln R)^3}V^5\right),
\end{aligned}
\tag{3.20}
$$

where

$$
\begin{aligned}
Q_1(L,R) =& \frac{L^3-R^3}{3(\ln L-\ln R)} + \frac{97\left(L^3+R^3\right)}{2}, \\
Q_2(L,R) =& \frac{(L-R)\left(L^5-R^5\right)}{2L^2R^2(\ln L-\ln R)} + \frac{(L-R)^2\left(L^3-R^3\right)\left(L^2+LR+R^2\right)}{9L^2R^2(\ln L-\ln R)^2} \\
&+\frac{13(L-R)\left(L^5-R^5\right)}{12L^2R^2(\ln L-\ln R)} + \frac{7\left(L^5-R^5\right)}{4LR} - \frac{(L-R)^2(L+R)}{2(\ln L-\ln R)} \\
&+\frac{(L-R)(L+R)\left(L^3-R^3\right)}{4LR(\ln L-\ln R)} - \frac{17(L-R)^2}{12(\ln L-\ln R)}, \\
Q_3(L,R) =& \frac{(L-R)\left(L^5-R^5\right)}{\ln L-\ln R} - \frac{(L-R)^2}{\ln L-\ln R} + L^5 - R^5, \\
Q_4(L,R) =& \frac{(L+R)\left(L^3-R^3\right)}{2LR(\ln L-\ln R)} - \frac{\left(L^3-R^3\right)^2}{3L^2R^2(\ln L-\ln R)^2} + \frac{3(L+R)^2}{4}.
\end{aligned}
$$

The derivation of the expressions in (3.20) is provided in the Appendix Section 3.6.

Remark 3.12. *Under the electroneutrality condition, up to the fourth order in ε, the I-V relation function $\mathscr{I}(V)$ is quintic instead of being cubic. However, for $\varepsilon > 0$ small,*

$\mathscr{I} = I_0 + \varepsilon I_1 + \varepsilon^2 I_2 + \varepsilon^3 I_3$ is good enough to approximate the I-V relation, which can be seen from last section.

To end this section, we have the following interesting result about the I-V relations, which can be checked directly from systems (2.27) and (2.28).

Proposition 3.13. *For all $\varepsilon > 0$, $\mathscr{I}(L,R,\bar{V};\varepsilon) = -\mathscr{I}(R,L,-\bar{V};\varepsilon)$. A direct observation shows that, for $j = 0,1,2,3,4$,*

$$I_j(L,R,V;0) = -I_j(R,L,-V;0), \quad T_j(L,R,V;0) = -T_j(R,L,-V;0).$$

3.5 Numerical simulations

In this section, numerical simulations are performed to system system (2.27) with the boundary condition (2.28) to check the cubic-like feature of the I-V curve and investigate the effects of the boundary conditions, the permanent charge on the I-V relations.

To apply the BVP solver mentioned in section 2.3, we first rewrite (2.27) into a system of first order equations as

$$\begin{aligned} &\varepsilon \frac{d}{dx}\phi = u, \quad \frac{\varepsilon}{h(x)}\frac{d}{dx}(h(x)u) = -(\alpha c_1 - \beta c_2 + Q(x)), \\ &\varepsilon h(x)\frac{dc_1}{dx} + \alpha h(x) c_1 u = -\varepsilon J_1, \\ &\varepsilon h(x)\frac{dc_2}{dx} - \beta h(x) c_2 u = -\varepsilon J_2, \quad \frac{dJ_i}{dx} = 0, \end{aligned} \tag{3.21}$$

with the same boundary condition (2.28).

For a general iteration step, we take the initial guess from the approximate solution of the previous fixed point iteration. At the first iteration, for the case where $Q = 0$, we take advantage of the analysis from [1] and choose the initial guess $\left(\phi^0, u^0, c_1^0, c_2^0, J_1^0, J_2^0\right)$ as follows.

We take the zeroth order outer solution from [1] as our initial guess for both $Q(x)=0$ and $Q(x)\neq 0$

$$
\begin{aligned}
\phi_0^0(x)=&\frac{\ln|L-(L-R)x|-\ln R}{\ln L-\ln R}\nu_0, \quad u_0^0(x)=\frac{(L-R)\nu_0}{(\ln L-\ln R)((L-R)x-L)},\\
c_{10}^0(x)=&c_{20}^0(x)=L-(L-R)x, \quad J_{10}^0=(L-R)\left(1+\frac{\nu_0}{\ln L-\ln R}\right),\\
J_{20}^0=&(L-R)\left(1-\frac{\nu_0}{\ln L-\ln R}\right).
\end{aligned}
\tag{3.22}
$$

We take a uniform mesh partition as initial mesh and evaluate the functions ($\phi_0^0, u_0^0, c_{10}^0$, $c_{20}^0, J_{10}^0, J_{20}^0$) at these mesh points as initial guess for "bvp4c" at our first fixed point iteration. We use the mesh and solution from previous fixed point iteration as our initial mesh and initial guess for late iteration.

3.5.1 Numerical experiments

In this section, three numerical experiments are conducted to system (3.21) with boundary conditions (2.28) respectively, which are stated as follows:

- Experiment 1: for $Q(x)=0$, fixing L and R, letting ε vary, we check the cubic-like feature of the I-V relation, and meanwhile, compare the I-V curves from numerical simulation with the ones obtained from asymptotic expansions;
- Experiment 2: for $Q(x)=0$, fixing R and ε, letting L vary, we investigate the effect of the concentration boundary condition on the I-V curve;

- Experiment 3: for $Q = \begin{cases} 0 & 0 \le x < a, \\ Q_0 & a \le x \le b, \\ 0 & b < x \le 1, \end{cases}$ fixing L, R and ε, letting Q_0 vary, we investigate the effect of the permanent charge on the I-V relation curve and check the cubic-like feature of the I-V curve.

For experiment 1, the following properties are predicted from the analytical results and can be observed from the numerical simulations: For the first part, we have (see Figure 1)

(i) all I-V curves pass through the point $(0,0)$, and for V close to 0, the value of ε has less effect on the I-V curve;

(ii) for $V > 0$, the I-V curve is decreasing in ε, and for $V < 0$, the I-V curve is increasing in ε;

(iii) the I-V curve is more cubic-like for larger $\varepsilon > 0$, and for ε small enough, the I-V relation curve $\mathscr{I}(V)$ is close to the zeroth order approximation $\mathscr{I}_0 = 2(L-R)V/(\ln L - \ln R)$ under the electroneutrality condition.

For the second part, one has (see Figure 2)

(i) the smaller ε is, the better approximation $\mathscr{I}_t$ (the third order approximation to the I-V curve) will be;

(ii) the approximation is sensitive to V, for V close to 0, the value of ε has less effect on the approximation.

For experiment 2, the following properties can be observed from the numerical simulations (see Figure 3):

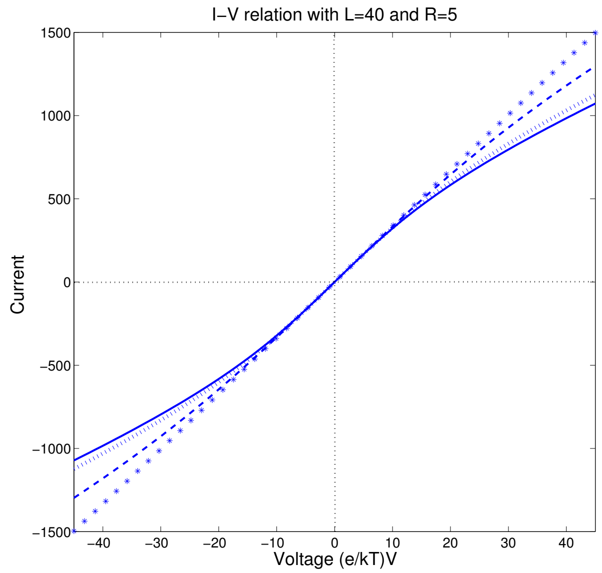

Figure 3.1: Numerical simulation of the I-V relation $\mathscr{I}(V)$ with $Q = 0$. $\mathscr{I}_1$(solid curve, $\varepsilon = 0.1$), $\mathscr{I}_2$(dotted curve, $\varepsilon = 0.08$), $\mathscr{I}_3$(dashed curve, $\varepsilon = 0.04$), and $\mathscr{I}_4$(stars, $\varepsilon = 0.008$)

(i) all curves pass the point $(0,0)$, for $V > 0$, the I-V curves are increasing in L, and for $V < 0$, they are decreasing in L;

(ii) for fixed ε and R, the I-V curve is more cubic-like for larger difference $L - R$.

For experiment 3, we investigate

(i) all curves pass through the point $(0,0)$, and the I-V curves still keep the cubic-like feature;

(ii) the I-V curves are decreasing in the permanent charge Q_0(see Figure 4).

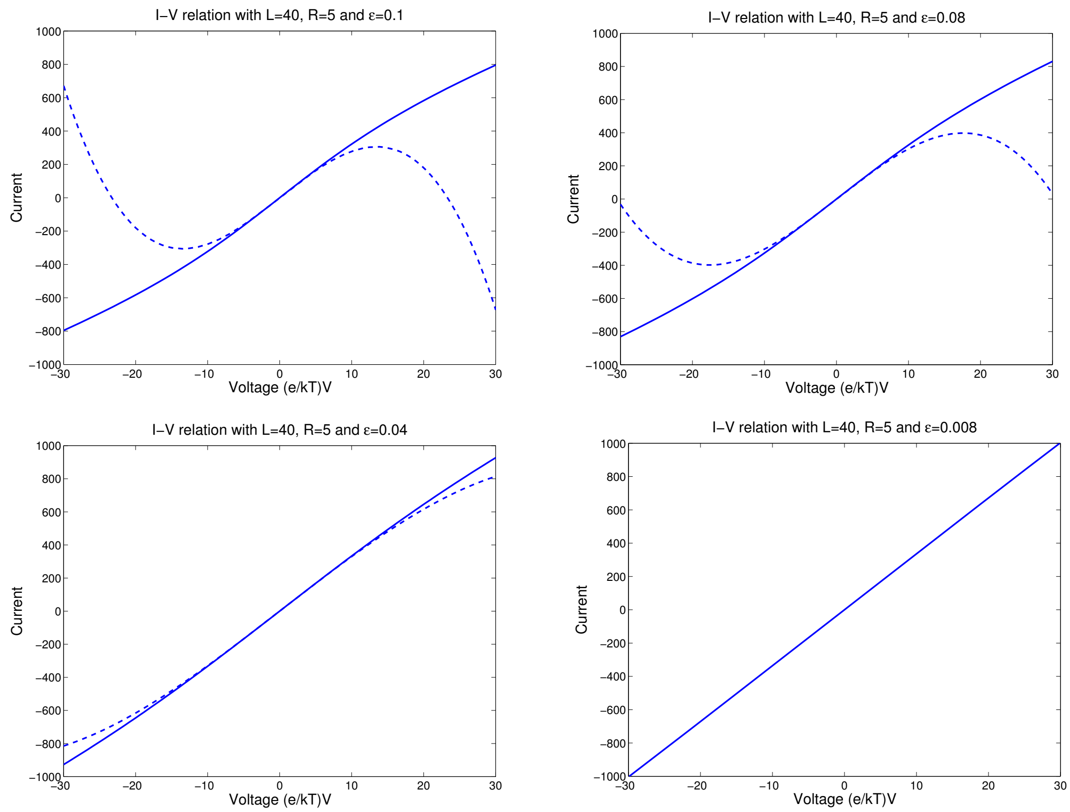

Figure 3.2: Plots of $\mathscr{I}(V)$ for $Q = 0$. $\mathscr{I}_t-$ third order approximation, and $\mathscr{I}_{ns}-$ numerical simulation.

3.6 Appendix: Fourth order matching under electroneutrality conditions

In this section, we study the fourth order asymptotic expansions in ε and the matching under electroneutrality conditions at the two ends of the ion channel.

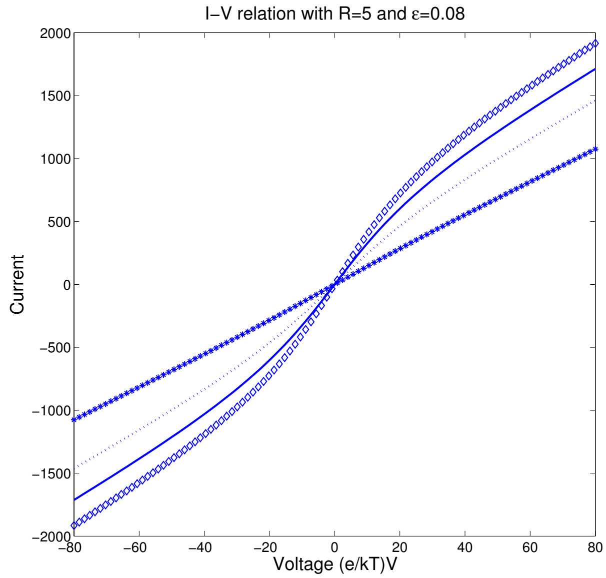

Figure 3.3: Numerical simulation of the I-V relation $\mathscr{I}(V)$ with $Q=0$. $\mathscr{I}_1$(stars, $L=10$), $\mathscr{I}_2$(dotted curve, $L=25$), $\mathscr{I}_3$(solid curve, $L=40$), and $\mathscr{I}_4$(diamonds, $L=55$).

3.6.1 Fourth order outer expansion

The fourth order outer system is

$$\begin{aligned}\ddot{\phi}_2 &= -c_{14}+c_{24},\\ \dot{c}_{14} &= -\left(c_{10}\dot{\phi}_4+c_{11}\dot{\phi}_3+c_{12}\dot{\phi}_2+c_{13}\dot{\phi}_1+c_{14}\dot{\phi}_0\right)-J_{14},\\ \dot{c}_{24} &= c_{20}\dot{\phi}_4+c_{21}\dot{\phi}_3+c_{22}\dot{\phi}_2+c_{23}\dot{\phi}_1+c_{24}\dot{\phi}_0-J_{24}.\end{aligned} \tag{3.23}$$

Under electroneutrality condition, that is, $L_1=L_2=L$ and $R_1=R_2=R$, adding the last two equations in (3.23), we get

$$c_{14}+c_{24} = a_4-T_4x+\frac{I_0^2(4T_0^2-I_0^2)}{2(a_0-T_0x)^5}-\frac{I_0^2(a_2-T_2x)}{(a_0-T_0x)^3}+\frac{I_0I_2}{(a_0-T_0x)^2},$$

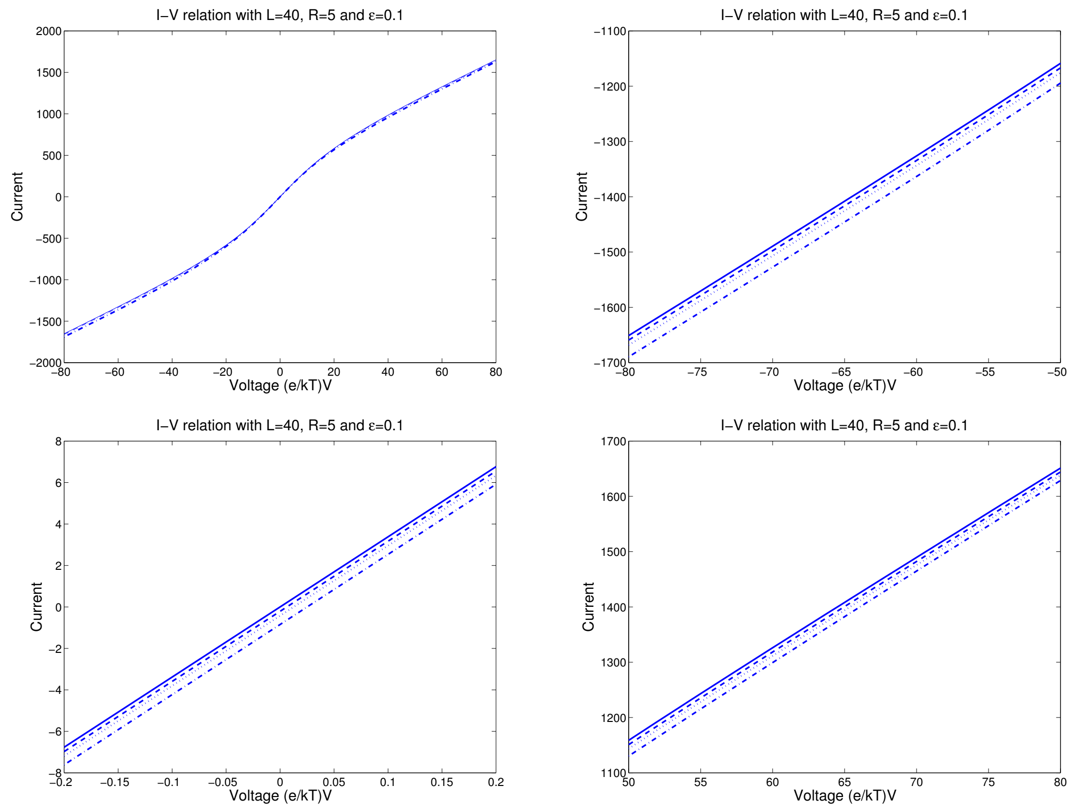

Figure 3.4: Plots of $I(V)$. The left graph in the first row is the simulation over the interval $[-80,80]$, for the other three graphs, we focus on different subintervals. $\mathscr{I}_0$(solid curve, Q=0), $\mathscr{I}_1$(dashed curve, Q=0.05), $\mathscr{I}_2$(dotted curve, Q=0.1) and $\mathscr{I}_3$(dash point, Q=0.2)

where a_4 is some constant that will be determined through matching. Subtracting the last two equations in (3.23) results in

$$\begin{aligned}\dot{\phi}_4 = &-\frac{I_4}{a_0 - T_0 x} + \frac{1}{a_0 - T_0 x}\dddot{\phi}_2 - \left(\frac{a_2 - T_2 x}{a_0 - T_0 x} + \frac{I_0^2}{2(a_0 - T_0 x)^3}\right)\dot{\phi}_2 \\ &- \left(\frac{a_4 - T_4 x}{a_0 - T_0 x} + \frac{I_0^2\left(4T_0^2 - I_0^2\right)}{2(a_0 - T_0 x)^6} - \frac{I_0^2(a_2 - T_2 x)}{(a_0 - T_0 x)^4} + \frac{I_0 I_2}{(a_0 - T_0 x)^3}\right)\dot{\phi}_0.\end{aligned}$$

Recall that

$$
\begin{aligned}
\dot{\phi}_0 =& -\frac{I_0}{a_0 - T_0 x}, \quad \dot{\phi}_2 = \frac{I_0(I_0^2 - 4T_0^2)}{2(a_0 - T_0 x)^4} + \frac{I_0(a_2 - T_2 x)}{(a_0 - T_0 x)^2} - \frac{I_2}{a_0 - T_0 x}, \\
\ddot{\phi}_2 =& \frac{2I_0 T_0\left(I_0^2 - 4T_0^2\right)}{(a_0 - T_0 x)^5} + \frac{2I_0 T_0(a_2 - T_2 x)}{(a_0 - T_0 x)^3} - \frac{I_0 T_2 + I_2 T_0}{(a_0 - T_0 x)^2}, \\
\dddot{\phi}_2 =& \frac{10 I_0 T_0^2 (I_0^2 - 4T_0^2)}{(a_0 - T_0 x)^6} + \frac{6 I_0 T_0^2 (a_2 - T_2 x)}{(a_0 - T_0 x)^4} - \frac{2T_0(2I_0 T_2 + I_2 T_0)}{(a_0 - T_0 x)^3}.
\end{aligned}
\tag{3.24}
$$

Therefore, we have

$$
\begin{aligned}
\dot{\phi}_4 =& \frac{I_0(I_0^2 - 4T_0^2)(40T_0^2 - 3I_0^2)}{4(a_0 - T_0 x)^7} + \frac{2a_2 I_0 (4T_0^2 - I_0^2)}{(a_0 - T_0 x)^5} + \frac{3I_0^2 I_2 - 8I_0 T_0 T_2 - 4T_0^2 I_2}{2(a_0 - T_0 x)^4} \\
&- \frac{a_2^2 I_0}{(a_0 - T_0 x)^3} + \frac{I_2 a_2 + a_4 I_0}{(a_0 - T_0 x)^2} - \frac{I_4}{a_0 - T_0 x} - \frac{2I_0 T_2 (4T_0^2 - I_0^2) x}{(a_0 - T_0 x)^5} \\
&- \frac{(I_2 T_2 + I_0 T_4) x}{(a_0 - T_0 x)^2} + \frac{2a_2 I_0 T_2 x}{(a_0 - T_0 x)^3} - \frac{I_0 T_2^2 x^2}{(a_0 - T_0 x)^3}.
\end{aligned}
$$

By careful computations, we have, with b_4 a constant to be determined through matching,

$$
\begin{aligned}
\phi_4(x) =& b_4 + \frac{I_0(I_0^2 - 4T_0^2)(40T_0^2 - 3I_0^2)}{24T_0(a_0 - T_0 x)^6} + \frac{I_0(a_2 T_0 - a_0 T_2)(4T_0^2 - I_0^2)}{2T_0^2(a_0 - T_0 x)^4} \\
&+ \frac{I_0(I_0^2 - 4T_0^2)(T_0 - 4T_2) + 2I_0 T_0 (I_0 I_2 - 4T_0 T_2)}{6T_0^2 (a_0 - T_0 x)^3} - \frac{I_0(a_2 T_0 - a_0 T_2)^2}{2T_0^3 (a_0 - T_0 x)^2} \\
&+ \frac{T_0^2 (I_2 a_2 + a_4 I_0) - a_0 T_0 (I_2 T_2 - I_0 T_4) + 2I_0 T_2 (a_0 T_2 - a_2 T_0)}{T_0^3 (a_0 - T_0 x)} \\
&+ \frac{T_0(I_4 T_0 - I_0 T_4) + T_2(I_0 T_2 - T_0 I_2)}{T_0^3} \ln|a_0 - T_0 x|.
\end{aligned}
\tag{3.25}
$$

Together with the first equation in (3.23) and the theird equation in (3.24), we obtain the solution to the fourth order outer system (3.23)

$$\begin{aligned}
c_{14}(x) =& \frac{a_4 - T_4 x}{2} + \frac{I_0\left(4T_0^2 - I_0^2\right)(I_0 + 4T_0)}{4(a_0 - T_0 x)^5} - \frac{I_0(I_0 + 2T_0)(a_2 - T_2 x)}{2(a_0 - T_0 x)^3} \\
&+ \frac{I_0(I_2 + T_2) + I_2 T_0}{2(a_0 - T_0 x)^2}, \\
c_{24}(x) =& \frac{a_4 - T_4 x}{2} + \frac{I_0(I_0^2 - 4T_0^2)(4T_0 - I_0)}{4(a_0 - T_0 x)^5} + \frac{I_0(2T_0 - I_0)(a_2 - T_2 x)}{2(a_0 - T_0 x)^3} \\
&+ \frac{I_0(I_2 - T_2) - I_2 T_0}{2(a_0 - T_0 x)^2}, \\
\phi_4(x) =& b_4 + \frac{I_0(I_0^2 - 4T_0^2)(40T_0^2 - 3I_0^2)}{24T_0(a_0 - T_0 x)^6} + \frac{I_0(a_2 T_0 - a_0 T_2)(4T_0^2 - I_0^2)}{2T_0^2(a_0 - T_0 x)^4} \\
&+ \frac{I_0(I_0^2 - 4T_0^2)(T_0 - 4T_2) + 2I_0 T_0(I_0 I_2 - 4T_0 T_2)}{6T_0^2(a_0 - T_0 x)^3} - \frac{I_0(a_2 T_0 - a_0 T_2)^2}{2T_0^3(a_0 - T_0 x)^2} \\
&+ \frac{T_0^2(I_2 a_2 + a_4 I_0) - a_0 T_0(I_2 T_2 - I_0 T_4) + 2I_0 T_2(a_0 T_2 - a_2 T_0)}{T_0^3(a_0 - T_0 x)} \\
&+ \frac{T_0(I_4 T_0 - I_0 T_4) + T_2(I_0 T_2 - T_0 I_2)}{T_0^3} \ln|a_0 - T_0 x|.
\end{aligned} \tag{3.26}$$

3.6.2 Fourth order inner expansion

The fourth order inner system at $x = 0$ is

$$\begin{aligned}
\Phi_4' =& U_4, \quad U_4' = -(C_{14} - C_{24}), \\
C_{14}' =& -(C_{10}U_4 + C_{11}U_3 + C_{12}U_2 + C_{13}U_1 + C_{14}U_0) - J_{13}, \\
C_{24}' =& (C_{20}U_4 + C_{21}U_3 + C_{22}U_2 + C_{23}U_1 + C_{24}U_0) - J_{23}.
\end{aligned} \tag{3.27}$$

Proposition 3.14. *System* (3.27) *has the following integrals:*

$$\begin{aligned}
G_1 =& C_{14}e^{\Phi_0} + C_{10}e^{\Phi_0}\Phi_4 + J_{13}F_1 + F_{141} + F_{142} + F_{143}, \\
G_2 =& C_{24}e^{-\Phi_0} - C_{20}e^{-\Phi_0}\Phi_4 + J_{23}F_2 - F_{241} - F_{242} - F_{243},
\end{aligned}$$

$$G_3 = U_0U_4 + U_1U_3 + U_2^2 - C_{14} - C_{24} - T_3\xi,$$

where F_1 and F_2 are given in Proposition 3.3, and

$$\begin{aligned}
F_{141}(\xi) &= \int_0^\xi C_{11}(s)U_3(s)e^{\Phi_0(s)}ds, \quad F_{142}(\xi) = \int_0^\xi C_{12}(s)U_2(s)e^{\Phi_0(s)}ds,\\
F_{143}(\xi) &= \int_0^\xi C_{13}(s)U_1(s)e^{\Phi_0(s)}ds, \quad F_{241}(\xi) = \int_0^\xi C_{21}(s)U_3(s)e^{-\Phi_0(s)}ds,\\
F_{242}(\xi) &= \int_0^\xi C_{22}(s)U_2(s)e^{-\Phi_0(s)}ds, \quad F_{243}(\xi) = \int_0^\xi C_{23}(s)U_1(s)e^{-\Phi_0(s)}ds.
\end{aligned}$$

Proof. The proof is straightforward. □

Under electroneutrality conditions, by careful computations, one has

$$\begin{aligned}
F_{141}(\xi) =& \frac{T_0}{2}\left[\frac{I_0T_0^2}{4(2L)^3}\xi^4 + \frac{1}{2L}\left(\frac{I_2}{2} + \frac{I_0T_0^2}{(2L)^3}\right)\xi^2 + \frac{9I_0T_0^2}{4(2L)^5} - \frac{I_0T_0^2}{4(2L)^3}\left(\frac{1}{\sqrt{2L}}\xi^3 + \frac{2}{L}\xi^2\right.\right.\\
&\left.\left. + \frac{9}{(2L)^{\frac{3}{2}}}\xi + \frac{9}{(2L)^2}\right)e^{-\sqrt{2L}\xi}\right]e^{\bar{V}},\\
F_{142}(\xi) =& \frac{I_0^2T_0^2}{2(2L)^4}\left[-\frac{1}{2}\xi^2 + \frac{1}{4L} - \frac{1}{\sqrt{2L}}e^{-\sqrt{2L}\xi}\left(\xi + \frac{1}{2\sqrt{2L}}e^{-\sqrt{2L}\xi}\right)\right]e^{\bar{V}},\\
F_{143}(\xi) =& -\frac{I_0}{2L}\left[\left(\frac{I_0T_0(I_0+2T_0)}{4(2L)^3} - \frac{T_2}{4}\right)\xi^2 - \frac{I_0^2T_0}{2(2L)^{\frac{7}{2}}}\xi + \frac{I_0T_0(I_0-T_0)}{4(2L)^4} + \frac{I_0T_0}{4(2L)^{\frac{5}{2}}}\right.\\
&\left.\times\left(\frac{T_0}{2(2L)^{\frac{1}{2}}}\xi^2 + \frac{I_0+T_0}{2L}\xi + \frac{T_0-I_0}{(2L)^{\frac{3}{2}}}\right)e^{-\sqrt{2L}\xi}\right]e^{\bar{V}},\\
F_{241}(\xi) =& \frac{T_0}{2}\left[\frac{I_0T_0^2}{4(2L)^3}\xi^4 + \frac{1}{2L}\left(\frac{I_2}{2} + \frac{I_0T_0^2}{(2L)^3}\right)\xi^2 + \frac{9I_0T_0^2}{4(2L)^5} - \frac{I_0T_0^2}{4(2L)^3}\left(\frac{1}{\sqrt{2L}}\xi^3 + \frac{2}{L}\xi^2\right.\right.\\
&\left.\left. + \frac{9}{(2L)^{\frac{3}{2}}}\xi + \frac{9}{(2L)^2}\right)e^{-\sqrt{2L}\xi}\right]e^{-\bar{V}},\\
F_{242}(\xi) =& \frac{I_0^2T_0^2}{2(2L)^4}\left[\frac{1}{2}\xi^2 - \frac{1}{4L} + \frac{1}{\sqrt{2L}}e^{-\sqrt{2L}\xi}\left(\xi + \frac{1}{2\sqrt{2L}}e^{-\sqrt{2L}\xi}\right)\right]e^{-\bar{V}},\\
F_{243}(\xi) =& -\frac{I_0}{2L}\left[\left(\frac{I_0T_0(I_0-2T_0)}{4(2L)^3} - \frac{T_2}{4}\right)\xi^2 - \frac{I_0^2T_0}{2(2L)^{\frac{7}{2}}}\xi + \frac{I_0T_0(I_0+T_0)}{(2L)^4} + \frac{I_0T_0}{4(2L)^{\frac{5}{2}}}\right.
\end{aligned}$$

$$\times\left(-\frac{T_0}{2(2L)^{\frac{1}{2}}}\xi^2-\frac{T_0}{L}\xi-\frac{2(I_0+T_0)}{(2L)^{\frac{3}{2}}}\right)e^{-\sqrt{2L}\xi}\Bigg]e^{-\bar{V}}.$$

To solve for (Φ_4, C_{14}, C_{24}) with $\Phi_4(0)=C_{14}(0)=C_{24}(0)=0$, we note that, from the integrals in Proposition 3.14

$$\begin{aligned}
C_{14}(\xi)=&\frac{I_0T_0}{2(2L)^4}\left[\frac{\sqrt{2L}T_0^2}{4}\xi^3+\frac{T_0(4T_0+I_0)}{4}\xi^2+\frac{T_0(6I_0+11T_0)}{4\sqrt{2L}}\xi+\frac{9T_0^2+2I_0T_0-2I_0^2}{8L}\right.\\
&\left.+\frac{I_0T_0}{4L}e^{-\sqrt{2L}\xi}\right]e^{-\sqrt{2L}\xi}+\frac{1}{8L}\left(\frac{I_0T_0(I_0^2+3I_0T_0-2T_0^2)}{(2L)^3}-I_2T_0-I_0T_2\right)\xi^2\\
&-\frac{I_0^3T_0}{2(2L)^{\frac{9}{2}}}\xi-\frac{I_0T_0^3}{8(2L)^3}\xi^4+\frac{I_0T_0(2I_0^2-4I_0T_0-9T_0^2)}{8(2L)^5}-J_{13}\xi-L\Phi_4,\\
C_{24}(\xi)=&\frac{I_0T_0}{2(2L)^4}\left[-\frac{\sqrt{2L}T_0^2}{4}\xi^3+\frac{T_0(I_0-4T_0)}{4}\xi^2+\frac{T_0(8I_0-9T_0)}{4\sqrt{2L}}\xi+\frac{4I_0^2+4I_0T_0-9T_0^2}{8L}\right.\\
&\left.+\frac{I_0T_0}{4L}e^{-\sqrt{2L}}\right]e^{-\sqrt{2L}\xi}+\frac{1}{8L}\left(\frac{I_0T_0(3I_0T_0+2T_0^2-I_0^2)}{(2L)^3}+I_2T_0+I_0T_2\right)\xi^2\\
&+\frac{I_0^3T_0}{2(2L)^{\frac{9}{2}}}\xi+\frac{I_0T_0^3}{8(2L)^3}\xi^4+\frac{I_0T_0(2I_0^2-4I_0T_0-9T_0^2)}{8(2L)^5}-J_{23}\xi+L\Phi_4.
\end{aligned}$$

Therefore,

$$\begin{aligned}
\Phi_4''=&\frac{I_0T_0}{2(2L)^4}\left[\frac{2I_0^2-6T_0^2}{2L}-\frac{6T_0^2}{\sqrt{2L}}\xi-\frac{7T_0^2}{2}\xi^2-\frac{\sqrt{2L}T_0^2}{2}\xi^3\right]e^{-\sqrt{2L}\xi}+\frac{I_0T_0^3}{4(2L)^3}\xi^4\\
&+\left(\frac{I_0T_0}{2(2L)^4}(2T_0^2-I_0^2)+\frac{I_0T_2+I_2T_0}{4L}\right)\xi^2+\frac{I_0^3T_0}{(2L)^{\frac{9}{2}}}\xi+I_3\xi+\frac{I_0T_0\left(3T_0^2-I_0^2\right)}{(2L)^5}\\
&+2L\Phi_4.
\end{aligned}$$

The solution with $\Phi_4(0)=0$ is

$$\begin{aligned}
\Phi_4=&\frac{I_0T_0}{4(2L)^{\frac{9}{2}}}\left[\frac{\sqrt{2L}T_0^2}{8}\xi^4+\frac{17T_0^2}{12}\xi^3+\frac{41T_0^2}{8\sqrt{2L}}\xi^2+\frac{89T_0^2-16I_0^2}{16L}\xi+\frac{38T_0^2-6I_0^2}{(2L)^{\frac{3}{2}}}\right.\\
&\left.+4\left(\frac{T_2}{T_0}+\frac{I_2}{I_0}\right)(2L)^{\frac{3}{2}}-\gamma_1\right]e^{-\sqrt{2L}\xi}-\left(\frac{I_0T_0}{(2L)^5}\left(4T_0^2-\frac{I_0^2}{2}\right)+\frac{I_0T_2+I_2T_0}{2(2L)^2}\right)\xi^2
\end{aligned}$$

$$
-\frac{I_0T_0^3}{4(2L)^4}\xi^4-\left(\frac{I_0^3T_0}{(2L)^{\frac{11}{2}}}+\frac{I_3}{2L}\right)\xi-\frac{I_0T_0(19T_0^2-3I_0^2)}{2(2L)^6}-\frac{I_0T_2+I_2T_0}{(2L)^3}+\gamma_1e^{\sqrt{2L}\xi}.
$$

The matching will force $\gamma_1=0$. Thus, the third order inner solution is, for $\xi\geq 0$,

$$
\begin{aligned}
\Phi_4(\xi)=&\frac{I_0T_0}{4(2L)^{\frac{9}{2}}}\left[\frac{\sqrt{2L}T_0^2}{8}\xi^4+\frac{17T_0^2}{12}\xi^3+\frac{41T_0^2}{8\sqrt{2L}}\xi^2+\frac{89T_0^2-16I_0^2}{16L}\xi\right.\\
&\left.+\frac{38T_0^2-6I_0^2}{(2L)^{\frac{3}{2}}}+4\left(\frac{T_2}{T_0}+\frac{I_2}{I_0}\right)(2L)^{\frac{3}{2}}\right]e^{-\sqrt{2L}\xi}-\frac{I_0T_0^3}{4(2L)^4}\xi^4\\
&-\left(\frac{I_0T_0}{(2L)^5}\left(4T_0^2-\frac{I_0^2}{2}\right)+\frac{I_0T_2+I_2T_0}{2(2L)^2}\right)\xi^2-\left(\frac{I_0^3T_0}{(2L)^{\frac{11}{2}}}+\frac{I_3}{2L}\right)\xi\\
&-\frac{I_0T_0(19T_0^2-3I_0^2)}{2(2L)^6}-\frac{I_0T_2+I_2T_0}{(2L)^3},\\
C_{14}(\xi)=&\left[-\frac{I_0T_0^3}{64(2L)^3}\xi^4-\frac{5I_0T_0^3}{96(2L)^{\frac{7}{2}}}\xi^3+\frac{I_0T_0^2(15T_0+8I_0)}{64(2L)^4}\xi^2\right.\\
&+\frac{I_0T_0(7T_0^2+64I_0T_0+16I_0^2)}{64(2L)^{\frac{9}{2}}}\xi+\frac{I_0T_0}{2(2L)^5}\left(\frac{I_0^2}{2}+I_0T_0-\frac{13T_0^2}{2}\right)\\
&\left.-\frac{I_0T_2+I_2T_0}{2(2L)^2}+\frac{I_0^2T_0^2}{4(2L)^5}e^{-\sqrt{2L}\xi}\right]e^{-\sqrt{2L}\xi}+\frac{3I_0T_0^2(I_0+2T_0)}{4(2L)^4}\xi^2\\
&-\frac{T_3}{2}\xi+\frac{I_0T_0(13T_0^2-I_0^2-3I_0T_0)}{4(2L)^5}+\frac{I_0T_2+I_2T_0}{8L^2},\\
C_{24}(\xi)=&\left[\frac{I_0T_0^3}{64(2L)^3}\xi^4+\frac{5I_0T_0^3}{96(2L)^{\frac{7}{2}}}\xi^3+\frac{I_0T_0^2(8I_0-15T_0)}{64(2L)^4}\xi^2\right.\\
&+\frac{I_0T_0(64I_0T_0-7T_0^2-16I_0^2)}{64(2L)^{\frac{9}{2}}}\xi+\frac{I_0T_0}{2(2L)^5}\left(I_0T_0-\frac{I_0^2}{2}+\frac{13T_0^2}{2}\right)\\
&\left.+\frac{I_0T_2+I_2T_0}{2(2L)^2}+\frac{I_0^2T_0^2}{4(2L)^5}e^{-\sqrt{2L}\xi}\right]e^{-\sqrt{2L}\xi}+\frac{3I_0T_0^2(I_0-2T_0)}{4(2L)^4}\xi^2\\
&-\frac{T_3}{2}\xi+\frac{I_0T_0(I_0^2-3I_0T_0-13T_0^2)}{4(2L)^5}-\frac{I_0T_2+I_2T_0}{8L^2}.
\end{aligned}
\tag{3.28}
$$

Similarly, at $x = 1$, the fourth order inner solution is, for $\xi \leq 0$,

$$
\begin{aligned}
\Psi_4(\xi) =& \frac{I_0 T_0}{4(2R)^{\frac{9}{2}}} \left[\frac{\sqrt{2R} T_0^2}{8} \xi^4 + \frac{17 T_0^2}{12} \xi^3 + \frac{41 T_0^2}{8\sqrt{2R}} \xi^2 + \frac{89 T_0^2 - 16 I_0^2}{16R} \xi \right. \\
& \left. + \frac{38 T_0^2 - 6 I_0^2}{(2R)^{\frac{3}{2}}} + 4\left(\frac{T_2}{T_0} + \frac{I_2}{I_0}\right)(2R)^{\frac{3}{2}} \right] e^{-\sqrt{2R}\xi} - \frac{I_0 T_0^3}{4(2R)^4} \xi^4 \\
& - \left(\frac{I_0 T_0}{(2R)^5} \left(4T_0^2 - \frac{I_0^2}{2}\right) + \frac{I_0 T_2 + I_2 T_0}{2(2R)^2} \right) \xi^2 - \left(\frac{I_0^3 T_0}{(2R)^{\frac{11}{2}}} + \frac{I_3}{2R} \right) \xi \\
& - \frac{I_0 T_0 (19 T_0^2 - 3 I_0^2)}{2(2R)^6} - \frac{I_0 T_2 + I_2 T_0}{(2R)^3}, \\
D_{14}(\xi) =& \left[-\frac{I_0 T_0^3}{64(2R)^3} \xi^4 - \frac{5 I_0 T_0^3}{96(2R)^{\frac{7}{2}}} \xi^3 + \frac{I_0 T_0^2 (15 T_0 + 8 I_0)}{64(2R)^4} \xi^2 \right. \\
& + \frac{I_0 T_0 (7 T_0^2 + 64 I_0 T_0 + 16 I_0^2)}{64(2R)^{\frac{9}{2}}} \xi + \frac{I_0 T_0}{2(2R)^5} \left(\frac{I_0^2}{2} + I_0 T_0 - \frac{13 T_0^2}{2} \right) \\
& \left. - \frac{I_0 T_2 + I_2 T_0}{2(2R)^2} + \frac{I_0^2 T_0^2}{4(2R)^5} e^{-\sqrt{2R}\xi} \right] e^{-\sqrt{2R}\xi} + \frac{3 I_0 T_0^2 (I_0 + 2T_0)}{4(2R)^4} \xi^2 \\
& - \frac{T_3}{2} \xi + \frac{I_0 T_0 (13 T_0^2 - I_0^2 - 3 I_0 T_0)}{4(2R)^5} + \frac{I_0 T_2 + I_2 T_0}{8R^2}, \\
D_{24}(\xi) =& \left[\frac{I_0 T_0^3}{64(2R)^3} \xi^4 + \frac{5 I_0 T_0^3}{96(2R)^{\frac{7}{2}}} \xi^3 + \frac{I_0 T_0^2 (8 I_0 - 15 T_0)}{64(2R)^4} \xi^2 \right. \\
& + \frac{I_0 T_0 (64 I_0 T_0 - 7 T_0^2 - 16 I_0^2)}{64(2R)^{\frac{9}{2}}} \xi + \frac{I_0 T_0}{2(2R)^5} \left(I_0 T_0 - \frac{I_0^2}{2} + \frac{13 T_0^2}{2} \right) \\
& \left. + \frac{I_0 T_2 + I_2 T_0}{2(2R)^2} + \frac{I_0^2 T_0^2}{4(2R)^5} e^{-\sqrt{2R}\xi} \right] e^{-\sqrt{2R}\xi} + \frac{3 I_0 T_0^2 (I_0 - 2T_0)}{4(2R)^4} \xi^2 \\
& - \frac{T_3}{2} \xi + \frac{I_0 T_0 (I_0^2 - 3 I_0 T_0 - 13 T_0^2)}{4(2R)^5} - \frac{I_0 T_2 + I_2 T_0}{8R^2}.
\end{aligned}
\tag{3.29}
$$

3.6.3 Fourth order matching

At $x = 0$, for the outer expansion, we have, in terns of the variable ξ, the outer expansion at $x = 0$ is

$$
E_\xi^4 E_x^4(\phi) = b_0 + \frac{I_0}{T_0} \ln a_0 - \varepsilon \frac{I_0}{a_0} \xi + \varepsilon^2 \left(b_2 - \frac{I_0 (4 T_0^2 - I_0^2)}{6 T_0 a_0^3} + \frac{I_0 (a_2 T_0 - a_0 T_2)}{T_0^2 a_0} \right.
$$

$$
\begin{aligned}
&+\frac{T_0I_2-I_0T_2}{T_0^2}\ln a_0-\frac{I_0T_0}{2a_0^2}\xi^2\Big)+\varepsilon^3\left(\frac{I_0(a_3T_0-a_0T_3)}{a_0T_0^2}+\frac{I_3T_0-I_0T_3}{T_0^2}\ln a_0\right.\\
&+b_3+\left(\frac{I_0(I_0^2-4T_0^2)}{2a_0^4}+\frac{a_2I_0-a_0I_2}{a_0^2}\right)\xi-\frac{I_0T_0^2}{3a_0^3}\xi^3\Big)\\
&+\varepsilon^4\left(\frac{a_3I_0-a_0I_3}{a_0^2}\xi+\left(\frac{a_2I_0T_0}{a_0^3}-\frac{I_0T_2+I_2T_0}{2a_0^2}+\frac{I_0T_0\left(I_0^2-4T_0^2\right)}{a_0^5}\right)\xi^2\right.\\
&\left.-\frac{I_0T_0^3}{4a_0^4}\xi^4+\phi_4(0)\right),
\end{aligned}
$$

$$
\begin{aligned}
E_\xi^4E_x^4(c_1)=&\frac{a_0}{2}-\varepsilon\frac{T_0}{2}\xi+\varepsilon^2\left(\frac{a_2}{2}+\frac{I_0^2+2I_0T_0}{4a_0}\right)+\varepsilon^3\left(\frac{a_3}{2}+\left(\frac{I_0T_0(I_0+2T_0)}{2a_0^3}-\frac{T_2}{2}\right)\xi\right)\\
&+\varepsilon^4\left(\frac{a_4}{2}+\frac{I_0\left(4T_0^2-I_0^2\right)(I_0+4T_0)}{4a_0^5}-\frac{a_2I_0(I_0+2T_0)}{2a_0^3}+\frac{I_0(I_2+T_2)+I_2T_0}{2a_0^2}\right.\\
&\left.-\frac{T_3}{2}\xi+\frac{3I_0T_0^2(I_0+2T_0)}{2a_0^4}\xi^2\right),\\
E_\xi^4E_x^4(c_2)=&\frac{a_0}{2}-\varepsilon\frac{T_0}{2}\xi+\varepsilon^2\left(\frac{a_2}{2}+\frac{I_0^2-2I_0T_0}{4a_0}\right)+\varepsilon^3\left(\frac{a_3}{2}+\left(\frac{I_0T_0(I_0-2T_0)}{2a_0^3}-\frac{T_2}{2}\right)\xi\right)\\
&+\varepsilon^4\left(\frac{a_4}{2}+\frac{I_0(I_0^2-4T_0^2)(4T_0-I_0)}{4a_0^5}+\frac{a_2I_0(2T_0-I_0)}{2a_0^3}+\frac{I_0(I_2-T_2)-I_2T_0}{2a_0^2}\right.\\
&\left.-\frac{T_3}{2}\xi+\frac{3I_0T_0^2(I_0-2T_0)}{2a_0^4}\xi^2\right),
\end{aligned}
$$

where

$$
\begin{aligned}
\phi_4(0)=&b_4+\frac{T_0\left(I_4T_0-I_2T_2-I_0T_4\right)+I_0T_2^2}{T_0^3}\ln a_0+\frac{I_0\left(52I_0^2T_0^2+160T_0^4-3I_0^4\right)}{24a_0^6T_0}\\
&+\frac{I_0\left(a_2T_0-a_0T_2\right)\left(4T_0^2-I_0^2\right)}{2T_0^2a_0^4}+\frac{I_0^2\left(3I_2T_0-4I_0T_2\right)}{6T_0^2a_0^3}+\frac{2\left(2I_0T_2-I_2T_0\right)}{3a_0^3}\\
&+\frac{a_2I_2+a_4I_0}{a_0T_0}-\frac{T_2\left(a_0I_2+a_2I_0\right)}{a_0T_0^2}+\frac{I_0\left(a_2T_2+a_0T_4\right)}{a_0T_0^2}-\frac{I_0\left(a_0T_2-a_2T_0\right)^2}{2T_0^3a_0^2}\\
&+\frac{2I_0T_2^2}{T_0^3}.
\end{aligned}
$$

Similarly, in terms of $\xi = (x-1)/\varepsilon$, the outer expansion at $x = 1$ is

$$
\begin{aligned}
E_\xi^4 E_x^4(\phi) =& b_0 + \frac{I_0}{T_0}\ln|a_0 - T_0| + \frac{I_0(2a_0 - 3T_0)}{2(a_0-T_0)^2} + \frac{I_0T_0^2}{3(a_0-T_0)^3} - \varepsilon\left(\frac{a_0I_0}{(a_0-T_0)^2}\right.\\
&\left.-\frac{I_0T_0^2}{(a_0-T_0)^3}\right)\xi\\
&+\varepsilon^2\left(b_2 - \frac{I_0(4T_0^2 - I_0^2)}{6T_0(a_0-T_0)^3} + \frac{I_0(a_2T_0 - a_0T_2)}{T_0^2(a_0-T_0)} + \frac{I_2T_0 - I_0T_2}{T_0^2}\ln|a_0-T_0|\right.\\
&\left.+\frac{I_0T_0(3T_0-a_0)}{2(a_0-T_0)^3}\xi^2\right)\\
&+\varepsilon^3\left(b_3 + \frac{I_3T_0 - I_0T_3}{T_0^2}\ln|a_0-T_0| + \frac{a_0I_3 - a_3I_0 + I_0T_3 - I_3T_0}{(a_0-T_0)^2}\right.\\
&+\frac{I_0(a_3T_0 - a_0T_3)}{T_0^2(a_0-T_0)} + \left(\frac{I_0(I_0^2 - 4T_0^2)}{2(a_0-T_0)^4} + \frac{(a_2-T_2)I_0 - (a_0-T_0)I_2}{(a_0-T_0)^2}\right)\xi\\
&\left.-\frac{I_0T_0^2}{3(a_0-T_0)^3}\xi^3\right)\\
&+\varepsilon^4\left(\left(\frac{I_0(a_3-T_3)}{(a_0-T_0)^2} - \frac{I_3}{a_0-T_0}\right)\xi + \left(\frac{I_0T_0\left(I_0^2 - 4T_0^2\right)}{(a_0-T_0)^5} + \frac{a_2I_0T_0}{(a_0-T_0)^3}\right.\right.\\
&\left.\left.-\frac{I_0T_2 + I_2T_0}{2(a_0-T_0)^2}\right)\xi^2 - \frac{I_0T_0^3}{4(a_0-T_0)^4}\xi^4 + \phi_4(1)\right),\\
E_\xi^4 E_x^4(c_1) =& \frac{a_0-T_0}{2} - \varepsilon\frac{T_0}{2}\xi + \varepsilon^2\left(\frac{a_2-T_2}{2} + \frac{I_0^2 + 2I_0T_0}{4(a_0-T_0)^2}\right)\\
&+\varepsilon^3\left(\frac{a_3-T_3}{2} + \left(\frac{I_0T_0(I_0+2T_0)}{2(a_0-T_0)^3} - \frac{T_2}{2}\right)\xi\right)\\
&+\varepsilon^4\left(\frac{a_4-T_4}{2} + \frac{I_0\left(4T_0^2 - I_0^2\right)(I_0+4T_0)}{4(a_0-T_0)^5} - \frac{I_0(I_0+2T_0)(a_2-T_2)}{2(a_0-T_0)^3}\right.\\
&\left.+\frac{I_0(I_2+T_2)}{2(a_0-T_0)^2} + \frac{I_2T_0}{2(a_0-T_0)^2} - \frac{T_3}{2}\xi + \frac{3I_0T_0^2(I_0+2T_0)}{2(a_0-T_0)^4}\xi^2\right),\\
E_\xi^4 E_x^4(c_2) =& \frac{a_0-T_0}{2} - \varepsilon\frac{T_0}{2}\xi + \varepsilon^2\left(\frac{a_2-T_2}{2} + \frac{I_0^2 - 2I_0T_0}{4(a_0-T_0)^2}\right)\\
&+\varepsilon^3\left(\frac{a_3-T_3}{2} + \left(\frac{I_0T_0(I_0-2T_0)}{2(a_0-T_0)^3} - \frac{T_2}{2}\right)\xi\right)\\
&+\varepsilon^4\left(\frac{a_4-T_4}{2} + \frac{I_0(I_0^2 - 4T_0^2)(4T_0 - I_0)}{4(a_0-T_0)^5} + \frac{I_0(2T_0-I_0)(a_2-T_2)}{2(a_0-T_0)^3}\right.\\
&\left.+\frac{I_0(I_2-T_2)}{2(a_0-T_0)^2} - \frac{I_2T_0}{2(a_0-T_0)^2} - \frac{T_3}{2}\xi + \frac{3I_0T_0^2(I_0-2T_0)}{2(a_0-T_0)^4}\xi^2\right),
\end{aligned}
$$

where

$$
\begin{aligned}
\phi_4(1) =& b_4 + \frac{T_0\left(I_4T_0 - I_2T_2 - I_0T_4\right) + I_0T_2^2}{T_0^3} \ln|a_0 - T_0| + \frac{I_0\left(52I_0^2T_0^2 + 160T_0^4 - 3I_0^4\right)}{24T_0\left(a_0 - T_0\right)^6} \\
&+ \frac{I_0\left(a_2T_0 - a_0T_2\right)\left(4T_0^2 - I_0^2\right)}{2T_0^2\left(a_0 - T_0\right)^4} + \frac{I_0^2\left(3I_2T_0 - 4I_0T_2\right)}{6T_0^2\left(a_0 - T_0\right)^3} + \frac{2\left(2I_0T_2 - I_2T_0\right)}{3\left(a_0 - T_0\right)^3} \\
&- \frac{I_0\left(a_0T_2 - a_2T_0\right)^2}{2T_0^3\left(a_0 - T_0\right)^2} + \frac{a_2I_2 + a_4I_0}{T_0(a_0 - T_0)} - \frac{T_2\left(a_0I_2 + a_2I_0\right)}{T_0^2(a_0 - T_0)} + \frac{I_0\left(a_2T_2 + a_0T_4\right)}{T_0^2(a_0 - T_0)} \\
&+ \frac{2a_0I_0T_2^2}{T_0^3(a_0 - T_0)}.
\end{aligned}
$$

From (3.28) and (3.29), the inner expansion at $x = 0$ is

$$
\begin{aligned}
E_x^3E_\xi^3(\Phi) =& \bar{V} - \varepsilon\frac{I_0}{2L}\xi - \varepsilon^2\left(\frac{I_0T_0}{8L^3} + \frac{I_0T_0}{8L^2}\xi^2\right) - \varepsilon^3\left(\frac{I_0T_0^2}{(2L)^{\frac{9}{2}}} + \left(\frac{I_2}{2L} + \frac{2I_0T_0^2}{(2L)^4}\right)\xi\right. \\
&\left. + \frac{I_0T_0^2}{3(2L)^3}\xi^3\right) \\
&- \varepsilon^4\left(\left(\frac{I_0^3T_0}{(2L)^{\frac{11}{2}}} + \frac{I_3}{2L}\right)\xi + \left(\frac{I_0T_0}{(2L)^5}\left(4T_0^2 - \frac{I_0^2}{2}\right) + \frac{I_0T_2 + I_2T_0}{2(2L)^2}\right)\xi^2\right. \\
&\left. + \frac{I_0T_0^3}{4(2L)^4}\xi^4 + \frac{I_0T_0(19T_0^2 - 3I_0^2)}{2(2L)^6} + \frac{I_0T_2 + I_2T_0}{(2L)^3}\right), \\
E_x^3E_\xi^3(C_1) =& L - \varepsilon\frac{T_0}{2}\xi + \varepsilon^2\frac{I_0T_0}{8L^2} - \varepsilon^3\left(\frac{I_0^2T_0}{2(2L)^{\frac{7}{2}}} - \left(\frac{I_0T_0^2}{8L^3} + \frac{I_0^2T_0}{16L^3} - \frac{T_2}{2}\right)\xi\right) \\
&+ \varepsilon^4\left(\frac{3I_0T_0^2(I_0 + 2T_0)}{4(2L)^4}\xi^2 - \frac{T_3}{2}\xi + \frac{I_0T_0(13T_0^2 - I_0^2 - 3I_0T_0)}{4(2L)^5}\right. \\
&\left. + \frac{I_0T_2 + I_2T_0}{8L^2}\right), \\
E_x^3E_\xi^3(C_2) =& L - \varepsilon\frac{T_0}{2}\xi - \varepsilon^2\frac{I_0T_0}{8L^2} - \varepsilon^3\left(\frac{I_0^2T_0}{2(2L)^{\frac{7}{2}}} - \left(\frac{I_0^2T_0}{16L^3} - \frac{I_0T_0^2}{8L^3} - \frac{T_2}{2}\right)\xi\right) \\
&+ \varepsilon^4\left(\frac{3I_0T_0^2(I_0 - 2T_0)}{4(2L)^4}\xi^2 - \frac{T_3}{2}\xi + \frac{I_0T_0(I_0^2 - 3I_0T_0 - 13T_0^2)}{4(2L)^5}\right. \\
&\left. - \frac{I_0T_2 + I_2T_0}{8L^2}\right),
\end{aligned}
$$

and the inner expansion at $x=1$ is

$$\begin{aligned}
E_x^3E_\xi^3(\Psi) =&\bar{V}-\varepsilon\frac{I_0}{2R}\xi-\varepsilon^2\left(\frac{I_0T_0}{8R^3}+\frac{I_0T_0}{8R^2}\xi^2\right)-\varepsilon^3\left(\frac{I_0T_0^2}{(2R)^{\frac{9}{2}}}+\left(\frac{I_2}{2R}+\frac{2I_0T_0^2}{(2R)^4}\right)\xi\right.\\
&\left.+\frac{I_0T_0^2}{3(2R)^3}\xi^3\right)\\
&-\varepsilon^4\left(\left(\left(\frac{I_0^3T_0}{(2R)^{\frac{11}{2}}}+\frac{I_3}{2R}\right)\xi+\left(\frac{I_0T_0}{(2R)^5}\left(4T_0^2-\frac{I_0^2}{2}\right)+\frac{I_0T_2+I_2T_0}{2(2R)^2}\right)\xi^2\right.\right.\\
&\left.+\frac{I_0T_0^3}{4(2R)^4}\xi^4+\frac{I_0T_0(19T_0^2-3I_0^2)}{2(2R)^6}+\frac{I_0T_2+I_2T_0}{(2R)^3}\right),\\
E_x^3E_\xi^3(D_1) =&R-\varepsilon\frac{T_0}{2}\xi+\varepsilon^2\frac{I_0T_0}{8R^2}-\varepsilon^3\left(\frac{I_0^2T_0}{2(2R)^{\frac{7}{2}}}-\left(\frac{I_0T_0^2}{8R^3}+\frac{I_0^2T_0}{16R^3}-\frac{T_2}{2}\right)\xi\right)\\
&+\varepsilon^4\left(\frac{3I_0T_0^2(I_0+2T_0)}{4(2R)^4}\xi^2-\frac{T_3}{2}\xi+\frac{I_0T_0(13T_0^2-I_0^2-3I_0T_0)}{4(2R)^5}\right.\\
&\left.+\frac{I_0T_2+I_2T_0}{8R^2}\right),\\
E_x^3E_\xi^3(D_2) =&R-\varepsilon\frac{T_0}{2}\xi-\varepsilon^2\frac{I_0T_0}{8R^2}-\varepsilon^3\left(\frac{I_0^2T_0}{2(2R)^{\frac{7}{2}}}-\left(\frac{I_0^2T_0}{16R^3}-\frac{I_0T_0^2}{8R^3}-\frac{T_2}{2}\right)\xi\right)\\
&+\varepsilon^4\left(\frac{3I_0T_0^2(I_0-2T_0)}{4(2R)^4}\xi^2-\frac{T_3}{2}\xi+\frac{I_0T_0(I_0^2-3I_0T_0-13T_0^2)}{4(2R)^5}\right.\\
&\left.-\frac{I_0T_2+I_2T_0}{8R^2}\right).
\end{aligned}$$

The matchings at $x=0$ and $x=1$, together with

$$a_0=2L,\quad T_0=2(L-R),\quad I_0=\frac{2(L-R)}{\ln L-\ln R}\bar{V},\quad a_2=-\frac{I_0^2}{8L^2},\quad T_2=\frac{I_0^2(L^2-R^2)}{8L^2R^2},$$

$$I_2=\frac{I_0T_2}{T_0}+\frac{I_0\left(2T_0^2+I_0^2\right)\left(L^3-R^3\right)}{48L^3R^3(\ln L-\ln R)}+\frac{I_0(a_2T_0-a_0T_2)}{4LR(\ln L-\ln R)},$$

give

$$a_4=\frac{I_0\left[I_0^2(I_0+3T_0)-T_0^2(3T_0+7I_0)\right]}{64L^5}+\frac{a_2I_0(I_0+2T_0)}{8L^3}-\frac{I_0I_2}{4L^2},$$

$$
\begin{aligned}
T_4 =& \frac{I_0 T_0\left(I_0^2-3T_0^2-7T_0 I_0\right)}{64}\left(\frac{1}{L^5}-\frac{1}{R^5}\right)-\frac{I_0 I_2}{4}\left(\frac{1}{L^2}-\frac{1}{R^2}\right),\\
I_4 T_0 =& \frac{I_0 T_0\left(3I_0^4-16I_0^2T_0^2-388T_0^4\right)}{1536(\ln L-\ln R)}\left(\frac{1}{L^6}-\frac{1}{R^6}\right)-\frac{I_0(a_2T_0-a_0T_2)\left(4T_0^2-I_0^2\right)}{32(\ln L-\ln R)}\\
&\times\left(\frac{1}{L^4}-\frac{1}{R^4}\right)-\frac{I_2T_0\left(2T_0^2+3I_0^2\right)+2I_0T_2\left(7T_0^2-2I_0^2\right)}{48(\ln L-\ln R)}\left(\frac{1}{L^3}-\frac{1}{R^3}\right)\\
&+\frac{I_0(a_0T_2-a_2T_0)^2}{8T_0(\ln L-\ln R)}\left(\frac{1}{L^2}-\frac{1}{R^2}\right)+\frac{a_0(I_2T_2-I_0T_4)-T_0(a_2I_2+a_4I_0)}{2(\ln L-\ln R)}\\
&\times\left(\frac{1}{L}-\frac{1}{R}\right)+\frac{I_0T_2^2}{R(\ln L-\ln R)}-\frac{I_0T_2^2}{T_0}+I_2T_2+I_0T_4.
\end{aligned}
$$

We conclude that

$$
\begin{aligned}
T_4 =& \frac{3(L-R)^4\left(L^5-R^5\right)}{4L^5R^5(\ln L-\ln R)}\bar{V}+\frac{(L-R)^4}{2L^5R^5(\ln L-\ln R)^2}\left(\frac{\left(L^2-R^2\right)\left(L^3-R^3\right)}{3(\ln L-\ln R)}\right.\\
&\left.+\frac{7\left(L^5-R^5\right)}{2}\right)V^2-\frac{(L-R)^4\left(L^5-R^5\right)}{4L^5R^5(\ln L-\ln R)^3}\bar{V}^3+\frac{(L-R)^5(L+R)}{2L^4R^4(\ln L-\ln R)^4}\\
&\times\left(\frac{(L+R)}{2}-\frac{L^3-R^3}{3LR(\ln L-\ln R)}\right)\bar{V}^4,\\
I_4 =& \frac{(L-R)^4}{L^4R^4(\ln L-\ln R)^2}\left(\frac{(L-R)\left(L^3-R^3\right)Q_1(L,R)}{6L^2R^2}\bar{V}+\frac{3Q_3(L,R)}{4LR}\bar{V}^2\right.\\
&\left.+\frac{Q_2(L,R)}{\ln L-\ln R}\bar{V}^3-\frac{Q_3(L,R)}{4LR(\ln L-\ln R)^2}\bar{V}^4+\frac{(L-R)Q_4(L,R)}{2(\ln L-\ln R)^3}\bar{V}^5\right),
\end{aligned}
\tag{3.30}
$$

where

$$
\begin{aligned}
Q_1(L,R) =& \frac{L^3-R^3}{3(\ln L-\ln R)}+\frac{97\left(L^3+R^3\right)}{2},\\
Q_2(L,R) =& \frac{(L-R)\left(L^5-R^5\right)}{2L^2R^2(\ln L-\ln R)}+\frac{(L-R)^2\left(L^3-R^3\right)\left(L^2+LR+R^2\right)}{9L^2R^2(\ln L-\ln R)^2}\\
&+\frac{13(L-R)\left(L^5-R^5\right)}{12L^2R^2(\ln L-\ln R)}+\frac{7\left(L^5-R^5\right)}{4LR}-\frac{(L-R)^2(L+R)}{2(\ln L-\ln R)}\\
&+\frac{(L-R)(L+R)\left(L^3-R^3\right)}{4LR(\ln L-\ln R)}-\frac{17(L-R)^2}{12(\ln L-\ln R)},\\
Q_3(L,R) =& \frac{(L-R)\left(L^5-R^5\right)}{\ln L-\ln R}-\frac{(L-R)^2}{\ln L-\ln R}+L^5-R^5,
\end{aligned}
$$

$$Q_4(L,R) = \frac{(L+R)\left(L^3-R^3\right)}{2LR(\ln L - \ln R)} - \frac{\left(L^3-R^3\right)^2}{3L^2R^2(\ln L - \ln R)^2} + \frac{3(L+R)^2}{4}.$$

In particular, the fourth order correction $I_4(\bar{V})$ to the zeroth order I-V relation $I_0(\bar{V})$ is quintic in $\bar{V}$. As $L \to R$, one finds that $T_4 \to 0$ and $I_4 \to \frac{3}{2R}\bar{V}^5$.

Chapter 4

A numerical study for ionic flows with hard sphere ion species: I-V relations and critical potentials

We consider a one-dimensional steady-state PNP type model for ionic flow through membrane channels. Improving the cPNP models where ion species are treated as point charges, this model includes ionic interaction due to finite sizes of ion species modeled by hard sphere potential from the Density Functional Theory. The resulting problem is a singularly perturbed boundary value problem of an integro-differential system. We examine the problem and investigate the ion size effect on the I-V relations numerically, focusing on the case where two oppositely charged ion species are involved and only the hard sphere components of the excess chemical potentials are included. Two numerical tasks are conducted. The first one is a numerical approach of solving the boundary value problem and obtaining I-V curves. This is accomplished through a numerical implement of the analytical strategy introduced by Ji and Liu in [46]. The second task is to numerically detect two critical potential values V_c and V^c. The existence of these two critical values is first realized for a relatively simple setting and analytical approximations of V_c and V^c are obtained in the above mentioned reference. Our numerical detections are based on the defining properties of V_c and V^c and are designed to use the numerical I-V curves directly. For the setting in the above mentioned reference, our numerical results agree well with the analytical predictions.

4.1 Introduction

We numerically examine singularly perturbed boundary value problems of an integro-differential system – a one-dimensional steady-state PNP type model for ionic flow through membrane channels (see [4, 5, 24, 30, 31, 32, 33, 43, 44, 46, 58]).

As mentioned in section 2.1.1, the simplest PNP system is the cPNP system, which treats ions as point-charges, and ignore the ion-to-ion interaction. To take into considerations of ion sizes, one needs to include the excess (beyond the ideal) chemical potential in the model. The PNP system combined with Density Functional Theory (DFT) for hard sphere potentials of ion species serves the purpose for this consideration and has been investigated computationally with great improvements ([9, 31, 32, 33], etc.). All these computations, however, lack sufficiently analytical supports. In a recent work [46], the authors analyzed a one-dimensional version of PNP-DFT system in a simple setting; they considered the case where two oppositely charged ions are involved, the permanent charge can be ignored and only the hard sphere component of the excess chemical potential is included beyond the ideal potential. The model, viewed as a singularly perturbed boundary value problem of an integro-differential system, was analyzed by a combination of geometric singular perturbation theory and functional analysis. They established the existence result for small ion sizes and, treating the sizes as small parameters, derived an approximation of the I-V relation. The approximation result allowed them to make the following finding: there is a critical potential value V_c so that, if $V > V_c$, then the ion size enhances the flow; if $V < V_c$, it reduces the current; There is another critical potential value V^c so that, if $V > V^c$, the current is increasing with respect to $\lambda = r_2/r_1$ where r_1

and r_2 are, respectively, the radii of the positively and negatively charged ions; if $V < V^c$, the current is decreasing in λ.

In this chapter, we perform numerical study of the one-dimensional version of PNP-DFT system in a more general setting than that in [46] to include non-trivial permanent charges. Two numerical tasks are conducted. The first one is a numerical approach for solving the boundary value problem and obtaining I-V curves. This is accomplished through a numerical implement of the analytical strategy introduced in [46]. The second task is to numerically detect two critical potential values V_c and V^c that are defined slightly general than these in [46]. Lacking of analytical formulas for general situations, our numerical detections of V_c and V^c are based on their defining properties and are designed to use the numerical I-V curves directly. For the relative simple setting in [46], our numerical results agree well with the analytical predictions.

The rest of the chapter is organized as follows. In Section 4.2, we briefly set up the one-dimensional PNP-DFT model for ionic flows and recall the analytic results from [46]. In Section 4.3, we discuss our numerical strategy for solving the model problem in detail. In Section 4.4, we introduce two critical potentials generalizing that defined in [46] and provide a design for detecting the critical potentials. In Section 4.5, we present a number of case studies to demonstrate the usage of the numerical activities in Sections 4.3 and 4.4.

4.2 Models and two critical potentials

In this section, we study system (2.27) with the boundary conditions (2.28) including the *nonlocal* hard-sphere component (see [29, 71, 72, 73, 74, 75]) by

$$\mu_i^{HS} = \frac{\delta\Omega(\{c_j\})}{\delta c_i}, \tag{4.1}$$

where

$$
\begin{aligned}
\Omega(\{c_j\}) =& -\int n_0(x;c_1,c_2)\ln(1-n_1(x;c_1,c_2))dx,\\
n_l(x;c_1,c_2) =& \sum_{j=1}^{2}\int c_j(x')\omega_l^j(x-x')dx', \quad (l=0,1),\\
\omega_0^j(x) =& \frac{\delta(x-r_j)+\delta(x+r_j)}{2}, \quad \omega_1^j(x)=\Theta(r_j-|x|),
\end{aligned}
\tag{4.2}
$$

where δ is the Dirac delta function, Θ is the Heaviside function, and r_j is the radius of the jth ion species.

Through out the chapter, we will also assume the electroneutrality conditions at the boundaries

$$
\sum_{j=1}^{n} z_jL_j = \sum_{j=1}^{n} z_jR_j = 0. \tag{4.3}
$$

In [46], the authors considered only the hard-sphere component μ_i^{HS} of μ_i^{ex} with two ion species ($n=2$) of opposite charges ($z_1>0$ and $z_2<0$) and $Q=0$. Based on a combination of geometric singular perturbation analysis and functional analysis, in addition to the existence and uniqueness result for the boundary value problem (BVP) (2.27)–(2.28), an approximation of I-V relation in $r=r_1$ is also obtained:

$$
I(V;\varepsilon,r) := z_1J_1+z_2J_2 = I_0(V;\varepsilon)+I_1(V;\varepsilon)r+o(r),
$$

where

$$
\begin{aligned}
I_0(V;0) =& (D_1-D_2)(L-R)+\frac{e(z_1D_1-z_2D_2)}{kT}f_0(L,R)V,\\
I_1(V;0) =& \frac{2(L-R)}{z_1z_2kT}[(\lambda-1)(z_1D_1-z_2D_2)f_0(L,R)-(z_1\lambda-z_2)(D_1-D_2)(L+R)]\\
&-\frac{2e(z_1\lambda-z_2)(z_1D_1-z_2D_2)}{z_1z_2k^2T^2}f_1(L,R)V,
\end{aligned}
$$

with $\lambda = r_2/r_1$, $L = z_1L_1 = -z_2L_2 > 0$, $R = z_1R_1 = -z_2R_2 > 0$,

$$f_0(L,R) = \frac{L-R}{\ln L - \ln R}, \quad f_1(L,R) = \frac{(L^2-R^2)(\ln L - \ln R) - 2(L-R)^2}{(\ln L - \ln R)^2}.$$

This explicit approximation allows the authors of [46] to realize the existence of two critical potential values V_c and V^c defined, respectively, by

$$I_1(V_c;0) = 0, \quad \frac{d}{d\lambda} I_1(V^c;0) = 0. \tag{4.4}$$

They are given, in this setting, by

$$\begin{aligned} V_c =& \frac{kT}{e}\left((\lambda-1)\frac{(L-R)f_0(L,R)}{(z_1\lambda - z_2)f_1(L,R)} - \frac{(D_1-D_2)(L^2-R^2)}{(z_1D_1-z_2D_2)f_1(L,R)}\right), \\ V^c =& \frac{kT}{e}\left(\frac{(L-R)f_0(L,R)}{z_1f_1(L,R)} - \frac{(D_1-D_2)(L^2-R^2)}{(z_1D_1-z_2D_2)f_1(L,R)}\right). \end{aligned} \tag{4.5}$$

The importance of V_c and V^c is evident and we summarize it here ([46]).

Theorem 4.1. *Let V_c and V^c be defined by (4.4).*

(i) If $V > V_c$, then for $\varepsilon > 0$ small and $r > 0$ small, the ion sizes enhance the current I; that is, $I(V;\varepsilon,r) > I(V;\varepsilon,0)$;

If $V < V_c$, then for $\varepsilon > 0$ small and $r > 0$ small, the ion sizes reduce the current I; that is, $I(V;\varepsilon,r) < I(V;\varepsilon,0)$;

(ii) If $V > V^c$, then for $\varepsilon > 0$ small and $r > 0$ small, the larger the negatively charged ion the larger the current I; that is, the current I is increasing in λ;

If $V < V^c$, then for $\varepsilon > 0$ small and $r > 0$ small, the smaller the negatively charged ion the larger the current I; that is, the current I is decreasing in λ.

4.3 Numerical solution of the BVP (2.27)–(2.28)

Motivated by the work in [46] and with a longterm goal of understanding effects of various variables (such as ion sizes, permanent charges, boundary conditions, etc.) on I-V relations of membrane channels, we examine the effect of ion sizes on the I-V relation based on numerical solutions of the BVP (2.27)–(2.28). We will conduct two numerical tasks.

Task 1. We will develop a numerical approach to the BVP (2.27)–(2.28) and, as a result, obtain numerical I-V curves.

Task 2. Based on numerical I-V curves and the defining properties of V_c and V^c (NOT the analytical formulas (4.5)), we will design a procedure for detecting them numerically for two cases:

(a) for $Q = 0$ that allows us to make a comparison between the analytical predications in [46] and our numerical results;

(b) for a piece-wise constant $Q \neq 0$.

In this section, we will carry out the first task. Task 2 is a critical component for the relevance of our mathematical studies of the PNP type models to ion channel properties and will be carried out in Section 4.4.

To this end, we study system (2.27) with the boundary conditions (2.28) including the *nonlocal* hard-sphere potential given by , for $x \in [0,1]$,

$$\begin{aligned}
\frac{d\mu_1^{HS}}{dx}(x) =& \frac{c_1(x+2r)+c_2(x+(\lambda+1)r)}{1-K_1(x)} - \frac{c_1(x-2r)+c_2(x-(\lambda+1)r)}{1-K_2(x)}, \\
\frac{d\mu_2^{HS}}{dx}(x) =& \frac{c_1(x+(\lambda+1)r)+c_2(x+2\lambda r)}{1-K_3(x)} - \frac{c_1(x-(\lambda+1)r)+c_2(x-2\lambda r)}{1-K_4(x)},
\end{aligned} \tag{4.6}$$

where

$$
\begin{aligned}
K_1(x) &= \int_x^{x+2r} c_1(s)ds + \int_{x-(\lambda-1)r}^{x+(\lambda+1)r} c_2(s)ds,\\
K_2(x) &= \int_{x-2r}^{x} c_1(s)ds + \int_{x-(\lambda+1)r}^{x+(\lambda-1)r} c_2(s)ds,\\
K_3(x) &= \int_{x+(\lambda-1)r}^{x+(\lambda+1)r} c_1(s)ds + \int_x^{x+2\lambda r} c_2(s)ds,\\
K_4(x) &= \int_{x-(\lambda+1)r}^{x-(\lambda-1)r} c_1(s)ds + \int_{x-2\lambda r}^{x} c_2(s)ds.
\end{aligned}
\tag{4.7}
$$

This technical result is from Lemma 4.2 in [46].

Remark 4.2. *The definition of* $\mu_i^{HS}(x)$ *for* $x \in [0,1]$ *requires* (c_1, c_2) *to be defined for* $x \in [-\rho, 1+\rho]$ *where* $\rho = \max\{r_1 + r_2, 2r_1, 2r_2\}$*, where* r_1 *and* r_2 *are the radii of the positively and negatively charged ions respectively. As remarked in [46], the effect of a specific extension is of order* $O(\rho^2)$*. In the sequel, we will fix an extension for our numerical simulations.*

4.3.1 Numerical strategy for solving problem (2.27)–(2.28) with μ_i^{HS} defined by (4.6)

In this part, we present our numerical strategy for *Task 1*. Note that, with μ_i^{HS} defined by (4.6), system (2.27) is an integro-differential system. Our numerical approach is to implement the analytical strategy in [46] that is one of the natural approaches to integro-differential systems.

We begin with a brief summary of the analytical strategy in [46]. For any $(G_1(x), G_2(x)) \in \mathscr{C}^0([0,1], \mathbb{R}^2)$, introduce the auxiliary problem, for convenience, setting $\alpha = z_1 > 0$ and

$\beta = -z_2 > 0$,

$$\begin{aligned}
&\frac{\varepsilon^2}{h(x)}\frac{d}{dx}\left(h(x)\frac{d}{dx}\phi\right) = -(\alpha c_1 - \beta c_2 + Q(x)), \quad \frac{dJ_i}{dx} = 0,\\
&h(x)\frac{dc_1}{dx} + \alpha h(x) c_1 \frac{d\phi}{dx} + G_1(x) = -J_1,\\
&h(x)\frac{dc_2}{dx} - \beta h(x) c_2 \frac{d\phi}{dx} + G_2(x) = -J_2
\end{aligned} \tag{4.8}$$

with the same boundary conditions in (2.28)

$$\phi(0) = \bar{V},\ \ c_i(0) = L_i;\ \ \phi(1) = 0,\ \ c_i(1) = R_i. \tag{4.9}$$

Let $(\phi(x;\varepsilon), c_i(x;\varepsilon))$ be the solution of (4.8) and (4.9) and define a mapping

$$\mathscr{F} : \mathscr{C}^0([0,1],\mathbb{R}^2) \to \mathscr{C}^1([0,1],\mathbb{R}^2) \ \text{ by } \ \mathscr{F}(G_1,G_2)(x) = (c_1(x;\varepsilon), c_2(x;\varepsilon)).$$

Define the second mapping

$$\mathscr{G} : \mathscr{C}^1([0,1],\mathbb{R}^2) \to \mathscr{C}^0([0,1],\mathbb{R}^2)$$

by

$$\mathscr{G}(c_1,c_2)(x) = \left(\frac{h(x)c_1(x)}{kT}\frac{d}{dx}\mu_1^{HS}(x), \frac{h(x)c_2(x)}{kT}\frac{d}{dx}\mu_2^{HS}(x)\right),$$

where μ_i^{HS} are given by the model (4.1) for the given (c_1, c_2).

The BVP (2.27) and (2.28) becomes a fixed point problem

$$(G_1,G_2) = \mathscr{H}(G_1,G_2) \ \text{ for } \ (G_1,G_2) \in \mathscr{C}^0([0,1],\mathbb{R}^2) \tag{4.10}$$

where $\mathscr{H} = (\mathscr{G} \circ \mathscr{F})$. It has been proved in [46, Theorem 5.1] that, for $\varepsilon > 0$ small and as $r \to 0$, the Fréchet derivative $D\mathscr{H}$ of $\mathscr{H}$ is of order $O(r)$. Hence, for $\varepsilon > 0$ small and $r \to 0$ small, the fixed point exists.

Our numerical approach, in a simple word, is to solve the above fixed point problem by numerical iterations. Since the mapping $\mathscr{H}$ is not explicit, a numerical approximation $\mathscr{H}_N$ of $\mathscr{H}$ cannot be directly constructed. Instead, we will numerically implement the above analytical strategy, that is, we proceed to construct numerical approximations of $\mathscr{F}$ and $\mathscr{G}$ with two subroutines. We now describe the iteration procedure.

Subroutine 1. Given fixed functions $G_1^{(0)}(x)$ and $G_2^{(0)}(x)$, we numerically solve the BVP (4.8) and (4.9) with $G_i(x) = G_i^{(0)}(x)$. This auxiliary problem is a BVP of ordinary differential equations (ODEs). We could use standard BVP solvers for ODEs to obtain the numerical solutions $\left(\phi^{(0)}, u^{(0)}, c_1^{(0)}, c_2^{(0)}, J_1^{(0)}, J_2^{(0)}\right)$ for $x \in [0,1]$.

Subroutine 2. After an extension of $(c_1^{(0)}, c_2^{(0)})$ to $x \in [-\rho, \rho+1]$, we numerically determine $\left(G_1^{(1)}(x), G_2^{(1)}(x)\right)$ from

$$G_i^{(1)}(x) = \frac{h(x)c_i^{(0)}(x)}{kT}\frac{d}{dx}\mu_i^{HS}(x)$$

using (4.6) with $c_i(x) = c_i^{(0)}(x)$. This completes one numerical iteration:

$$\left(G_1^{(1)}, G_2^{(1)}\right) = \mathscr{H}_N\left(G_1^{(0)}, G_2^{(0)}\right). \tag{4.11}$$

The mapping $\mathscr{H}_N$ can be viewed as a numerical realization of $\mathscr{H} = \mathscr{G} \circ \mathscr{F}$. Our numerical fixed point iteration method can be formulated as

$$\left(G_1^{(n+1)}, G_2^{(n+1)}\right) = \mathscr{H}_N\left(G_1^{(n)}, G_2^{(n)}\right). \tag{4.12}$$

Subroutine 2 is straightforward because of the explicit formula (4.6). The convergence of this numerical fixed point iteration depends more on BVP solvers for (4.8)–(4.9) involved in Subroutine 1. Our numerical experiments show that, with the BVP solvers and the initial guess we used, the iterations (4.12) converge quite fast (usually need 5-7 iterations to reduce the L_2-error to 10^{-6}). We will thus discuss our BVP solvers and the initial guess in more detail below.

4.3.2 BVP solvers for (4.8)–(4.9) and the initial guess

We use "bvp4c" in Matlab ([52]) as the solver for our auxiliary BVP (4.8) and (4.9). The basic ideas has been illustrated in section 2.3.

Due to the piecewise cubic approximate solution $S(x)$ given by "bvp4c", we could obtain the K_i's in (4.7) analytically and evaluate $G_1^{(n)}(x)$ and $G_2^{(n)}(x)$ accurately in each fixed point iteration. Moreover, we could extend the solution to $[-\rho, 1+\rho]$ easily for polynomials. In our numerical experiments, we use a constant extension.

To apply "bvp4c", we first rewrite (4.8) into a system of 1st-order equations as

$$\begin{aligned}
&\varepsilon \frac{d}{dx}\phi = u,\\
&\frac{\varepsilon}{h(x)}\frac{d}{dx}(h(x)u) = -(\alpha c_1 - \beta c_2 + Q(x)), \quad \frac{dJ_i}{dx} = 0,\\
&\varepsilon h(x)\frac{dc_1}{dx} + \alpha h(x) c_1 u + \varepsilon G_1(x) = -\varepsilon J_1,\\
&\varepsilon h(x)\frac{dc_2}{dx} - \beta h(x) c_2 u + \varepsilon G_2(x) = -\varepsilon J_2
\end{aligned} \tag{4.13}$$

with the same boundary conditions in (4.8).

For a general iteration step, we take the initial guess from the approximate solution of the previous fixed point iteration. At the first iteration, for the case where $Q = 0$, we take advantage of the analysis from [46] and choose the initial guess $\big(\phi^{(0,0)}, u^{(0,0)}, c_1^{(0,0)}, c_2^{(0,0)}, J_1^{(0,0)}, J_2^{(0,0)}\big)$ as follows.

The leading term for the analytical solution (G_1, G_2) is provided in [46, Theorem 6.1]. We take it as our initial guess

$$G_1^{(0)}(x) = n_1(L-(L-R)x), \quad G_2^{(0)}(x) = n_2(L-(L-R)x), \tag{4.14}$$

where

$$n_1 = -\frac{2(\alpha(\lambda+1)+2\beta)(L-R)r}{\alpha^2\beta kT}, \;\; n_2 = -\frac{2(2\alpha\lambda+\beta(\lambda+1))(L-R)r}{\alpha\beta^2 kT}.$$

The leading terms for c_1 and c_2 are also provided in [46, Proposition 3.4] as

$$c_1^{(0,0)}(x) = \frac{L-(L-R)x+mx(1-x)}{\alpha}, \;\; c_2^{(0,0)}(x) = \frac{L-(L-R)x+mx(1-x)}{\beta},$$

where

$$m = \frac{2(\alpha\lambda+\beta)(L-R)^2}{\alpha\beta kT}r.$$

Using the expressions for $\bar{J}_1^{(0,0)}$, $\bar{J}_2^{(0,0)}$ and $\bar{\phi}^{(0,0)}$ in [46], we obtain

$$\begin{aligned}J_1^{(0,0)} =& L_1 - R_1 - \frac{\alpha\beta(n_1+n_2)(L_1+R_1)}{2(\alpha+\beta)}\\ &+ \frac{-\alpha m\bar{V} + \frac{\alpha(\beta n_2-\alpha n_1)}{\alpha+\beta}\left(\frac{(L_1-R_1)s_1-L_1}{s_2-s_1}\ln\left|\frac{1-s_1}{s_1}\right| + \frac{(R_1-L_1)s_2+L_1}{s_2-s_1}\ln\left|\frac{1-s_2}{s_2}\right|\right)}{\left(\frac{1}{s_1-s_2}\ln\left|\frac{1-s_1}{s_1}\right| + \frac{1}{s_2-s_1}\ln\left|\frac{1-s_2}{s_2}\right|\right)},\end{aligned}$$

$$\begin{aligned}J_2^{(0,0)} =& L_2 - R_2 - \frac{\alpha^2(n_1+n_2)(L_1+R_1)}{2(\alpha+\beta)}\\ &+ \frac{-\alpha m\bar{V} + \frac{\alpha(\beta n_2-\alpha n_1)}{\alpha+\beta}\left(\frac{(L_1-R_1)s_1-L_1}{s_2-s_1}\ln\left|\frac{1-s_1}{s_1}\right| + \frac{(R_1-L_1)s_2+L_1}{s_2-s_1}\ln\left|\frac{1-s_2}{s_2}\right|\right)}{\left(\frac{1}{s_1-s_2}\ln\left|\frac{1-s_1}{s_1}\right| + \frac{1}{s_2-s_1}\ln\left|\frac{1-s_2}{s_2}\right|\right)},\end{aligned}$$

and

$$\phi^{(0,0)}(x) = \bar{V} - \frac{\beta J_2 - \alpha J_1}{m(\alpha+\beta)} \left(\frac{1}{s_1 - s_2} \ln\left|\frac{x-s_1}{s_1}\right| + \frac{1}{s_2 - s_1} \ln\left|\frac{x-s_2}{s_2}\right| \right)$$
$$- \frac{\alpha(\beta n_2 - \alpha n_1)\left(\frac{\alpha((L_1-R_1)s_1 - L_1)\ln\left|\frac{x-s_1}{s_1}\right|}{s_2 - s_1} + \frac{\alpha((R_1-L_1)s_2 + L_1)\ln\left|\frac{x-s_2}{s_2}\right|}{s_2-s_1} \right)}{m(\alpha+\beta)}.$$

Here

$$s_1 = \frac{m - \alpha(L_1 - R_1) + \sqrt{(m-\alpha(L_1-R_1))^2 + 4mL_1}}{2m}$$

and

$$s_2 = \frac{m - \alpha(L_1 - R_1) - \sqrt{(m-\alpha(L_1-R_1))^2 + 4mL_1}}{2m}$$

are two roots of the equation $\alpha(L_1 - (L_1 - R_1)s) + ms(1-s) = 0$.

At our first fixed point iteration, we take a uniform mesh partition as initial mesh and evaluate the functions $(\phi^{(0,0)}, u^{(0,0)}, c_1^{(0,0)}, c_2^{(0,0)}, J_1^{(0,0)}, J_2^{(0,0)})$ at these mesh points as initial guess for "bvp4c". We use the mesh and solution from previous fixed point iteration as our initial mesh and initial guess for late iteration.

4.4 Design for numerical detections of V_c and V^c

In this section, we will describe our numerical methods for conducting *Task 2*. For the relative simple settings in [46], explicit approximation formulas for two critical voltages V_c and V^c are obtained analytically. For general situations, no relevant analytical result is available at this moment. *To be able to take the advantage of numerical I-V curves obtained in Task 1, one needs to design numerical methods to detect these two critical voltages*. Our design relies on *analytical characterizations* of two critical potentials V_c and V^c based on their *defining properties*.

Since we focus on the *ion size effect* on I-V relations, we will treat the radii $r = r_1$ and r_2 (hence $\lambda = r_2/r_1$) as variable parameters, and view L_j's, R_j's, $\varepsilon > 0$ small and a piece-wise constant $Q(x)$ as fixed parameters. Thus, we denote the I-V relation by $I = I(V;\lambda,r)$. For I-V relation corresponding to the classical PNP (ignoring the size effects), we denote it by $I = I_0(V)$.

Definition 4.3. *A solution V_c of*

$$I(V;\lambda,r) = I_0(V), \tag{4.15}$$

will be called a size balance potential. *A solution V^c of*

$$I_\lambda(V;\lambda,r) := \frac{\partial I}{\partial\lambda}(V;\lambda,r) = 0. \tag{4.16}$$

will be called a relative size effect potential.

For fixed (λ,r), the potential V_c will depend on the boundary concentrations L_i's, R_i's and the permanent charge Q. It is the balance potential under which ion sizes do not have effects on the current. The potential V^c is meant to distinguish the magnitudes of effects among different relative ion sizes λ.

Corollary 4.4. *For fixed $(\bar\lambda,\bar r)$, let $\bar V_c$ be a size balance potential defined by (4.15).*

(i) If $I_V(\bar V_c;\bar\lambda,\bar r) > I_{0V}(V_c)$, then $I(V;\lambda,r) > I_0(V)$ for $V > \bar V_c$ but close (that is, the ion sizes enhance the current) and $I(V;\lambda,r) < I_0(V)$ for $V < \bar V_c$ but close (that is, the ion sizes reduce the current).

(ii) If $I_V(\bar V_c;\bar\lambda,\bar r) < I_{0V}(V_c)$, then $I(V;\lambda,r) > I_0(V)$ for $V < \bar V_c$ but close (that is, the ion sizes enhance the current) and $I(V;\lambda,r) < I_0(V)$ for $V > \bar V_c$ but close (that is, the ion sizes reduce the current).

Proof. The proof is simple and we omit it here. $\square$

Remark 4.5. *For the setting considered in ([46]), it was shown ([46, Lemma 6.2]) that $I_V(V;\lambda,r) > I_{0V}(V)$ in (i) holds for all (V,λ) if $r>0$ is small enough.*

Corollary 4.6. *For fixed (λ_*, r_*), let V_*^c be a potential defined in (4.16). Suppose $I_{\lambda V}(V_*^c;\lambda_*,r_*) \neq 0$. One has, for (V,λ) in a neighborhood of (V_*^c,λ_*),*

(i) if $I_{\lambda V}(V_*^c;\lambda_*,r_*) > 0$, then, for $V > V_*^c$, $I(V;\lambda,r_*)$ is increasing in λ and, for $V < V_*^c$, $I(V;\lambda,r_*)$ is decreasing in λ;

(ii) if $I_{\lambda V}(V_*^c;\lambda_*,r_*) < 0$, then, for $V > V_*^c$, $I(V;\lambda,r_*)$ is increasing in λ and, for $V < V_*^c$, $I(V;\lambda,r_*)$ is decreasing in λ.

Proof. We write, for some function $p(V,\lambda)$,

$$I(V;\lambda,r_*) - I(V;\lambda_*,r_*) = p(V,\lambda)(\lambda-\lambda_*).$$

Differentiate with respect to λ and V, and set $\lambda=\lambda_*$ to get

$$I_\lambda(V;\lambda_*,r_*) = p(V,\lambda_*), \quad I_{\lambda V}(V;\lambda_*,r_*) = p_V(V,\lambda_*).$$

In particular, $p(V_*^c,\lambda_*)=0$ and $p_V(V_*^c,\lambda_*) \neq 0$. It follows from the Implicit Function Theory that there is a function $\Gamma(\lambda)$ for λ near λ_* such that $V_*^c = \Gamma(\lambda_*)$ and $p(\Gamma(\lambda),\lambda) = 0$. Therefore, $p(V,\lambda) = q(V,\lambda)(V-\Gamma(\lambda))$ for some function $q(V,\lambda)$, and

$$q(V_*^c,\lambda_*) = p_V(V_*^c,\lambda_*) = I_{\lambda V}(V_*^c;\lambda_*,r_*).$$

We conclude

$$I_\lambda(V;\lambda_*,r_*) = p(V,\lambda_*) = q(V;\lambda_*)(V-V_*^c).$$

In particular, $I_\lambda(V;\lambda,r_*)$ and $I_{\lambda V}(V_*^c;\lambda_*,r_*)(V-V_*^c)$ have the same sign for (V,λ) in a neighborhood of (V_*^c,λ_*). Both (i) and (ii) then follow immediately. □

Remark 4.7. *For the setting considered in ([46]), it was shown ([46, Lemma 6.2]) that the condition $I_{\lambda V}(V;\lambda,r)>0$ in (i) holds for all (V,λ) if $r>0$ is small enough.*

Given (λ,r), to numerically detect the corresponding critical value(s) V_c, one can simply plot the difference $I(V;\lambda,r)-I_0(V)$ and search for the roots.

Our numerical design for a direct detecting of the critical value(s) V^c is a numerical interpretation of the following analytical result. For fixed (λ_*,r_*), define

$$H(V,\lambda)=I(V;\lambda,r_*)-I(V;\lambda_*,r_*). \tag{4.17}$$

Proposition 4.8. *For fixed $(\lambda,r)=(\lambda_*,r_*)$, V_*^c is the value defined in (4.16) if and only if the point (V_*^c,λ_*) is a saddle point of $H(V,\lambda)$ under the condition that $H_{\lambda V}(V_*^c,\lambda_*)=I_{\lambda V}(V_*^c;\lambda_*,r_*)\neq 0$.*

Proof. Note that $H(V,\lambda_*)=0$ for all V. Thus, $H_V(V,\lambda_*)=H_{VV}(V,\lambda_*)=0$. From the definition of V_*^c, one has $H_\lambda(V_*^c,\lambda_*)=I_\lambda(V_*^c;\lambda_*,r_*)=0$. Therefore, (V_*^c,λ_*) is a critical point of $H(V,\lambda)$. It then follows from

$$\left(H_{VV}H_{\lambda\lambda}-H_{\lambda V}^2\right)(V_*^c,\lambda_*)=-H_{\lambda V}^2(V_*^c,\lambda_*)<0$$

that (V_*^c,λ_*) is a saddle point of $H(V,\lambda)$. □

Numerically, for fixed (λ_*,r_*), we can computer $I(V;\lambda,r_*)$ and hence $H(V,\lambda)$ for any λ near λ_* and apply Proposition 4.8 to estimate V_*^c from the saddle point of $H(V,\lambda)$. Another approach for detecting V^c is to numerically compute the solution(s) V of $I_\lambda(V;\lambda,r)=$

0. This will involve a numerical evaluation of the partial derivative and a numerical root finding.

We remark that, for real biological situations, one is interested in only discrete values of (λ, r). For the critical potential V_c, one can take an experimental I-V relation as $I(V;\lambda, r)$ and numerically (or analytically) compute $I_0(V)$ for ideal case that allows one to get an estimate of V_c. On the other hand, it is not clear to us how to design a procedure of using experimental data to detect the value V^c.

4.5 Numerical experiments: case studies

In this section, we perform numerical simulations for different values of α, β, and λ for $Q = 0$ and $Q \neq 0$. For simplicity, we make the following assumptions for the parameters involved in the PNP-DFT model:

- The elementary charge $e = 1$, the Boltzmann constant $k = 1$ and the absolute temperature $T = 1$.
- We take $\varepsilon = 0.002$, $h(x) = 1$, and the diffusion coefficient $D_i(x) = 1,\ i = 1, 2$.
- The radius of the positively charged ion $r_1 = r = 0.0001$.

4.5.1 Numerical values vs analytical predications for $Q = 0$

For $Q = 0$, we compare the numerical values V_c and V^c with those analytical approximations obtained in [46]. We remark that the analytical values of V_c and V^c in [46] are zeroth order in ε and first order in r approximations. For $\varepsilon > 0$ small and $r > 0$ small, the numerical values V_c and V^c should be close to the ones obtained from the zeroth order approximation given by (4.5).

In our first set of experiments, we compute V_c for the following 6 different choices of parameter values:

- Case 1: $\alpha = \beta = 1$, $\lambda = 1.885$, $L = \alpha L_1 = \beta L_2 = 4$, and $R = \alpha R_1 = \beta R_2 = 20$;
- Case 2: $\alpha = \beta = 1$, $\lambda = 1.382$, $L = \alpha L_1 = \beta L_2 = 4$, and $R = \alpha R_1 = \beta R_2 = 20$;
- Case 3: $\alpha = 2\beta = 2$, $\lambda = 1.885$, $L = \alpha L_1 = \beta L_2 = 4$, and $R = \alpha R_1 = \beta R_2 = 20$;
- Case 4: $\alpha = \beta = 1$, $\lambda = 1.885$, $L = \alpha L_1 = \beta L_2 = 20$, and $R = \alpha R_1 = \beta R_2 = 4$;
- Case 5: $\alpha = \beta = 1$, $\lambda = 1.382$, $L = \alpha L_1 = \beta L_2 = 20$, and $R = \alpha R_1 = \beta R_2 = 4$;
- Case 6: $\alpha = 2\beta = 2$, $\lambda = 1.885$, $L = \alpha L_1 = \beta L_2 = 20$, and $R = \alpha R_1 = \beta R_2 = 4$.

The choice of $\lambda = 1.885$ in Cases 1, 3, 4, and 6 is motivated by the corresponding λ values for Na^+Cl^- and $Ca^{2+}Cl_2^-$, and $\lambda = 1.382$ in Cases 2 and 5 for K^+Cl^-.

For each case, we plot $I(V;\lambda,r) - I_0(V)$ as a function of V and the critical potential V_c is the root of the difference. The results are reported in Figure 4.1. The analytical values of V_c from (4.5) are -1.1921, -0.6232, and -0.7210 for Cases 1–3, respectively. The numerical values of V_c are -1.2020, -0.6274, and -0.7310, which agree well with the analytical predictions. From the numerical simulations, we observe that V_c's for $L = 4 < R = 20$ (Cases 1–3) and $L = 20 > R = 4$ (Cases 4–6) differ by a sign and the analytical formulas (4.5) for $D_1 = D_2$ verify the observation.

In our second set of experiments, we compute V^c for above 6 cases in the first set of experiments. For each case, we fix $\lambda_* = \lambda/2$ and plot $H(V,\lambda)$, defined in (4.17), as a function of V with 4 different λ values ($3/4\lambda$, λ, $5/4\lambda$, and $6/4\lambda$). The results are in Figure 4.2. The analytical results for zeroth order in ε and first order in r tell us that the graphs for these 4 different λ values should have a common intersection point with $V = V_c$. Also, the analytical values of V^c are -3.8861, -3.8861, and -1.9430 for

Cases 1–3, respectively. From Figure 4.2, one sees that these graphs almost go through the same point and the numerical values of V^c are -3.92, -3.92, and -1.96, which are close to the analytical approximations. Similarly, V^c's for $L < R$ and $L > R$ differ by a sign and the analytical formulas (4.5) for $D_1 = D_2$ verify the observation.

4.5.2 Numerical values of V_c and V^c for piecewise constant $Q(x) \neq 0$

In this section, we consider the problem (2.27)–(2.28) with $Q(x) = Q_0 = 1$ on $(1/3, 2/3)$ and $Q(x) = 0$ otherwise on $[0,1]$. Due to the jumps of Q, the singularly perturbed auxiliary BVP (4.8)–(4.9) is much near singular for small ε. Since we are focusing on the numerical examinations of the critical potentials V_c and V^c, we thus take $\varepsilon = 0.02$ for this study rather than $\varepsilon = 0.002$ as in previous part. Other parameters are the same as the previous section and we will only consider the setting of Case 1.

Applying the strategy described in Section 4.3.1, we first solve the BVP (2.27)–(2.28) for $V = -0.5960$. The profiles of $\bar{\phi}$ and $\bar{u}$ are shown in Figure 4.3, and those of c_1 and c_2 in Figure 4.4. We observe that $\bar{u}$ have corners around $x = 1/3$ and $x = 2/3$; $c_2 - c_1 \approx Q_0 = 1$ on the interval $(1/3, 2/3)$, where $Q \neq 0$. The presence of the corners of $\bar{u}$ reflects the fact that each transition layer (one at $x = 1/3$ and the other at $x = 2/3$) consists of two portions (see [24, 58]).

The critical potential V_c is determined as we did for $Q = 0$ case and the result is shown in Figure 4.5.

For the critical potential V^c, based on Proposition 4.8, we look for saddle points of $H(V, \lambda)$, whose graph is plotted in Figure 4.6. One clearly sees a saddle point of the surface. The saddle point of this surface will give us the numerical value of V^c.

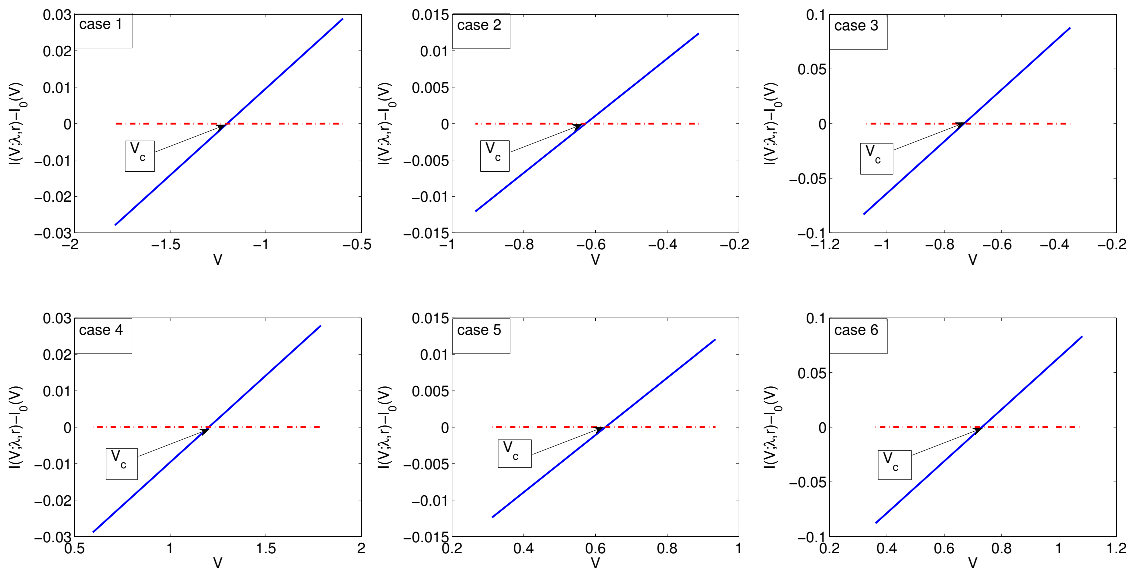

Figure 4.1: Plots of $I(V;\lambda,r)-I_0(V)$ and V_c for $Q=0$.

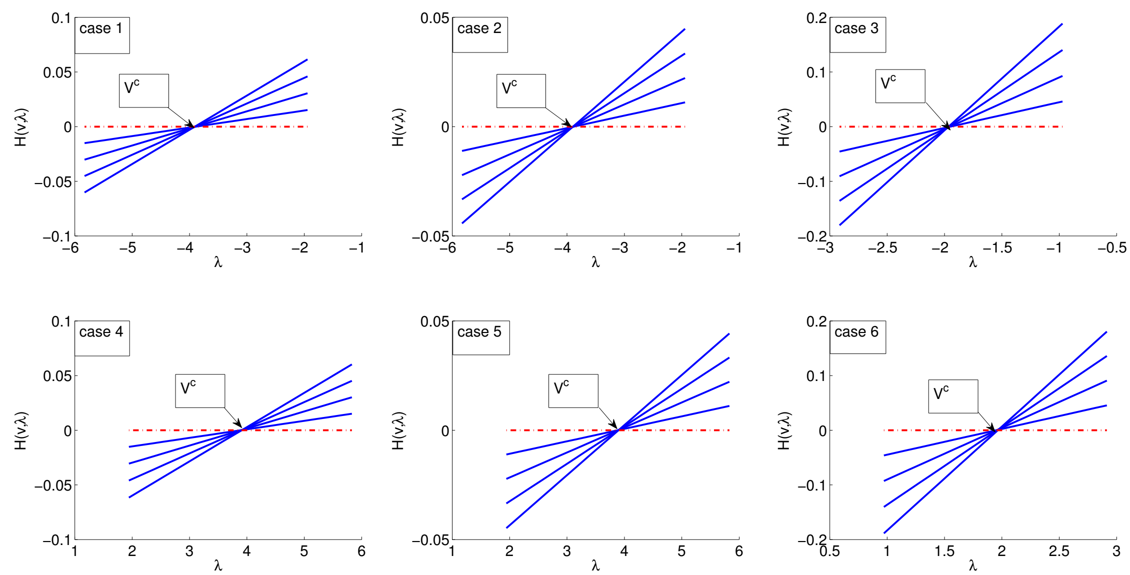

Figure 4.2: Plots of $H(V,\lambda)$ with four values of λ and V^c for $Q=0$.

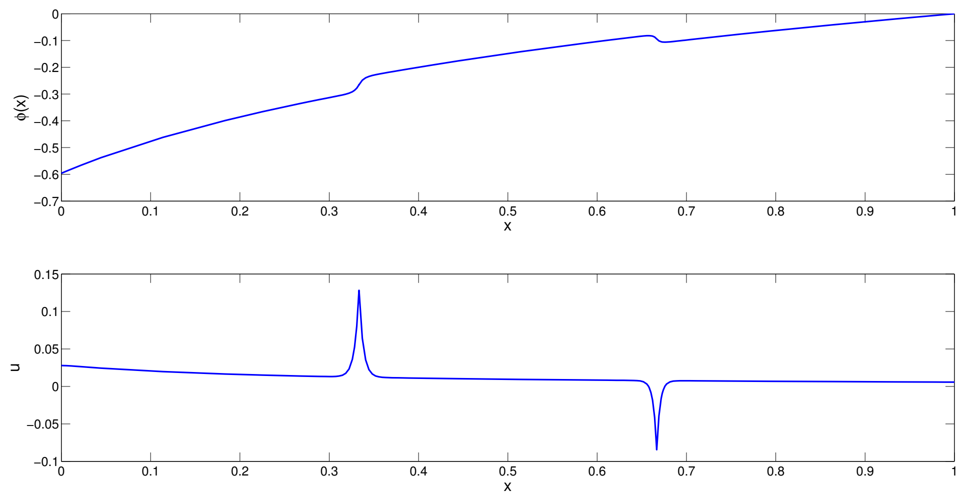

Figure 4.3: Profiles of $\bar{\phi}$ (top) and $\bar{u}$ (bottom) for $Q \neq 0$.

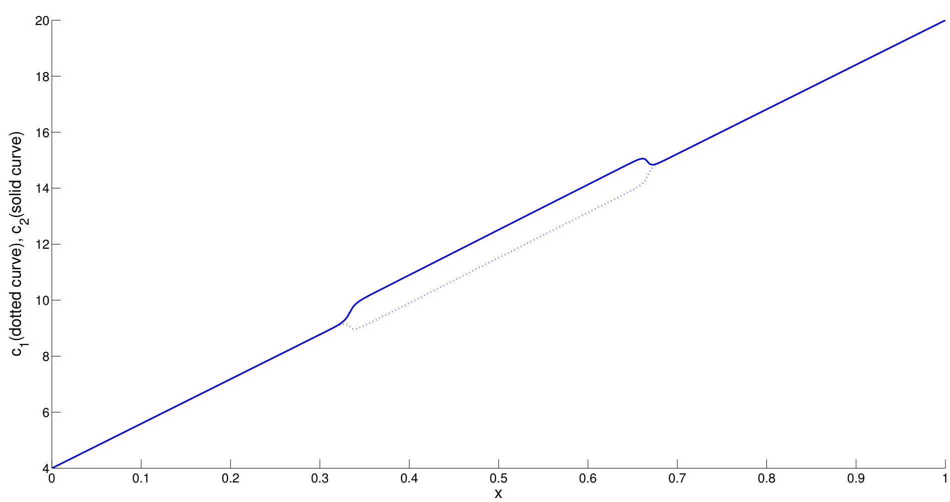

Figure 4.4: Profiles of c_1 and c_2 for $Q \neq 0$.

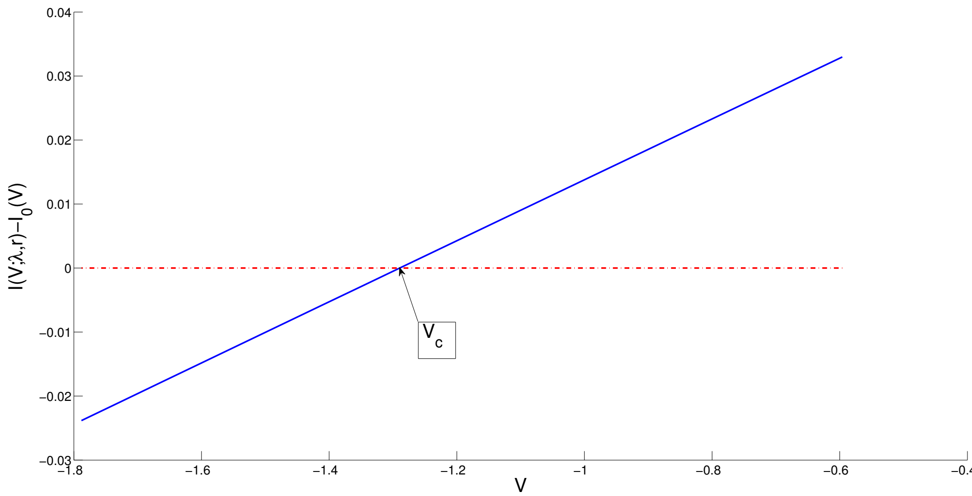

Figure 4.5: Plot of $I(V;\lambda,r) - I_0(V)$ and V_c for $Q \neq 0$.

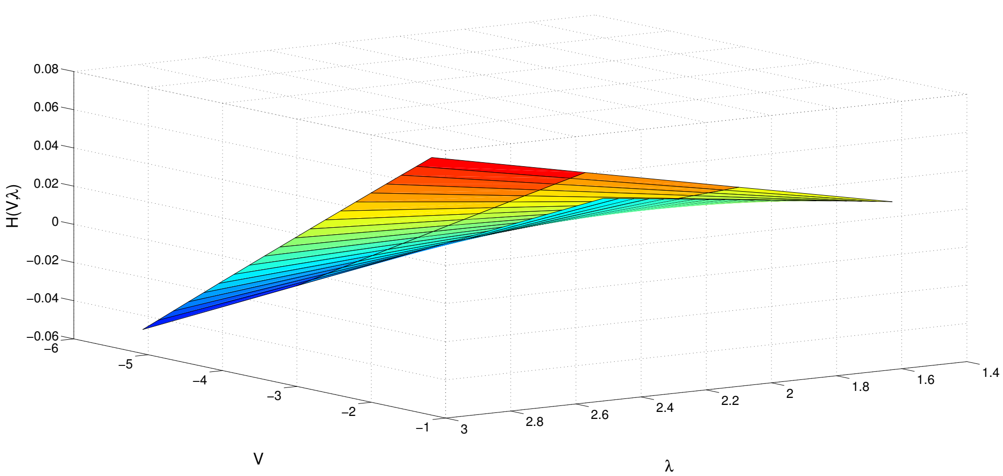

Figure 4.6: Plot of $H(V,\lambda)$ whose saddle points give V^c.

Chapter 5

Poisson-Nernst-Planck systems for ion flow with a local hard-sphere potential for ion size effects

In this chapter, we analyze system (2.27), a one-dimensional steady-state PNP type model for ionic flow through a membrane channel with fixed boundary ion concentrations (charges) and electric potentials (2.28). A local hard-sphere potential that depends pointwise on ion concentrations is included in the model to account for ion size effects on the ionic flow. The model problem is treated as a boundary value problem of a singularly perturbed differential system. Our analysis is based on the geometric singular perturbation theory but, most importantly, on specific structures of this concrete model. The existence of solutions to the boundary value problem for small ion sizes is established and, treating the ion sizes as small parameters, we also derive an approximation of the I-V relation and identify two critical potentials or voltages for ion size effects. Under electroneutrality (zero net charge) boundary conditions, each of these two critical potentials separates the potential into two regions over which the ion size effects are qualitatively opposite to each other. On the other hand, without electroneutrality boundary conditions, the qualitative effects of ion sizes will depend not only on the critical potentials but also on boundary concentrations. Important scaling laws of I-V relations and critical potentials in boundary concentrations are obtained. Similar results about ion size effects on the flow of matter are also discussed. Under electroneutrality boundary conditions, the results on the first order approximation in ion diameters of solutions, I-V relations and critical potentials agree with those with a nonlocal hard-sphere potential examined in [46].

5.1 Introduction

In this chapter, we study the dynamics of ionic flow, the electrodiffusion of charges, through ion channels via system (2.27), a one-dimensional steady-state PNP type system including an additional component, a *local* hard-sphere (HS) potential, to account for *ion size effects*. We are particularly interested in ion size effects on the I-V relation.

In ([46]), the authors provided an analytical treatment of system (2.27) with *electroneutrality* (zero net charge) boundary conditions and including a *nonlocal* hard-sphere potential of the excess component in addition to the ideal component. They treated the model as a singularly perturbed system and rigorously established the existence and uniqueness results of the boundary value problem for small ion sizes. Treating ion sizes as small parameters, they derived an approximation of the I-V relation. Most importantly, the approximate I-V relation allows them to establish the following results.

(i) There is a critical potential or voltage V_c so that, if the boundary potential V satisfies $V > V_c$, then ion sizes *enhance* the current I in the sense that the contribution of ion sizes to the current I is positive; if $V < V_c$, then ion sizes *reduce* the current I.

(ii) There is another critical potential V^c so that, if $V > V^c$, then the current I *increases* in $\lambda = d_2/d_1$ where d_1 and d_2 are, respectively, the diameters of the positively and negatively charged ions; if $V < V^c$, then the current I *decreases* in λ.

In [61], among other things, the authors designed an algorithm for numerically detecting these critical potentials *without using any analytical formulas for I-V relations*. They demonstrated the effectiveness of this algorithm by conducting two numerical tasks. In the first one, the authors took the model problem with the same setting as in [46] for which analytical formulas for V_c and V^c are available. The authors numerically computed I-V relations and, applying the algorithm, computed the critical potentials V_c and V^c. They found that the computed values V_c and V^c agree well with the values obtained from the analytical formulas. For the second numerical task, the authors examined a PNP type model that includes also a nonzero permanent charge Q. For this case, no analytical formulas for the I-V relations and for the critical potentials are currently available. But the authors were able to numerically identify the critical potentials by applying their algorithm.

In this chapter, we study a one-dimensional steady-state PNP system with a *local* model for the hard-sphere (HS) potential. The problem has basically the same setting as that in [46] except that we take a *local* model for the hard-sphere potential and allow *non-electroneutrality* boundary conditions. It is clear that local models have the advantage of simplicity relative to nonlocal ones. In this chapter, we take a local hard-sphere model derived from the nonlocal model used in [46] for two reasons: to provide a mathematical framework for the study of the problem with local hard-sphere models; to compare the results for the local hard-sphere model with those for the nonlocal hard-sphere model in [46].

Under electroneutrality boundary conditions, we will show that the local hard-sphere model yields exactly the same results on the first order approximation (in the diameters of the ion species) I-V relation and the critical potentials V_c and V^c as those of the nonlocal hard-sphere model in [46]. This is perhaps well expected. To the contrary, in the absence of electroneutrality, it is rather surprising that the roles of critical potentials V_c

and V^c on ion size effects are significantly different: the opposite effects of ion sizes separated by V_c and V^c described in (i) and (ii) above now depend on other quantities in terms of boundary concentrations (Theorems 5.14 and 5.15 and Proposition 5.17). Many important biological properties of ion channels are controlled through the boundary conditions. Our results provide a concrete situation for which the important I-V relations of ion channels can depend on boundary conditions sensitively. An observation based on the I-V relation also reveals the following scaling laws (Theorem 5.28):

(a) the contribution I_0 to the I-V relation from the ideal component scales *linearly* in boundary concentrations (that is, if one scales the boundary concentrations by a factor s, then I_0 is scaled by s);

(b) the contribution (up to the leading order) to the I-V relation from the hard-sphere component scales *quadratically* in boundary concentrations;

(c) both V_c and V^c scale *invariantly* in boundary concentrations.

Results on ion size effects to the *flow of matter* in Section 5.4.2 again indicate the richness of ion size effects on the electrodiffusion process.

The general framework for the analysis is the geometric singular perturbation theory–essentially the same as that for the nonlocal hard-sphere potential in [46]. A major difference is that the nonlocal hard-sphere potentials disappear in the limiting fast system but the local ones survive in this limit, and hence, more is involved in the treatment of the limiting fast dynamics for the local hard-sphere potential case. On the other hand, for the local hard-sphere potential case, we need not introduce an auxiliary problem as that for nonlocal case in [46]. A crucial ingredient for the success of our analysis is again the revealing of a set of integrals that allows us to handle the limiting fast dynamics with details as for the classical PNP cases.

The rest of this chapter is organized as follows. In Section 5.2, we describe the one-dimensional PNP-HS model for ion flows, a local model for hard-sphere potentials, and the setup of the boundary value problem of the singularly perturbed PNP-HS system. In Section 5.3, the existence and (local) uniqueness result for the boundary value problem is established in the framework of the geometric singular perturbation theory. Section 5.4 contains two parts. In Section 5.4.1, we derive an approximation of the I-V relation based on the analysis in Section 5.3, identify three critical potentials, and examine significant roles of two of the critical potentials for ion size effects on ionic flows. Important scaling laws of I-V relations and critical potentials in boundary concentrations are obtained. In Section 5.4.2, we discuss ion size effects on the flow of matter. This is presented briefly due to a simple relation between the flow rate of charge and the flow rate of matter.

5.2 Problem Setup

We assume the channel is narrow so that it can be effectively viewed as a one-dimensional channel and normalize it as the interval $[0,1]$ that connects the interior and the exterior of the channel. The one-dimensional steady-state Poisson-Nernst-Planck system (2.27) with the boundary condition (2.28) is studied. An important feature for system (2.27) in this chapter is that for the electrochemical potential, besides the ideal component, a *local* hard-sphere component is included, which is modeled by

$$\frac{1}{kT}\mu_i^{LHS}(x) = -\ln\left(1-\sum_{j=1}^{n} d_j c_j(x)\right) + \frac{d_i \sum_{j=1}^{n} c_j(x)}{1-\sum_{j=1}^{n} d_j c_j(x)}, \tag{5.1}$$

where d_j is the diameter of the jth ion species.

As mentioned in the introduction, this local model is an approximation of the well-known nonlocal model for hard-sphere (hard-rod) used in [46]. Its derivation is provided in Chapter 2.

The main goal of this paper is to examine the qualitative effect of ion sizes via the steady-state boundary value problem of (2.27) and (2.28) with the local hard-sphere (LHS) model (5.1) for the excess potential. We will examine the steady-state boundary value problem in Section 5.3. In Section 5.4, we will obtain approximations for (2.29) and (2.30) to study ion size effects on the I-V relation and on the flow rate $\mathscr{T}$.

For definiteness, we will take essentially the same setting as that in [46] but without assuming electroneutrality boundary conditions: $z_1L_1 + z_2L_2 = z_1R_1 + z_2R_2 = 0$. Using the expression (2.5) for the ideal component $\mu_i^{id}(x)$, together with

$$\begin{aligned}\frac{1}{kT}\frac{d}{dx}\mu_1^{LHS} =& \frac{d_1(2+d_1(c_2-c_1)-2d_2c_2)}{(1-d_1c_1-d_2c_2)^2}\frac{dc_1}{dx} + \frac{d_1+d_2-d_1^2c_1-d_2^2c_2}{(1-d_1c_1-d_2c_2)^2}\frac{dc_2}{dx},\\ \frac{1}{kT}\frac{d}{dx}\mu_2^{LHS} =& \frac{d_1+d_2-d_1^2c_1-d_2^2c_2}{(1-d_1c_1-d_2c_2)^2}\frac{dc_1}{dx} + \frac{d_2(2+d_2(c_1-c_2)-2d_1c_1)}{(1-d_1c_1-d_2c_2)^2}\frac{dc_2}{dx},\end{aligned} \tag{5.2}$$

system (2.27) becomes

$$\begin{aligned}&\frac{\varepsilon^2}{h(x)}\frac{d}{dx}\left(h(x)\frac{d}{dx}\phi\right) = -z_1c_1 - z_2c_2, \quad \frac{dJ_1}{dx} = \frac{dJ_2}{dx} = 0,\\ &\frac{dc_1}{dx} = -f_1(c_1,c_2;d_1,d_2)\frac{d\phi}{dx} - \frac{1}{h(x)}g_1(c_1,c_2,J_1,J_2;d_1,d_2),\\ &\frac{dc_2}{dx} = f_2(c_1,c_2;d_1,d_2)\frac{d\phi}{dx} - \frac{1}{h(x)}g_2(c_1,c_2,J_1,J_2;d_1,d_2)\end{aligned} \tag{5.3}$$

where

$$
\begin{aligned}
f_1(c_1,c_2;d_1,d_2) =& z_1c_1-(d_1+d_2-d_1^2c_1-d_2^2c_2)(z_1c_1+z_2c_2)c_1 \\
& -z_1(d_1-d_2)c_1^2, \\
f_2(c_1,c_2;d_1,d_2) =& -z_2c_2+(d_1+d_2-d_1^2c_1-d_2^2c_2)(z_1c_1+z_2c_2)c_2 \\
& +z_2(d_2-d_1)c_2^2, \\
g_1(c_1,c_2,J_1,J_2;d_1,d_2) =& \big((1-d_1c_1)^2+d_2^2c_1c_2\big)J_1 \\
& -c_1(d_1+d_2-d_1^2c_1-d_2^2c_2)J_2, \\
g_2(c_1,c_2,J_1,J_2;d_1,d_2) =& \big((1-d_2c_2)^2+d_1^2c_1c_2\big)J_2 \\
& -c_2(d_1+d_2-d_1^2c_1-d_2^2c_2)J_1.
\end{aligned}
\tag{5.4}
$$

Recall the boundary conditions are

$$
\phi(0)=\bar{V},\ c_i(0)=L_i>0;\ \phi(1)=0,\ c_i(1)=R_i>0. \tag{5.5}
$$

5.3 Geometric singular perturbation theory for (5.3)–(5.5)

We will rewrite system (5.3) into a standard form for singularly perturbed systems and convert the boundary value problem (5.3) and (5.5) to a connecting problem.

Denote the derivative with respect to x by overdot and introduce $u=\varepsilon\dot{\phi}$ and $\tau=x$. System (5.3) becomes

$$
\begin{aligned}
\varepsilon\dot{\phi} =& u, \quad \varepsilon\dot{u}=-z_1c_1-z_2c_2-\varepsilon\frac{h_\tau(\tau)}{h(\tau)}u, \\
\varepsilon\dot{c}_1 =& -f_1(c_1,c_2;d_1,d_2)u-\frac{\varepsilon}{h(\tau)}g_1(c_1,c_2,J_1,J_2;d_1,d_2), \\
\varepsilon\dot{c}_2 =& f_2(c_1,c_2;d_1,d_2)u-\frac{\varepsilon}{h(\tau)}g_2(c_1,c_2,J_1,J_2;d_1,d_2) \\
\dot{J}_1 =& \dot{J}_2=0, \quad \dot{\tau}=1.
\end{aligned}
\tag{5.1}
$$

System (5.1) will be treated as a singularly perturbed system with ε as the singular parameter. Its phase space is $\mathbb{R}^7$ with state variables $(\phi, u, c_1, c_2, J_1, J_2, \tau)$. We have included constants J_1 and J_2 in the phase space. A reason for this is explained in the paragraph below that of display (5.3).

For $\varepsilon > 0$, the rescaling $x = \varepsilon\xi$ of the independent variable x gives rise to

$$\begin{aligned}
\phi' =& u, \quad u' = -z_1 c_1 - z_2 c_2 - \varepsilon \frac{h_\tau(\tau)}{h(\tau)} u, \\
c_1' =& -f_1(c_1, c_2; d_1, d_2) u - \frac{\varepsilon}{h(\tau)} g_1(c_1, c_2, J_1, J_2; d_1, d_2), \\
c_2' =& f_2(c_1, c_2; d_1, d_2) u - \frac{\varepsilon}{h(\tau)} g_2(c_1, c_2, J_1, J_2; d_1, d_2), \\
J_1' =& J_2' = 0, \quad \tau' = \varepsilon,
\end{aligned} \tag{5.2}$$

where prime denotes the derivative with respect to the variable ξ.

For $\varepsilon > 0$, systems (5.1) and (5.2) have exactly the same phase portrait. But their limiting systems at $\varepsilon = 0$ are different. The limiting system of (5.1) is called the *limiting slow system*, whose orbits are called *slow orbits* or regular layers. The limiting system of (5.2) is the *limiting fast system*, whose orbits are called *fast orbits* or singular (boundary and/or internal) layers. By *a singular orbit* of system (5.1) or (5.2), we mean a continuous and piecewise smooth curve in $\mathbb{R}^7$ that is a union of finitely many slow and fast orbits. Very often, limiting slow and fast systems provide complementary information on state variables. Therefore, the main task of singularly perturbed problems is to patch the limiting information together to form a solution for the entire $\varepsilon > 0$ system.

Let B_L and B_R be the subsets of the phase space $\mathbb{R}^7$ defined by

$$\begin{aligned}
B_L =& \{(\bar{V}, u, L_1, L_2, J_1, J_2, 0) \in \mathbb{R}^7 : \text{arbitrary } u, J_1, J_2\}, \\
B_R =& \{(0, u, R_1, R_2, J_1, J_2, 1) \in \mathbb{R}^7 : \text{arbitrary } u, J_1, J_2\},
\end{aligned} \tag{5.3}$$

where $\bar{V}$, L_1, L_2, R_1 and R_2 are given in (5.5). Then the original boundary value problem is equivalent to a connecting problem, namely, finding a solution of (5.1) or (5.2) from B_L to B_R (see, for example, [47]).

For $\varepsilon > 0$ small, let $M_L(\varepsilon)$ be the collection of forward orbits from B_L under the flow and let $M_R(\varepsilon)$ be that of backward orbits from B_R. Since the flow is not tangent to B_L and B_R and $\dim B_L = \dim B_R = 3$, we have $\dim M_L(\varepsilon) = \dim M_R(\varepsilon) = 4$. We will show that $M_L(\varepsilon)$ and $M_R(\varepsilon)$ intersect transversally in the phase space $\mathbb{R}^7$. Transversality of the intersection implies $\dim(M_L(\varepsilon) \cap M_R(\varepsilon)) = \dim M_L(\varepsilon) + \dim M_R(\varepsilon) - \dim \mathbb{R}^7$. It then follows that $\dim(M_L(\varepsilon) \cap M_R(\varepsilon)) = 1$ which would allow us to conclude the existence and (local) uniqueness of a solution for the connecting problem. This is the reason that we include J_1 and J_2 in the phase space. Alternatively, one can treat J_1 and J_2 as parameters and work in the phase space $\mathbb{R}^5$. Then the corresponding B_L and B_R would each be of dimension one, and hence, $M_L(\varepsilon)$ and $M_R(\varepsilon)$ would each be of dimension two. Should $M_L(\varepsilon)$ and $M_R(\varepsilon)$ intersect, the intersection cannot be transversal due to the dimension counting. To establish the existence and uniqueness result with this alternative approach, one would have to apply perturbation argument with J_1 and J_2 as perturbation parameters.

In what follows, we will consider the equivalent connecting problem for system (5.1) or (5.2) and construct its solution from B_L to B_R. The construction process involves two main steps: the first step is to construct a singular orbit to the connecting problem, and the second step is to apply geometric singular perturbation theory to show that there is a unique solution near the singular orbit for small $\varepsilon > 0$.

5.3.1 Geometric construction of singular orbits

Following the idea in [24, 57, 58], we will first construct a singular orbit on $[0,1]$ that connects B_L to B_R. Such an orbit will generally consist of two boundary layers and a regular layer.

Limiting fast dynamics and boundary layers

By setting $\varepsilon = 0$ in (5.1), we obtain the so-called *slow manifold*

$$\mathscr{Z} = \{u = 0,\ z_1c_1 + z_2c_2 = 0\}. \tag{5.4}$$

By setting $\varepsilon = 0$ in (5.2), we get the *limiting fast system*

$$\begin{aligned}
\phi' =& u, \quad u' = -z_1c_1 - z_2c_2,\\
c_1' =& -f_1(c_1,c_2;d_1,d_2)u,\\
c_2' =& f_2(c_1,c_2;d_1,d_2)u,\\
J_1' =& J_2' = 0, \quad \tau' = 0.
\end{aligned} \tag{5.5}$$

Note that the slow manifold $\mathscr{Z}$ is the set of equilibria of (5.5).

Lemma 5.1. *For system (5.5), the slow manifold $\mathscr{Z}$ is normally hyperbolic.*

Proof. The slow manifold $\mathscr{Z}$ is precisely the set of equilibria of (5.5). The linearization of (5.5) at each point of $(\phi,0,c_1,c_2,J_1,J_2,\tau) \in \mathscr{Z}$ has five zero eigenvalues whose generalized eigenspace is the tangent space of the five-dimensional slow manifold $\mathscr{Z}$ of equilibria, and the other two eigenvalues are $\pm\sqrt{z_1f_1 - z_2f_2}$. On the slow manifold $\mathscr{Z}$ where $z_1c_1 + z_2c_2 = 0$, one has, from (5.4),

$$z_1f_1(c_1,c_2;d_1,d_2) - z_2f_2(c_1,c_2;d_1,d_2) = z_1^2c_1 + z_2^2c_2.$$

Note that $f_1(c_1,c_2;d_1,d_2)$ has a factor c_1 and $f_2(c_1,c_2;d_1,d_2)$ has a factor c_2. It follows from (c_1,c_2)-subsystem of (5.5) that $\{c_1>0\}$ and $\{c_2>0\}$ are invariant under (5.5). Since c_1 and c_2 have positive boundary values, c_1 and c_2 are positive for all $x\in[0,1]$. Therefore, $z_1f_1(c_1,c_2;d_1,d_2)-z_2f_2(c_1,c_2;d_1,d_2)>0$. Thus $\mathscr{Z}$ is normally hyperbolic.

□

We denote the stable (resp. unstable) manifold of $\mathscr{Z}$ by $W^s(\mathscr{Z})$ (resp. $W^u(\mathscr{Z})$). Let M_L be the collection of orbits from B_L in forward time under the flow of system (5.5) and M_R be the collection of orbits from B_R in backward time under the flow of system (5.5). Then, for a singular orbit connecting B_L to B_R, the boundary layer at $\tau=x=0$ must lie in $N_L=M_L\cap W^s(\mathscr{Z})$ and the boundary layer at $\tau=x=1$ must lie in $N_R=M_R\cap W^u(\mathscr{Z})$. In this subsection, we will determine the boundary layers N_L and N_R, and their landing points $\omega(N_L)$ and $\alpha(N_R)$ on the slow manifold $\mathscr{Z}$. The regular layer, determined by the limiting slow system in §5.3.1, will lie in $\mathscr{Z}$ and connect the landing points $\omega(N_L)$ at $\tau=0$ and $\alpha(N_R)$ at $\tau=1$. A singular orbit $\Gamma^0\cup\Lambda\cup\Gamma^1$ is illustrated in Figure 5.1 where $\Gamma^0\subset N_L$ is a boundary layer at $\tau=0$ and $\Gamma^1\subset N_R$ is a boundary layer at $\tau=1$, and Λ is a regular layer connecting the landing points of Γ^0 and Γ^1 on the slow manifold $\mathscr{Z}$ to be constructed in Section 5.3.1. We remark that the boundary layers $\Gamma^0\subset N_L$ and $\Gamma^1\subset N_R$ cannot be uniquely determined untill the construction of Λ.

Recall that d_1 and d_2 are the diameters of the two ion species. For small $d_1>0$ and $d_2>0$, we treat (5.5) as a regular perturbation of that with $d_1=d_2=0$. While d_1 and d_2 are small, their ratio is of order $O(1)$. We thus set

$$d_1=d \ \text{ and } \ d_2=\lambda d \tag{5.6}$$

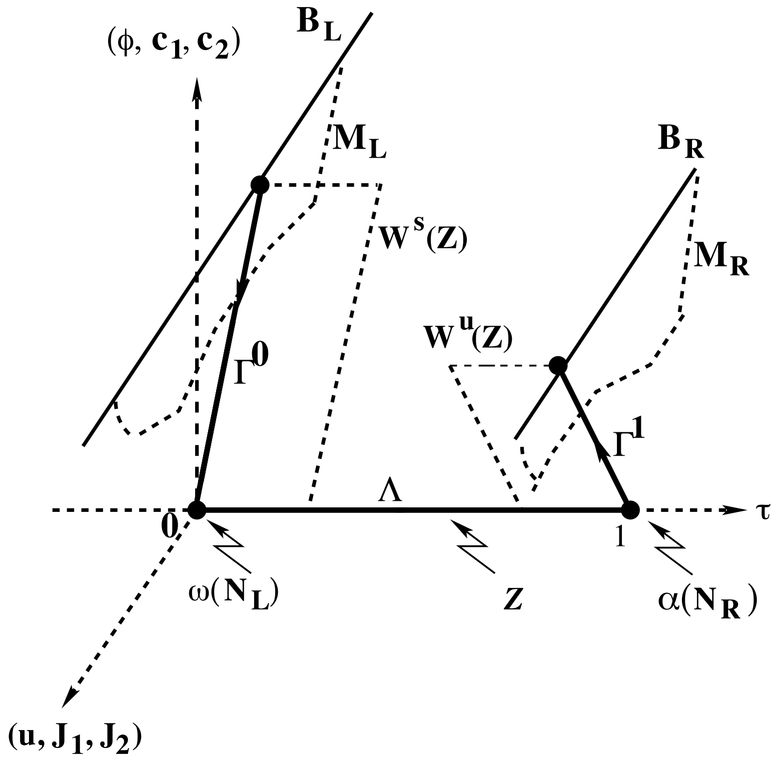

Figure 5.1: *A singular orbit* $\Gamma^0 \cup \Lambda \cup \Gamma^1$ *on* $[0,1]$*: a boundary layer* Γ^0 *at* $\tau = 0$*, a regular layer* Λ *on* $\mathscr{Z}$ *from* $\tau = 0$ *to* $\tau = 1$*, and a boundary layer* Γ^1 *at* $\tau = 1$.

and look for solutions

$$\Gamma(\xi;d) = (\phi(\xi;d), u(\xi;d), c_1(\xi;d), c_2(\xi;d), J_1(d), J_2(d), \tau)$$

of system (5.5) of the form

$$\begin{aligned}
&\phi(\xi;d) = \phi_0(\xi) + \phi_1(\xi)d + o(d), \quad u(\xi;d) = u_0(\xi) + u_1(\xi)d + o(d), \\
&c_1(\xi;d) = c_{10}(\xi) + c_{11}(\xi)d + o(d), \quad c_2(\xi) = c_{20}(\xi) + c_{21}(\xi)d + o(d), \\
&J_1(d) = J_{10} + J_{11}d + o(d), \quad J_2(d) = J_{20} + J_{21}d + o(d).
\end{aligned} \tag{5.7}$$

Substituting (5.7) into system (5.5), we obtain, for the zeroth order in d,

$$\begin{aligned}
\phi_0' =& u_0, \quad u_0' = -z_1c_{10} - z_2c_{20}, \\
c_{10}' =& -z_1c_{10}u_0, \quad c_{20}' = -z_2c_{20}u_0, \\
J_{10}' =& J_{20}' = 0, \quad \tau' = 0,
\end{aligned} \tag{5.8}$$

and, for the first order in d,

$$\begin{aligned}
\phi_1' =& u_1, \quad u_1' = -z_1c_{11} - z_2c_{21}, \\
c_{11}' =& -z_1u_0c_{11} - z_1c_{10}u_1 + u_0\left((\lambda+1)z_2c_{10}c_{20} + 2z_1c_{10}^2\right), \\
c_{21}' =& -z_2u_0c_{21} - z_2c_{20}u_1 + u_0\left((\lambda+1)z_1c_{10}c_{20} + 2\lambda z_2c_{20}^2\right), \\
J_{11}' =& J_{21}' = 0, \quad \tau' = 0.
\end{aligned} \tag{5.9}$$

Recall that we are interested in the solutions $\Gamma^0(\xi;d) \subset N_L = M_L \cap W^s(\mathscr{Z})$ with $\Gamma^0(0;d) \in B_L$ and $\Gamma^1(\xi;d) \subset N_R = M_R \cap W^u(\mathscr{Z})$ with $\Gamma^1(0;d) \in B_R$.

Proposition 5.2. *Assume that $d \geq 0$ is small.*

(i) The stable manifold $W^s(\mathscr{Z})$ intersects B_L transversally at points

$$\left(\bar{V}, u_0^l + u_1^l d + o(d), L_1, L_2, J_1(d), J_2(d), 0\right),$$

and the ω-limit set of $N_L = M_L \bigcap W^s(\mathscr{Z})$ is

$$\omega(N_L) = \left\{(\phi_0^L + \phi_1^L d + o(d), 0, c_{10}^L + c_{11}^L d + o(d), c_{20}^L + c_{21}^L d + o(d), J_1(d), J_2(d), 0)\right\},$$

where $J_i(d) = J_{i0} + J_{i1}d + o(d)$, $i = 1,2$, can be arbitrary and

$$\phi_0^L = \bar{V} - \frac{1}{z_1 - z_2}\ln\frac{-z_2L_2}{z_1L_1}, \quad z_1c_{10}^L = -z_2c_{20}^L = (z_1L_1)^{\frac{-z_2}{z_1-z_2}}(-z_2L_2)^{\frac{z_1}{z_1-z_2}},$$

$$
\begin{aligned}
u_0^l =& sgn(z_1L_1+z_2L_2)\sqrt{2\left(L_1+L_2+\frac{z_1-z_2}{z_1z_2}(z_1L_1)^{\frac{-z_2}{z_1-z_2}}(-z_2L_2)^{\frac{z_1}{z_1-z_2}}\right)};\\
\phi_1^L =& \frac{1-\lambda}{z_1-z_2}(L_1+L_2-c_{10}^L-c_{20}^L),\\
z_1c_{11}^L =& -z_2c_{21}^L = z_1c_{10}^L\left(L_1+\lambda L_2+\frac{\lambda z_1-z_2}{z_1-z_2}(L_1+L_2)+\frac{2(\lambda z_1-z_2)}{z_2}c_{10}^L\right),\\
u_1^l =& \frac{(L_1+L_2)(L_1+\lambda L_2)-(c_{10}^L+c_{20}^L)(c_{10}^L+\lambda c_{20}^L)-c_{11}^L-c_{21}^L}{u_0^l}.
\end{aligned}
$$

(ii) The unstable manifold $W^u(\mathscr{Z})$ intersects B_R transversally at points

$$
(0,u_0^r+u_1^rd+o(d),R_1,R_2,J_1(d),J_2(d),1),
$$

and the α-limit set of N_R is

$$
\alpha(N_R)=\left\{(\phi_0^R+\phi_1^Rd+o(d),0,c_{10}^R+c_{11}^Rd+o(d),c_{20}^R+c_{21}^Rd+o(d),J_1(d),J_2(d),1)\right\},
$$

where $J_i(d)=J_{i0}+J_{i1}d+o(d)$, $i=1,2$, can be arbitrary and

$$
\begin{aligned}
\phi_0^R =& -\frac{1}{z_1-z_2}\ln\frac{-z_2R_2}{z_1R_1},\quad z_1c_{10}^R=-z_2c_{20}^R=(z_1R_1)^{\frac{-z_2}{z_1-z_2}}(-z_2R_2)^{\frac{z_1}{z_1-z_2}},\\
u_0^r =& -sgn(z_1R_1+z_2R_2)\sqrt{2\left(R_1+R_2+\frac{z_1-z_2}{z_1z_2}(z_1R_1)^{\frac{-z_2}{z_1-z_2}}(-z_2R_2)^{\frac{z_1}{z_1-z_2}}\right)};\\
\phi_1^R =& \frac{1-\lambda}{z_1-z_2}(R_1+R_2-c_{10}^R-c_{20}^R),\\
z_1c_{11}^R =& -z_2c_{21}^R = z_1c_{10}^R\left(R_1+\lambda R_2+\frac{\lambda z_1-z_2}{z_1-z_2}(R_1+R_2)+\frac{2(\lambda z_1-z_2)}{z_2}c_{10}^R\right),\\
u_1^r =& \frac{(R_1+R_2)(R_1+\lambda R_2)-(c_{10}^R+c_{20}^R)(c_{10}^R+\lambda c_{20}^R)-c_{11}^R-c_{21}^R}{u_0^r}.
\end{aligned}
$$

Remark 5.3. *When $z_1L_1+z_2L_2=0$, $u_0^l=0$. In this case, u_1^l is defined as the limit of its expression as $z_1L_1+z_2L_2\to 0$ and it is zero. Similar remark applies to u_1^r when $z_1R_1+z_2R_2=0$.*

Proof. The stated result for system (5.8) has been obtained in [24, 57, 58]. For system (5.9), one can check that it has three nontrivial first integrals:

$$\begin{aligned}
F_1 =& z_1\phi_1 + \frac{c_{11}}{c_{10}} + 2c_{10} + (\lambda+1)c_{20},\\
F_2 =& z_2\phi_1 + \frac{c_{21}}{c_{20}} + 2\lambda c_{20} + (\lambda+1)c_{10},\\
F_3 =& u_0u_1 - c_{11} - c_{21} - (\lambda+1)c_{10}c_{20} - c_{10}^2 - \lambda c_{20}^2.
\end{aligned}$$

We now establish the results for $\phi_1^L, c_{11}^L, c_{21}^L$ and u_1^l for system (5.9). Those for $\phi_1^R, c_{11}^R, c_{21}^R$ and u_1^r can be established in the similar way.

We note that $\phi_1(0) = c_{11}(0) = c_{21}(0) = 0$. Using the integrals F_1 and F_2, we have

$$\begin{aligned}
&z_1\phi_1 + \frac{c_{11}}{c_{10}} + 2c_{10} + (\lambda+1)c_{20} = 2L_1 + (\lambda+1)L_2,\\
&z_2\phi_1 + \frac{c_{21}}{c_{20}} + 2\lambda c_{10} + (\lambda+1)c_{10} = 2\lambda L_2 + (\lambda+1)L_1.
\end{aligned}$$

Therefore

$$\begin{aligned}
c_{11} =& c_{10}\left(2L_1 + (\lambda+1)L_2 - 2c_{10} - (\lambda+1)c_{20} - z_1\phi_1\right),\\
c_{21} =& c_{20}\left(2\lambda L_2 + (\lambda+1)L_1 - 2\lambda c_{20} - (\lambda+1)c_{10} - z_2\phi_1\right).
\end{aligned}$$

Taking the limit as $\xi \to \infty$, we have

$$\begin{aligned}
\phi_1^L =& \frac{1-\lambda}{z_1 - z_2}(L_1 + L_2 - c_{10}^L - c_{20}^L),\\
c_{11}^L =& c_{10}^L\left(2L_1 + (\lambda+1)L_2 - 2c_{10}^L - (\lambda+1)c_{20}^L - z_1\phi_1^L\right),\\
c_{21}^L =& c_{20}^L\left(2\lambda L_2 + (\lambda+1)L_1 - 2\lambda c_{20}^L - (\lambda+1)c_{10}^L - z_2\phi_1^L\right).
\end{aligned}$$

In view of the relations $z_1c_{10}^L + z_2c_{20}^L = z_1c_{11}^L + z_2c_{21}^L = 0$, one can get the formulas for c_{11}^L, c_{21}^L and ϕ_1^L. We now derive the formula for $u_1^l = u_1(0)$.

In view of $F_3(0) = F_3(\infty)$, we have

$$u_0^l u_1^l - (\lambda+1)L_1L_2 - L_1^2 - \lambda L_2^2 = -c_{11}^L - c_{21}^L - (\lambda+1)c_{10}^L c_{20}^L - (c_{10}^L)^2 - \lambda(c_{20}^L)^2.$$

The formula for u_1^l follows directly. $\square$

For later use, let Γ^0 denote the potential boundary layer at $x=0$ for system (5.5) and Let Γ^1 denote the potential boundary layer at $x=1$ for system (5.5).

Corollary 5.4. *Under electroneutrality boundary conditions, that is, $z_1L_1 = -z_2L_2 = L$ and $z_1R_1 = -z_2R_2 = R$,*

$$\phi_0^L = \bar{V},\ z_1c_{10}^L = -z_2c_{20}^L = L;\ \phi_0^R = 0,\ z_1c_{10}^R = -z_2c_{20}^R = R,$$

$$\phi_1^L = c_{11}^L = c_{21}^L = \phi_1^R = c_{11}^R = c_{21}^R = 0.$$

In particular, up to $O(d)$, there is no boundary layer at $x=0$ and $x=1$.

Limiting slow dynamics and regular layer

Next we construct the regular layer on $\mathscr{Z}$ that connects $\omega(N_L)$ and $\alpha(N_R)$. Note that, for $\varepsilon = 0$, system (5.1) loses most information. To remedy this degeneracy, we follow the idea in [24, 57, 58] and make a rescaling $u = \varepsilon p$ and $-z_2c_2 = z_1c_1 + \varepsilon q$ in system (5.1). In term of the new variables, system (5.1) becomes

$$\begin{aligned} \dot{\phi} =& p, \quad \varepsilon\dot{p} = q - \varepsilon\frac{h_\tau(\tau)}{h(\tau)}p, \quad \varepsilon\dot{q} = (z_1f_1 - z_2f_2)\,p + \frac{z_1g_1 + z_2g_2}{h(\tau)}, \\ \dot{c}_1 =& -f_1p - \frac{g_1}{h(\tau)}, \quad \dot{J}_1 = \dot{J}_2 = 0, \quad \dot{\tau} = 1 \end{aligned} \tag{5.10}$$

where, for $i = 1, 2$,

$$f_i = f_i\left(c_1, -\frac{z_1 c_1 + \varepsilon q}{z_2}; d, \lambda d\right) \text{ and } g_i = g_i\left(c_1, -\frac{z_1 c_1 + \varepsilon q}{z_2}, J_1, J_2; d, \lambda d\right).$$

It is again a singular perturbation problem and its limiting slow system is

$$\begin{aligned}
q =& 0, \quad p = -\frac{1}{z_1(z_1 - z_2)h(\tau)c_1}\sum_{i=1}^{2} z_i g_i\big(c_1, -\frac{z_1}{z_2}c_1, J_1, J_2; d, \lambda d\big),\\
\dot{\phi} =& p,\\
\dot{c}_1 =& -f_1\big(c_1, -\frac{z_1}{z_2}c_1; d, \lambda d\big)p - \frac{1}{h(\tau)}g_1\big(c_1, -\frac{z_1}{z_2}c_1, J_1, J_2; d, \lambda d\big),\\
\dot{J}_1 =& \dot{J}_2 = 0, \quad \dot{\tau} = 1.
\end{aligned} \tag{5.11}$$

In the above, for the expression for p, we have used (5.4) to find

$$z_1 f_1\Big(c_1, -\frac{z_1 c_1}{z_2}; d, \lambda d\Big) - z_2 f_2\Big(c_1, -\frac{z_1 c_1}{z_2}; d, \lambda d\Big) = z_1(z_1 - z_2)c_1.$$

From system (5.11), the slow manifold is

$$\mathscr{S} = \left\{ q = 0,\ p = -\frac{z_1 g_1\big(c_1, -\frac{z_1}{z_2}c_1, J_1, J_2; d, \lambda d\big) + z_2 g_2\big(c_1, -\frac{z_1}{z_2}c_1, J_1, J_2; d, \lambda d\big)}{z_1(z_1 - z_2)h(\tau)c_1} \right\}.$$

Therefore, the limiting slow system on $\mathscr{S}$ is

$$\begin{aligned}
\dot{\phi} =& p,\\
\dot{c}_1 =& -f_1\big(c_1, -\frac{z_1}{z_2}c_1; d, \lambda d\big)p - \frac{1}{h(\tau)}g_1\big(c_1, -\frac{z_1}{z_2}c_1, J_1, J_2; d, \lambda d\big),\\
\dot{J}_1 =& \dot{J}_2 = 0, \quad \dot{\tau} = 1,
\end{aligned} \tag{5.12}$$

where

$$p = -\frac{z_1 g_1\left(c_1, -\frac{z_1}{z_2}c_1, J_1, J_2; d, \lambda d\right) + z_2 g_2\left(c_1, -\frac{z_1}{z_2}c_1, J_1, J_2; d, \lambda d\right)}{z_1(z_1 - z_2)h(\tau)c_1}.$$

As for the layer problem, we look for solutions of (5.12) of the form

$$\begin{aligned} \phi(x) &= \phi_0(x) + \phi_1(x)d + o(d), \\ c_1(x) &= c_{10}(x) + c_{11}(x)d + o(d), \\ J_1 &= J_{10} + J_{11}d + o(d), \quad J_2 = J_{20} + J_{21}d + o(d) \end{aligned} \tag{5.13}$$

to connect $\omega(N_L)$ and $\alpha(N_R)$ given in Proposition 5.2; in particular, for $j = 0, 1$,

$$\left(\phi_j(0), c_{1j}(0)\right) = \left(\phi_j^L, c_{1j}^L\right), \quad \left(\phi_j(1), c_{1j}(1)\right) = \left(\phi_j^R, c_{1j}^R\right).$$

From system (5.12) and the definitions of f_j's and g_j's in (5.4), we have

$$\begin{aligned} \dot{\phi}_0 &= -\frac{z_1 J_{10} + z_2 J_{20}}{z_1(z_1 - z_2)h(\tau)c_{10}}, \quad \dot{c}_{10} = \frac{z_2\left(J_{10} + J_{20}\right)}{(z_1 - z_2)h(\tau)}, \\ \dot{J}_{10} &= \dot{J}_{20} = 0, \quad \dot{\tau} = 1, \end{aligned} \tag{5.14}$$

and

$$\begin{aligned} \dot{\phi}_1 =& \frac{(z_1 J_{10} + z_2 J_{20})c_{11}}{z_1(z_1 - z_2)h(\tau)c_{10}^2} + \frac{z_1(1-\lambda)(J_{10} + J_{20})c_{10} - (z_1 J_{11} + z_2 J_{21})}{z_1(z_1 - z_2)h(\tau)c_{10}}, \\ \dot{c}_{11} =& \frac{2(\lambda z_1 - z_2)(J_{10} + J_{20})c_{10} + z_2(J_{11} + J_{21})}{(z_1 - z_2)h(\tau)}, \\ \dot{J}_{11} =& \dot{J}_{21} = 0, \quad \dot{\tau} = 1. \end{aligned} \tag{5.15}$$

For convenience, we denote

$$H(x) = \int_0^x h^{-1}(s)ds. \tag{5.16}$$

Lemma 5.5. *There is a unique solution $(\phi_0(x), c_{10}(x), J_{10}, J_{20}, \tau(x))$ of (5.14) such that*

$$(\phi_0(0), c_{10}(0), \tau(0)) = (\phi_0^L, c_{10}^L, 0) \text{ and } (\phi_0(1), c_{10}(1), \tau(1)) = (\phi_0^R, c_{10}^R, 1), \tag{5.17}$$

where ϕ_0^L, ϕ_0^R, c_{10}^L, and c_{10}^R are given in Proposition 5.2. It is given by

$$\begin{aligned}
\phi_0(x) =& \phi_0^L + \frac{\phi_0^R - \phi_0^L}{\ln c_{10}^R - \ln c_{10}^L} \ln\left(1 - \frac{H(x)}{H(1)} + \frac{H(x)}{H(1)} \frac{c_{10}^R}{c_{10}^L}\right),\\
c_{10}(x) =& \left(1 - \frac{H(x)}{H(1)}\right) c_{10}^L + \frac{H(x)}{H(1)} c_{10}^R,\\
J_{10} =& \frac{c_{10}^L - c_{10}^R}{H(1)} \left(1 + \frac{z_1\left(\phi_0^L - \phi_0^R\right)}{\ln c_{10}^L - \ln c_{10}^R}\right),\\
J_{20} =& -\frac{z_1(c_{10}^L - c_{10}^R)}{z_2 H(1)} \left(1 + \frac{z_2\left(\phi_0^L - \phi_0^R\right)}{\ln c_{10}^L - \ln c_{10}^R}\right),\\
\tau(x) =& x.
\end{aligned}$$

Proof. The solution of system (5.14) with the initial condition $(\phi_0^L, c_{10}^L, J_{10}, J_{20}, 0)$ that corresponds to the point $(\phi_0^L, 0, c_{10}^L, c_{20}^L, J_{10}, J_{20}, 0)$ is

$$\begin{aligned}
\phi_0(x) &= \phi_0^L - \frac{z_1 J_{10} + z_2 J_{20}}{z_1(z_1 - z_2)} \int_0^x h^{-1}(s) c_{10}^{-1}(s) ds,\\
c_{10}(x) &= c_{10}^L + \frac{z_2\left(J_{10} + J_{20}\right)}{z_1 - z_2} H(x), \quad \tau(x) = x.
\end{aligned} \tag{5.18}$$

It follows from the c_{10}-equation and $c_{10}(1) = c_{10}^R$ that

$$J_{10} + J_{20} = -\frac{(z_1 - z_2)(c_{10}^L - c_{10}^R)}{z_2 H(1)}. \tag{5.19}$$

Note that, from (5.14),

$$\int_0^x h^{-1}(s) c_{10}^{-1}(s) ds = \frac{z_1 - z_2}{z_2(J_{10} + J_{20})} \int_0^x \frac{\dot{c}_{10}(s)}{c_{10}(s)} ds = H(1) \frac{\ln c_{10}^L - \ln c_{10}(x)}{c_{10}^L - c_{10}^R}.$$

Thus,

$$\phi_0(x) = \phi_0^L - H(1)\frac{z_1 J_{10} + z_2 J_{20}}{z_1(z_1 - z_2)} \frac{\ln c_{10}^L - \ln c_{10}(x)}{c_{10}^L - c_{10}^R}.$$

Applying the boundary condition $c_{10}(1) = c_{10}^R$ and $\phi_0(1) = \phi_0^R$, we have

$$\begin{aligned} J_{10} + J_{20} =& -\frac{(z_1 - z_2)(c_{10}^L - c_{10}^R)}{z_2 H(1)}, \\ z_1 J_{10} + z_2 J_{20} =& \frac{z_1(z_1 - z_2)(c_{10}^L - c_{10}^R)(\phi_0^L - \phi_0^R)}{H(1)(\ln c_{10}^L - \ln c_{10}^R)}. \end{aligned} \tag{5.20}$$

The expressions for J_{10} and J_{20}, and hence, for $\phi_0(x)$ and $c_{10}(x)$ follow directly. $\square$

For convenience, we define three functions

$$M = M(L_1, L_2, R_1, R_2; \lambda),\ N = N(L_1, L_2, R_1, R_2; \lambda),\ P(x) = P(x; L_1, L_2, R_1, R_2; \lambda)$$

as

$$\begin{aligned} M =& z_1 c_{10}^L w(L_1, L_2) - z_1 c_{10}^R w(R_1, R_2) + \frac{z_1(\lambda z_1 - z_2)}{z_2}\left((c_{10}^L)^2 - (c_{10}^R)^2\right), \\ N =& \frac{z_1(c_{10}^L - c_{10}^R)}{\ln c_{10}^L - \ln c_{10}^R}(\phi_1^L - \phi_1^R) - \frac{(1-\lambda)z_1}{z_2}\frac{(c_{10}^L - c_{10}^R)^2}{\ln c_{10}^L - \ln c_{10}^R} + \frac{\phi_0^L - \phi_0^R}{\ln c_{10}^L - \ln c_{10}^R}M \\ & - \frac{z_1(c_{10}^L - c_{10}^R)(w(L_1, L_2) - w(R_1, R_2))}{(\ln c_{10}^L - \ln c_{10}^R)^2}(\phi_0^L - \phi_0^R), \\ P(x) =& \frac{\lambda z_1 - z_2}{z_2}\frac{(c_{10}^L - c_{10}^R)H(x)}{(\ln c_{10}^L - \ln c_{10}^R)H(1)} \\ & + \frac{c_{10}^L - c_{10}(x)}{\ln c_{10}^L - \ln c_{10}^R}\left(\frac{w(L_1, L_2)}{c_{10}(x)} + \frac{\lambda z_1 - z_2}{z_2}\frac{c_{10}^L}{c_{10}(x)}\right) \\ & - \frac{H(x)}{z_1(\ln c_{10}^L - \ln c_{10}^R)c_{10}(x)H(1)}M + \frac{\ln c_{10}^L - \ln c_{10}(x)}{z_1(\ln c_{10}^L - \ln c_{10}^R)(c_{10}^L - c_{10}^R)}M \end{aligned} \tag{5.21}$$

where

$$w(\alpha, \beta) = \alpha + \lambda\beta + \frac{\lambda z_1 - z_2}{z_1 - z_2}(\alpha + \beta).$$

Lemma 5.6. *There is a unique solution $(\phi_1(x), c_{11}(x), J_{11}, J_{21}, \tau(x))$ of (5.15) such that*

$$(\phi_1(0), c_{11}(0), \tau(0)) = (\phi_1^L, c_{11}^L, 0) \text{ and } (\phi_1(1), c_{11}(1), \tau(1)) = (\phi_1^R, c_{11}^R, 1), \tag{5.22}$$

where ϕ_1^L, ϕ_1^R, c_{11}^L, and c_{11}^R are given in Proposition 5.2. It is given by

$$\begin{aligned}
\phi_1(x) =& \phi_1^L - \frac{(1-\lambda)(c_{10}^L - c_{10}^R)H(x)}{z_2 H(1)} + (\phi_0^L - \phi_0^R)P(x) - \frac{\ln c_{10}(x) - \ln c_{10}^L}{z_1(z_1 - z_2)(c_{10}^R - c_{10}^L)} N, \\
c_{11}(x) =& c_{11}^L + \frac{\lambda z_1 - z_2}{z_2}\left(c_{10}^2(x) - (c_{10}^L)^2\right) - \frac{H(x)}{z_1 H(1)} M, \\
J_{11} =& \frac{M}{z_1 H(1)} + \frac{N}{H(1)}, \quad J_{21} = -\frac{M}{z_2 H(1)} - \frac{N}{H(1)},
\end{aligned}$$

where M, N, and P are defined in (5.21).

Proof. It follows from (5.15) that

$$c_{11}(x) = c_{11}^L + \frac{\lambda z_1 - z_2}{z_2}\left(c_{10}^2(x) - (c_{10}^L)^2\right) + \frac{z_2(J_{11} + J_{21})}{z_1 - z_2} H(x).$$

Thus, from Proposition 5.2,

$$\begin{aligned}
\frac{z_2(J_{11} + J_{21})}{z_2 - z_1} H(1) =& c_{11}^L - c_{11}^R + \frac{\lambda z_1 - z_2}{z_2}\left((c_{10}^R)^2 - (c_{10}^L)^2\right) \\
=& c_{10}^L w(L_1, L_2) - c_{10}^R w(R_1, R_2) + \frac{\lambda z_1 - z_2}{z_2}\left((c_{10}^L)^2 - (c_{10}^R)^2\right),
\end{aligned}$$

or, by the definition of M in (5.21),

$$J_{11} + J_{21} = \frac{z_2 - z_1}{z_1 z_2 H(1)} M. \tag{5.23}$$

Hence,

$$c_{11}(x) = c_{11}^L + \frac{\lambda z_1 - z_2}{z_2}\left(c_{10}^2(x) - (c_{10}^L)^2\right) - \frac{H(x)}{z_1 H(1)} M. \tag{5.24}$$

Again, from (5.15)

$$\begin{aligned}\phi_1(x) =& \phi_1^L + \frac{z_1 J_{10} + z_2 J_{20}}{z_1(z_1 - z_2)} \int_0^x \frac{c_{11}(s)}{h(s) c_{10}^2(s)} ds + \frac{(1-\lambda)(J_{10} + J_{20})}{z_1 - z_2} H(x) \\ & - \frac{z_1 J_{11} + z_2 J_{21}}{z_1(z_1 - z_2)} \int_0^x \frac{1}{h(s) c_{10}(s)} ds.\end{aligned}$$

Note that, from (5.14) and (5.19),

$$\begin{aligned}\int_0^x \frac{c_{10}(s)}{h(s)} ds =& \frac{z_1 - z_2}{z_2(J_{10} + J_{20})} \int_0^x c_{10}(s) \dot{c}_{10}(s) ds = \frac{H(1)}{2} \frac{(c_{10}^L)^2 - c_{10}^2(x)}{c_{10}^L - c_{10}^R}, \\ \int_0^x \frac{1}{h(s) c_{10}^2(s)} ds =& \frac{z_1 - z_2}{z_2(J_{10} + J_{20})} \int_0^x \frac{\dot{c}_{10}(s)}{c_{10}^2(s)} ds = H(1) \frac{c_{10}^L - c_{10}(x)}{(c_{10}^L - c_{10}^R) c_{10}^L c_{10}(x)}, \\ \int_0^x \frac{\int_0^s h^{-1}(\sigma) d\sigma}{h(s) c_{10}^2(s)} ds =& - \frac{z_1 - z_2}{z_2(J_{10} + J_{20})} \int_0^x \int_0^s h^{-1}(\sigma) d\sigma \frac{d}{ds} c_{10}^{-1}(s) ds \\ =& \frac{H(1)}{c_{10}^L - c_{10}^R} \left(\frac{H(x)}{c_{10}(x)} - \int_0^x h^{-1}(s) c_{10}^{-1}(s) ds \right) \\ =& \frac{H(1) H(x)}{(c_{10}^L - c_{10}^R) c_{10}(x)} - H^2(1) \frac{\ln c_{10}^L - \ln c_{10}(x)}{(c_{10}^L - c_{10}^R)^2}.\end{aligned}$$

These, together with (5.24) and (5.20), yield

$$\begin{aligned}\int_0^x \frac{c_{11}(s)}{h(s) c_{10}^2(s)} ds = & \left(w(L_1, L_2) + \frac{\lambda z_1 - z_2}{z_2} c_{10}^L \right) \frac{H(1)(c_{10}^L - c_{10}(x))}{(c_{10}^L - c_{10}^R) c_{10}(x)} \\ & + \frac{\lambda z_1 - z_2}{z_2} H(x) - \frac{M}{z_1(c_{10}^L - c_{10}^R)} \left(\frac{H(x)}{c_{10}(x)} - \frac{\ln c_{10}^L - \ln c_{10}(x)}{c_{10}^L - c_{10}^R} H(1) \right).\end{aligned}$$

A careful calculation then gives

$$\phi_1(x) = \phi_1^L - \frac{(1-\lambda)(c_{10}^L - c_{10}^R) H(x)}{z_2 H(1)} + (\phi_0^L - \phi_0^R) P(x)$$

$$-\frac{z_1J_{11}+z_2J_{21}}{z_1(z_1-z_2)}\frac{\ln c_{10}^L-\ln c_{10}(x)}{c_{10}^L-c_{10}^R}H(1).$$

Hence,

$$\begin{aligned}
\phi_1^R =&\phi_1^L-\frac{1-\lambda}{z_2}(c_{10}^L-c_{10}^R)+(\phi_0^L-\phi_0^R)P(1)\\
&-\frac{z_1J_{11}+z_2J_{21}}{z_1(z_1-z_2)}\frac{\ln c_{10}^L-\ln c_{10}^R}{c_{10}^L-c_{10}^R}H(1)\\
=&\phi_1^L-\frac{1-\lambda}{z_2}(c_{10}^L-c_{10}^R)-\frac{w(L_1,L_2)-w(R_1,R_2)}{\ln c_{10}^L-\ln c_{10}^R}(\phi_0^L-\phi_0^R)\\
&+\frac{M(\phi_0^L-\phi_0^R)}{z_1(c_{10}^L-c_{10}^R)}-\frac{(z_1J_{11}+z_2J_{21})(\ln c_{10}^L-\ln c_{10}^R)}{z_1(z_1-z_2)(c_{10}^L-c_{10}^R)}H(1).
\end{aligned}$$

Thus,

$$\begin{aligned}
H(1)\frac{z_1J_{11}+z_2J_{21}}{z_1-z_2}&=z_1\frac{c_{10}^L-c_{10}^R}{\ln c_{10}^L-\ln c_{10}^R}(\phi_1^L-\phi_1^R)-\frac{(1-\lambda)z_1}{z_2}\frac{(c_{10}^L-c_{10}^R)^2}{\ln c_{10}^L-\ln c_{10}^R}\\
&+\frac{M(\phi_0^L-\phi_0^R)}{\ln c_{10}^L-\ln c_{10}^R}-z_1\frac{(c_{10}^L-c_{10}^R)(w(L_1,L_2)-w(R_1,R_2))}{(\ln c_{10}^L-\ln c_{10}^R)^2}(\phi_0^L-\phi_0^R)=N.
\end{aligned}$$

Formulas for J_{11}, J_{21}, and ϕ_1 follow directly. □

Corollary 5.7. *Under the electroneutrality conditions at the boundaries, that is,* $z_1L_1=-z_2L_2=L$ *and* $z_1R_1=-z_2R_2=R$*, we have,*

$$\begin{aligned}
J_{10}=&\frac{L-R}{z_1H(1)}\left(1+\frac{z_1\bar{V}}{\ln L-\ln R}\right),\quad J_{20}=\frac{L-R}{z_2H(1)}\left(1+\frac{z_2\bar{V}}{\ln L-\ln R}\right);\\
J_{11}=&\frac{\lambda z_1-z_2}{z_1z_2H(1)}\frac{R-L}{\ln R-\ln L}\left(\frac{2(R-L)}{\ln R-\ln L}-(R+L)\right)\bar{V}\\
&+\frac{1-\lambda}{z_1z_2H(1)}\frac{(R-L)^2}{\ln R-\ln L}+\frac{\lambda z_1-z_2}{z_1^2z_2H(1)}\left(R^2-L^2\right),\\
J_{21}=&-\frac{\lambda z_1-z_2}{z_1z_2H(1)}\frac{R-L}{\ln R-\ln L}\left(\frac{2(R-L)}{\ln R-\ln L}-(R+L)\right)\bar{V}\\
&-\frac{1-\lambda}{z_1z_2H(1)}\frac{(R-L)^2}{\ln R-\ln L}-\frac{\lambda z_1-z_2}{z_1z_2^2H(1)}\left(R^2-L^2\right).
\end{aligned}$$

Proof. This follows directly from Lemmas 5.5 and 5.6 and Proposition 5.2. □

The slow orbit, up to $O(d)$,

$$\Lambda(x;d) = (\phi_0(x) + \phi_1(x)d, c_{10}(x) + c_{11}(x)d, J_{10} + J_{11}d, J_{20} + J_{21}d, \tau(x)) \tag{5.25}$$

given in Lemmas 5.5 and 5.6 connects $\omega(N_L)$ and $\alpha(N_R)$. Let $\bar{M}_L$ (resp., $\bar{M}_R$) be the forward (resp., backward) image of $\omega(N_L)$ (resp., $\alpha(N_R)$) under the slow flow (5.12) on the five-dimensional slow manifold $\mathscr{S}$. Following the idea in [57], we have

Proposition 5.8. *There exists $d_0 > 0$ small depending on boundary conditions so that, if $0 \le d \le d_0$, then, on the five-dimensional slow manifold $\mathscr{S}$, $\bar{M}_L$ and $\bar{M}_R$ intersects transversally along the unique orbit $\Lambda(x;d)$ given in (5.25).*

Proof. To see the transversality of the intersection, it suffices to show that $\omega(N_L)\cdot 1$ (the image of $\omega(N_L)$ under the time-one map of the flow of system (5.12)) is transversal to $\alpha(N_R)$ on $\mathscr{S}\bigcap\{\tau = 1\}$. We will show first that, for $d = 0$, $\omega(N_L)\cdot 1$ and $\alpha(N_R)$ intersect transversally on $\mathscr{S}\bigcap\{\tau = 1\}$. We will use (ϕ, c_1, J_1, J_2) as a coordinate system on $\mathscr{S}\bigcap\{\tau = 1\}$. It follows from (5.18) that, for $d = 0$, $\omega(N_L)\cdot 1$ is given by

$$\omega(N_L)\cdot 1 = \{(\phi(J_1,J_2), c_1(J_1,J_2), J_1, J_2) : \text{ arbitrary } J_1,\, J_2\}$$

with

$$\begin{aligned}
\phi(J_1,J_2) =& \phi_0^L - \frac{z_1J_1 + z_2J_2}{z_1z_2(J_1+J_2)}\ln\frac{c_1(J_1,J_2)}{c_{10}^L},\\
c_1(J_1,J_2) =& c_{10}^L + \frac{z_2H(1)(J_1+J_2)}{z_1 - z_2}.
\end{aligned}$$

Thus, the tangent space to $\omega(N_L)\cdot 1$ restricted on $\mathscr{S}\bigcap\{\tau=1\}$ is spanned by the vectors

$$(\phi_{J_1},(c_1)_{J_1},1,0)=\left(\phi_{J_1},\frac{z_2}{z_1-z_2}H(1),1,0\right)$$

and

$$(\phi_{J_2},(c_1)_{J_2},0,1)=\left(\phi_{J_2},\frac{z_2}{z_1-z_2}H(1),0,1\right).$$

In view of the display in Proposition 5.2, the set $\alpha(N_R)$ is parameterized by J_1 and J_2, and hence, the tangent space to $\alpha(N_R)$ restricted on $\mathscr{S}\bigcap\{\tau=1\}$ is spanned by (0,0,1,0) and (0,0,0,1). Note that $\mathscr{S}\bigcap\{\tau=1\}$ is four dimensional. Thus, it suffices to show that the above four vectors are linearly independent or, equivalently, $\phi_{J_1}\neq\phi_{J_2}$ at $(J_1,J_2)=(J_{10},J_{20})$. The latter can be verified by a direct computation as follows:

$$\phi_{J_1}-\phi_{J_2}=-\frac{z_1-z_2}{z_1z_2(J_1+J_2)}\ln\left[1+\frac{z_2(J_1+J_2)}{(z_1-z_2)c_{10}^L}H(1)\right]\neq 0,$$

even as $J_1+J_2\to 0$. This establishes the transversal intersection of $\omega(N_L)\cdot 1$ and $\alpha(N_R)$ on $\mathscr{S}\bigcap\{\tau=1\}$. From the smooth dependence of solutions on parameter d, we conclude that there exists $d_0>0$ small, so that, if $0\leq d\leq d_0$, then $\omega(N_L)\cdot 1$ and $\alpha(N_R)$ intersect transversally on $\mathscr{S}\bigcap\{\tau=1\}$. This completes the proof. □

5.3.2 Existence of solutions near the singular orbit

We have constructed a unique singular orbit on [0,1] that connects B_L to B_R. It consists of two boundary layer orbits Γ^0 from the point

$$(\bar{V},u_0^l+u_1^ld+o(d),L_1,L_2,J_{10}+J_{11}d+o(d),J_{20}+J_{21}d+o(d),0)\in B_L$$

to the point

$$(\phi^L, 0, c_1^L, c_2^L, J_1, J_2, 0) \in \omega(N_L) \subset \mathscr{Z}$$

and Γ^1 from the point

$$(\phi^R, 0, c_1^R, c_2^R, J_1, J_2, 1) \in z_1(N_R) \subset \mathscr{Z}$$

to the point

$$(0, u_0^r + u_1^r + o(d), R_1, R_2, J_1, J_2, 1) \in B_R,$$

and a regular layer Λ on $\mathscr{Z}$ that connects the two landing points

$$(\phi^L, 0, c_1^L, c_2^L, J_1, J_2, 0) \in \omega(N_L)$$

and

$$(\phi^R, 0, c_1^R, c_2^R, J_1, J_2, 1) \in \alpha(N_R)$$

of the two boundary layers.

We now establish the existence of a solution of (5.3) and (5.5) near the singular orbit constructed above which is a union of two boundary layers and one regular layer $\Gamma^0 \bigcup \Lambda \bigcup \Gamma^1$. The proof follows the same line as that in [24, 57, 58] and the main tool used is the Exchange Lemma (see, for example [47, 48, 49, 93]) of the geometric singular perturbation theory.

Theorem 5.9. *Let $\Gamma^0 \bigcup \Lambda \bigcup \Gamma^1$ be the singular orbit of the connecting problem system (5.1) associated to B_L and B_R in system (5.3). Let $d_0 > 0$ be as in Proposition 5.8. Then, there exists $\varepsilon_0 > 0$ small (depending on the boundary conditions and d_0) so that, if $0 \le d \le d_0$ and $0 < \varepsilon \le \varepsilon_0$, then the boundary value problem (5.3) and (5.5) has a unique smooth solution near the singular orbit $\Gamma^0 \bigcup \Lambda \bigcup \Gamma^1$.*

Proof. Let $d_0 > 0$ be as in Proposition 5.8. For $0 \le d \le d_0$, denote $u^l = u_0^l + u_1^l d$, $J_1(d) = J_{10} + J_{11}d$ and $J_2(d) = J_{20} + J_{21}d$. Fix $\delta > 0$ small to be determined. Let

$$B_L(\delta) = \{(\bar{V}, u, L_1, L_2, J_1, J_2, 0) \in \mathbb{R}^7 : |u - u^l| < \delta, |J_i - J_i(d)| < \delta\}.$$

For $\varepsilon > 0$, let $M_L(\varepsilon, \delta)$ be the forward trace of $B_L(\delta)$ under the flow of system (5.1) or equivalently of system (5.2) and let $M_R(\varepsilon)$ be the backward trace of B_R. To prove the existence and uniqueness statement, it suffices to show that $M_L(\varepsilon, \delta)$ intersects $M_R(\varepsilon)$ transversally in a neighborhood of the singular orbit $\Gamma^0 \bigcup \Lambda \bigcup \Gamma^1$. The latter will be established by an application of Exchange Lemmas.

Note that $\dim B_L(\delta)$=3. It is clear that the vector field of the fast system (5.2) is not tangent to $B_L(\delta)$ for $\varepsilon \ge 0$, and hence, $\dim M_L(\varepsilon, \delta)$=4. We next apply Exchange Lemma to track $M_L(\varepsilon, \delta)$ in the vicinity of $\Gamma^0 \bigcup \Lambda \bigcup \Gamma^1$. First of all, the transversality of the intersection $B_L(\delta) \bigcap W^s(\mathscr{Z})$ along Γ^0 in Proposition 5.2 implies the transversality of intersection $M_L(0, \delta) \bigcap W^s(\mathscr{Z})$. Secondly, we have also established that $\dim \omega(N_L) = \dim N_L - 1 = 2$ in Proposition 5.2 and that the limiting slow flow is not tangent to $\omega(N_L)$ in Section 5.3.1. With these conditions, Exchange Lemma ([47, 48, 49, 93]) states that there exist $\rho > 0$ and $\varepsilon_1 > 0$ so that, if $0 < \varepsilon \le \varepsilon_1$, then $M_L(\varepsilon, \delta)$ will first follow Γ^0 toward $\omega(N_L) \subset \mathscr{Z}$, then follow the trace of $\omega(N_L)$ in the vicinity of Λ toward $\{\tau = 1\}$, leave the vicinity of $\mathscr{Z}$, and, upon exit, a portion of $M_L(\varepsilon, \delta)$ is C^1 $O(\varepsilon)$-close to $W^u(\omega(N_L) \times (1-\rho, 1+\rho))$ in the vicinity of Γ^1 (see Figure 5.2 for an illustration). Note that $\dim W^u(\omega(N_L) \times (1-\rho, 1+\rho)) = \dim M_L(\varepsilon, \delta) = 4$.

It remains to show that $W^u(\omega(N_L) \times (1-\rho, 1+\rho))$ intersects $M_R(\varepsilon)$ transversally since $M_L(\varepsilon, \delta)$ is C^1 $O(\varepsilon)$-close to $W^u(\omega(N_L) \times (1-\rho, 1+\rho))$. Recall that, for $\varepsilon = 0$, M_R intersects $W^u(\mathscr{Z})$ transversally along N_R (Proposition 5.2); in particular, at $\gamma_1 :=$

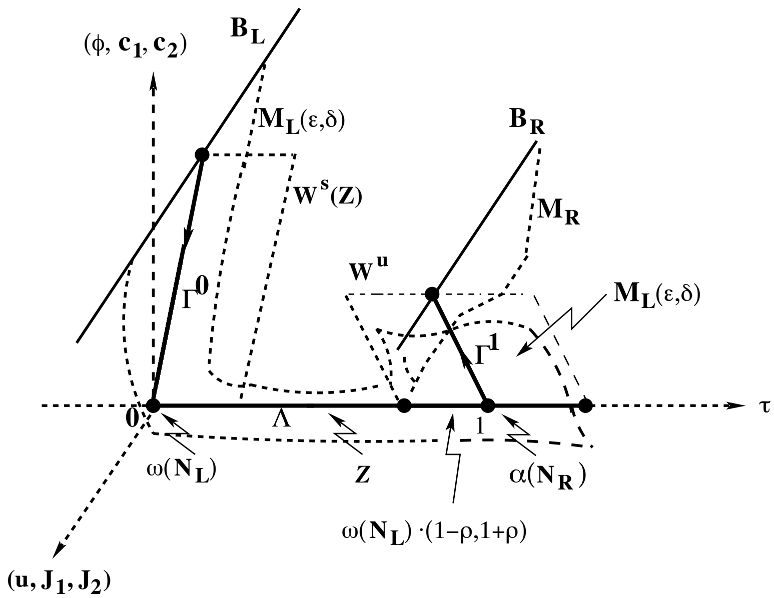

Figure 5.2: *Illustration of the evolution of $M_L(\varepsilon,\delta)$ from the vicinity of $\tau = 0$ to that of $\tau = 1$: On the left, $M_L(\varepsilon,\delta)$ intersects $W^s(\mathscr{Z})$ transversally and approaches $\omega(N_L)$ in the vicinity of Γ^0; It then follows the trace of $\omega(N_L)$ in the vicinity of Λ on $\mathscr{Z}$ toward the vicinity of $\omega(N_L)\cdot(1-\rho,1+\rho)$; A portion of it will leave the vicinity of $\mathscr{Z}$, and, upon exit from $\mathscr{Z}$, $M_L(\varepsilon,\delta)$ is C^1 $O(\varepsilon)$-close to $W^u(\omega(N_L)\times(1-\rho,1+\rho))$ in the vicinity of Γ^1. In the figure, $W^u(\omega(N_L)\times(1-\rho,1+\rho))$ is denoted by W^u.*

$\alpha(\Gamma^1) \in \alpha(N_R) \subset \mathscr{Z}$, we have

$$T_{\gamma_1} M_R = T_{\gamma_1}\alpha(N_R) + T_{\gamma_1} W^u(\gamma_1) + \operatorname{span}\{V_s\}$$

where, $T_{\gamma_1} W^u(\gamma_1)$ is the tangent space of the one-dimensional unstable fiber $W^u(\gamma_1)$ at γ_1 and the vector $V_s \notin T_{\gamma_1} W^u(\mathscr{Z})$ (the latter follows from the transversality of the intersection of M_R and $W^u(\mathscr{Z})$). Also,

$$T_{\gamma_1} W^u(\omega(N_L)\times(1-\rho,1+\rho)) = T_{\gamma_1}(\omega(N_L)\cdot 1) + \operatorname{span}\{V_\tau\} + T_{\gamma_1} W^u(\gamma_1)$$

where the vector V_τ is the tangent vector to the τ-axis as the result of the interval factor $(1-\rho,1+\rho)$. Recall from Proposition 5.8 that $\omega(N_L)\cdot 1$ and $\alpha(N_R)$ are transversal on

$\mathscr{X} \cap \{\tau = 1\}$. Therefore, at γ_1, the tangent spaces $T_{\gamma_1}M_R$ and $T_{\gamma_1}W^u(\omega(N_L)\times(1-\rho, 1+\rho))$ contain seven linearly independent vectors: V_s, V_τ, $T_{\gamma_1}W^u(\gamma_1)$ and the other four from $T_{\gamma_1}(\omega(N_L)\cdot 1)$ and $T_{\gamma_1}\alpha(N_R)$; that is, M_R and $W^u(\omega(N_L)\times(1-\rho, 1+\rho))$ intersect transversally. We thus conclude that, there exists $0 < \varepsilon_0 \le \varepsilon_1$ so that, if $0 < \varepsilon \le \varepsilon_0$, then $M_L(\varepsilon, \delta)$ intersects $M_R(\varepsilon)$ transversally.

For uniqueness, note that the transversality of the intersection $M_L(\varepsilon,\delta)\bigcap M_R(\varepsilon)$ implies $\dim(M_L(\varepsilon,\delta)\bigcap M_R(\varepsilon)) = \dim M_L(\varepsilon,\delta) + \dim M_R(\varepsilon) - 7 = 1$. Thus, there exists $\delta_0 > 0$ such that, if $0 < \delta \le \delta_0$, the intersection $M_L(\varepsilon,\delta)\bigcap M_R(\varepsilon)$ consists of precisely one solution near the singular orbit $\Gamma^0 \bigcup \Lambda \bigcup \Gamma^1$. $\square$

5.4 Ion size effects on the flows of charge and matter

The analysis in the previous sections not only establishes the existence of solutions for the boundary value problem (5.3) and (5.5) but also provides quantitative information on the solution that allows us to extract explicit approximations to the current $\mathscr{I}$ and the flow rate of matter, $\mathscr{T}$, for small ε and d. From the explicit approximations, we are able to identify some critical values for potential V that characterize ion size effects on the ionic flow. A number of scaling laws will be also obtained. Their consequences of ion size effects are discussed.

5.4.1 I-V relation, critical potentials, and scaling laws

I-V relation and its approximation

For fixed boundary concentrations L_1, L_2, R_1 and R_2 in (**??**), we express the I-V relation in (5.1) as

$$\mathscr{I}(V;\lambda,\varepsilon,d) = I_0(V;\varepsilon) + I_1(V;\lambda,\varepsilon)d + o(d), \tag{5.1}$$

where $I_0(V;\varepsilon)$ is the I-V relation without counting the ion size effect and $I_1(V;\lambda,\varepsilon)d$ is the leading term containing ion size effect on I-V relation.

Recall that we denote $H(1)=\int_0^1 h^{-1}(s)ds$ in (5.16).

Theorem 5.10. *In formula (5.1), one has*

$$\begin{aligned}
I_0(V;0)=&\rho_{00}(L_1,L_2,R_1,R_2)+\rho_{01}(L_1,L_2,R_1,R_2)\frac{e}{kT}V,\\
I_1(V;\lambda,0)=&\rho_{10}(L_1,L_2,R_1,R_2,\lambda)+\rho_{11}(L_1,L_2,R_1,R_2;\lambda)\frac{e}{kT}V,
\end{aligned}$$

where

$$\begin{aligned}
\rho_{00}=&\frac{z_1(D_1-D_2)(c_{10}^L-c_{10}^R)}{H(1)}+\frac{z_1(z_1D_1-z_2D_2)(c_{10}^L-c_{10}^R)}{H(1)(\ln c_{10}^L-\ln c_{10}^R)}\ln\frac{L_1R_2}{L_2R_1},\\
\rho_{01}=&\frac{z_1(z_1D_1-z_2D_2)(c_{10}^L-c_{10}^R)}{H(1)(\ln c_{10}^L-\ln c_{10}^R)},
\end{aligned}$$

$$\begin{aligned}
\rho_{10}=&\frac{z_1(D_1-D_2)}{H(1)}\left[c_{10}^Lw(L_1,L_2)-c_{10}^Rw(R_1,R_2)+\frac{\lambda z_1-z_2}{z_2}\left((c_{10}^L)^2-(c_{10}^R)^2\right)\right]\\
&-\frac{z_1(z_1D_1-z_2D_2)}{H(1)}\left[\frac{1-\lambda}{z_2}\frac{(c_{10}^L-c_{10}^R)^2}{\ln c_{10}^L-\ln c_{10}^R}-\frac{c_{10}^L-c_{10}^R}{\ln c_{10}^L-\ln c_{10}^R}(\phi_1^L-\phi_1^R)\right]\\
&+\frac{z_1(z_1D_1-z_2D_2)}{(z_1-z_2)H(1)}\frac{c_{10}^Lw(L_1,L_2)-c_{10}^Rw(R_1,R_2)}{\ln c_{10}^L-\ln c_{10}^R}\ln\frac{L_1R_2}{L_2R_1}\\
&+\frac{z_1(\lambda z_1-z_2)(z_1D_1-z_2D_2)}{(z_1-z_2)z_2H(1)}\frac{(c_{10}^L)^2-(c_{10}^R)^2}{\ln c_{10}^L-\ln c_{10}^R}\ln\frac{L_1R_2}{L_2R_1}\\
&-\frac{z_1(z_1D_1-z_2D_2)}{(z_1-z_2)H(1)}\frac{(c_{10}^L-c_{10}^R)(w(L_1,L_2)-w(R_1,R_2))}{(\ln c_{10}^L-\ln c_{10}^R)^2}\ln\frac{L_1R_2}{L_2R_1},
\end{aligned}$$

$$\begin{aligned}
\rho_{11}=&\frac{z_1(z_1D_1-z_2D_2)}{H(1)}\frac{c_{10}^Lw(L_1,L_2)-c_{10}^Rw(R_1,R_2)}{\ln c_{10}^L-\ln c_{10}^R}\\
&+\frac{z_1(\lambda z_1-z_2)(z_1D_1-z_2D_2)}{z_2H(1)}\frac{(c_{10}^L)^2-(c_{10}^R)^2}{\ln c_{10}^L-\ln c_{10}^R}
\end{aligned}$$

$$-\frac{z_1(z_1D_1-z_2D_2)}{H(1)}\frac{(c_{10}^L-c_{10}^R)(w(L_1,L_2)-w(R_1,R_2))}{(\ln c_{10}^L-\ln c_{10}^R)^2},$$

where c_{10}^L, c_{10}^R, ϕ_1^L and ϕ_1^R are given in Proposition 5.2 and

$$w(\alpha,\beta)=\alpha+\lambda\beta+\frac{\lambda z_1-z_2}{z_1-z_2}(\alpha+\beta).$$

Proof. For the zeroth order in ε, it follows from

$$\begin{aligned}\mathscr{I}(V;\lambda,0,d)=&z_1\mathscr{J}_1+z_2\mathscr{J}_2=z_1D_1J_1+z_2D_2J_2\\ &=(z_1D_1J_{10}+z_2D_2J_{20})+(z_1D_1J_{11}+z_2D_2J_{21})\,d+o(d)\end{aligned}\tag{5.2}$$

that

$$I_0(V;0)=z_1D_1J_{10}+z_2D_2J_{20}\ \text{ and }\ I_1(V;\lambda,0)=z_1D_1J_{11}+z_2D_2J_{21}.$$

The formulas for $I_0(V;0)$ and $I_1(V;0)$ follow directly from Lemmas 5.5 and 5.6. □

Corollary 5.11. *Under the electroneutrality conditions $z_1L_1=-z_2L_2=L$ and $z_1R_1=-z_2R_2=R$, one has*

$$\begin{aligned}I_0(V;0)=&\frac{(D_1-D_2)(L-R)}{H(1)}+\frac{(z_1D_1-z_2D_2)(L-R)}{H(1)(\ln L-\ln R)}\frac{e}{kT}V,\\ I_1(V;\lambda,0)=&\frac{(\lambda z_1-z_2)(D_2-D_1)(L^2-R^2)}{z_1z_2H(1)}-\frac{(1-\lambda)(z_1D_1-z_2D_2)(L-R)^2}{z_1z_2H(1)(\ln L-\ln R)}\\ &-\frac{(\lambda z_1-z_2)(z_1D_1-z_2D_2)(L-R)^2}{z_1z_2H(1)(\ln L-\ln R)^2}\left(\frac{(L+R)(\ln L-\ln R)}{L-R}-2\right)\frac{e}{kT}V.\end{aligned}$$

In particular, for fixed $R>0$, one has

$$\lim_{L\to R}I_0(V;0)=\frac{(z_1D_1-z_2D_2)R}{H(1)}\frac{e}{kT}V\ \text{ and }\ \lim_{L\to R}I_1(V;\lambda,0)=0.$$

Proof. Assume $z_1L_1 = -z_2L_2 = L$ and $z_1R_1 = -z_2R_2 = R$. It can be checked directly that

$$\begin{aligned}
\rho_{00} =& \frac{(D_1-D_2)(L-R)}{H(1)}, \quad \rho_{01} = \frac{(z_1D_1-z_2D_2)(L-R)}{H(1)(\ln L-\ln R)},\\
\rho_{10} =& \frac{(\lambda z_1-z_2)(D_2-D_1)(L^2-R^2)}{z_1z_2H(1)} - \frac{(1-\lambda)(z_1D_1-z_2D_2)(L-R)^2}{z_1z_2H(1)(\ln L-\ln R)},\\
\rho_{11} =& -\frac{(\lambda z_1-z_2)(z_1D_1-z_2D_2)(L-R)^2}{z_1z_2H(1)(\ln L-\ln R)^2}\left(\frac{(L+R)(\ln L-\ln R)}{L-R}-2\right).
\end{aligned} \tag{5.3}$$

The formulas for $I_0(V;0)$ and $I_1(V;0)$ then follow easily. The two limits can be shown easily too. □

Remark 5.12. *The above formulas for $I_0(V;0)$ and $I_1(V;\lambda,0)$ agree with those in [46] except for a factor $2H(1)$. The factor $H(1)$ does not appear in [46] since it is assumed there that $h(x)=1$, and hence, $H(1)=1$. The factor 2 in front of $H(1)$ is due to the fact that we are expending the I-V relation in the diameter d here instead of the radius r in [46]. As we mentioned in the introduction that there is a major difference between the analysis for the local hard sphere in this paper and that for the nonlocal model in [46]. Nevertheless, the agreement on $I_0(V;0)$ and $I_1(V;\lambda,0)$ is not a surprise since we are using the local hard sphere potential which is obtained as the expansion in the variable d from the nonlocal one used in [46].*

Critical potentials and ion size effects on I-V relations

Based on the approximation of I-V relations in Theorem 5.10, we will identify three critical potentials and discuss their roles in characterizing ion size effects on I-V relations.

Definition 5.13. *We define three potentials V_0, V_c and V^c by*

$$I_0(V_0;0)=0, \quad I_1(V_c;\lambda,0)=0, \quad \frac{d}{d\lambda}I_1(V^c;\lambda,0)=0.$$

For ion channels, the *reversal potential* is defined to be the potential V such that $\mathscr{I}(V;\lambda,\varepsilon)=0$. Thus, the potential V_0 is simply the zeroth order approximation in ε and d of the reversal potential. The critical potentials V_c and V^c are examined for the first time in [46] for a nonlocal hard-sphere model. The significance of the two critical values V_c and V^c is apparent from their definitions. The value V_c is the potential that balances ion size effect on I-V relations and the value V^c is the potential that separates the relative size effect on I-V relations. We provide precise statements below. First of all, note that $I_1(V;\lambda,0)$ is affine in V and in λ. Thus, quantities $\partial_V I_1(V;\lambda,0)$ and V_c depend on the boundary conditions L_1, L_2, R_1, R_2 and the ratio λ of ion sizes only; $\partial^2_{V\lambda} I_1(V;\lambda,0)$ and V^c depend on the boundary conditions L_1, L_2, R_1, R_2 but not on λ.

Theorem 5.14. *Suppose $\partial_V I_1(V;\lambda,0)>0$ (resp. $\partial_V I_1(V;\lambda,0)<0$).*

If $V>V_c$ (resp. $V<V_c$), then, for small $\varepsilon>0$ and $d>0$, the ion sizes enhance the current $\mathscr{I}$; that is, $\mathscr{I}(V;\varepsilon,d)>\mathscr{I}(V;\varepsilon,0)$;

If $V<V_c$ (resp. $V>V_c$), then, for small $\varepsilon>0$ and $d>0$, the ion sizes reduce the current $\mathscr{I}$; that is, $\mathscr{I}(V;\varepsilon,d)<\mathscr{I}(V;\varepsilon,0)$.

Theorem 5.15. *Suppose $\partial^2_{V\lambda} I_1(V;\lambda,0)>0$ (resp. $\partial^2_{V\lambda} I_1(V;\lambda,0)<0$).*

If $V>V^c$ (resp. $V<V^c$), then, for small $\varepsilon>0$ and $d>0$, the larger the negatively charged ion the larger the current; that is, the current $\mathscr{I}$ is increasing in λ;

If $V<V^c$ (resp. $V>V^c$), then, for small $\varepsilon>0$ and $d>0$, the smaller the negatively charged ion the larger the current; that is, the current $\mathscr{I}$ is decreasing in λ.

The following result in [46] can be checked easily.

Proposition 5.16. *Assume electroneutrality conditions $z_1L_1=-z_2L_2=L$ and $z_1R_1=-z_2R_2=R$, and $L\neq R$. Then,*

$$\partial_V I_1(V;\lambda,0)>0 \ \textit{and}\ \partial^2_{V\lambda} I_1(V;\lambda,0)>0.$$

As $R \to L$, $\partial_V I_1(V;\lambda,0) \to 0$ and $\partial^2_{V\lambda} I_1(V;\lambda,0) = O((L-R)^2)$. □

While both $\partial_V I_1(V;\lambda,0)$ and $\partial^2_{V\lambda} I_1(V;\lambda,0)$ are non-negative under electroneutrality conditions, in general, they can be negative. We do not have a complete result for the general case but the following partial result.

Proposition 5.17. *For any $L > 0$, $R_1^* > 0$ and $R_2^* > 0$ with $R_1^* R_2^* = L^2$, as $(R_1,R_2) \to (R_1^*,R_2^*)$,*

$$\begin{aligned}\partial_V I_1(V;\lambda,0) =& \frac{e}{kT}\rho_{11}(L,L,R_1,R_2;\lambda)\\ &\to \frac{e(D_1+D_2)L}{4kTH(1)R_1^*}(R_1^*-L)\left((3+\lambda)R_1^*-(1+3\lambda)L\right).\end{aligned}$$

The latter is negative if

$$\text{either } L < R_1^* < \frac{1+3\lambda}{3+\lambda}L \text{ for } \lambda > 1 \text{ or } \frac{1+3\lambda}{3+\lambda}L < R_1^* < L \text{ for } \lambda < 1.$$

As $(R_1,R_2) \to (R_1^*,R_2^*)$,

$$\partial_{V\lambda} I_1(V;\lambda,0) = \frac{e}{kT}\partial_\lambda \rho_{11}(L,L,R_1,R_2;\lambda) \to \frac{e(D_1+D_2)L}{4kTH(1)R_1^*}(R_1^*-L)(R_1^*-3L).$$

The latter is negative if $L < R_1^* < 3L$.

Proof. For $z_1 = -z_2 = 1$, we have

$$\begin{aligned}\partial_V I_1(V;\lambda,0) =& \frac{e}{kT}\rho_{11}(L_1,L_2,R_1,R_2;\lambda),\\ =& \frac{2e(D_1+D_2)}{kTH(1)}\frac{R_1^{1/2}R_2^{1/2}w(R_1,R_2)-L_1^{1/2}L_2^{1/2}w(L_1,L_2)}{\ln(R_1R_2)-\ln(L_1L_2)}\\ &-\frac{2e(1+\lambda)(D_1+D_2)}{kTH(1)}\frac{R_1R_2-L_1L_2}{\ln(R_1R_2)-\ln(L_1L_2)}\\ &-\frac{4e(D_1+D_2)}{kTH(1)}\frac{R_1^{1/2}R_2^{1/2}-L_1^{1/2}L_2^{1/2}}{\ln(R_1R_2)-\ln(L_1L_2)}\frac{w(R_1,R_2)-w(L_1,L_2)}{\ln(R_1R_2)-\ln(L_1L_2)}.\end{aligned}$$

Recall from Theorem 5.10 that, for $z_1 = -z_2 = 1$,

$$w(\alpha,\beta) = \alpha + \lambda\beta + \frac{1+\lambda}{2}(\alpha+\beta).$$

For fixed $a > 0$ and $b > 0$, we set

$$\rho(x,y;a,b) = \frac{H(1)}{D_1+D_2}\rho_{11}(a^2,b^2;x^2,y^2;\lambda).$$

Then, a direct calculation yields

$$\begin{aligned}\rho(x,y;a,b) =& \frac{xy-ab}{\ln(xy)-\ln(ab)}w_1(x^2,y^2) - (1+\lambda)\frac{x^2y^2-a^2b^2}{\ln(xy)-\ln(ab)} \\ &- \frac{xy-ab-ab(\ln(xy)-\ln(ab))}{(\ln(xy)-\ln(ab))^2}(w_1(x^2,y^2)-w_1(a^2,b^2)).\end{aligned}$$

Note that, as $z = xy \to ab$,

$$\frac{z-ab}{\ln z-\ln(ab)} \to ab, \quad \frac{z-ab-ab(\ln z-\ln(ab))}{(\ln z-\ln(ab))^2} \to \frac{ab}{2}, \quad \frac{z^2-a^2b^2}{\ln z-\ln(ab)} \to 2a^2b^2.$$

Thus, as $x \to x_0$ and $y \to y_0$ with $x_0y_0 = ab$,

$$\begin{aligned}\rho(x,y;a,b) \to& abw_1(x_0^2,y_0^2) - \frac{ab}{2}\left(w_1(x_0^2,y_0^2)-w_1(a^2,b^2)\right) - 2(1+\lambda)a^2b^2 \\ =& \frac{ab}{2}\left(w_1(x_0^2,y_0^2)+w_1(a^2,b^2)\right) - 2(1+\lambda)a^2b^2 \\ =& \frac{ab}{2}\left(w_1(x_0^2,y_0^2)+w_1(a^2,b^2)-4(1+\lambda)ab\right) \\ =& \frac{ab}{2}\left(\frac{3+\lambda}{2}x_0^2+\frac{1+3\lambda}{2}y_0^2+\frac{3+\lambda}{2}a^2+\frac{1+3\lambda}{2}b^2-4(1+\lambda)ab\right) \\ =& \frac{ab}{2x_0^2}\left(\frac{3+\lambda}{2}x_0^4+\left(\frac{3+\lambda}{2}a^2+\frac{1+3\lambda}{2}b^2-4(1+\lambda)ab\right)x_0^2+\frac{1+3\lambda}{2}a^2b^2\right).\end{aligned}$$

In particular, for $a = b$, as $x \to x_0$ and $y \to y_0$ with $x_0 y_0 = a^2$,

$$\begin{aligned}\rho(x,y;a,a) \to & \frac{a^2}{2x_0^2}\left(\frac{3+\lambda}{2}x_0^4 - 2(1+\lambda)a^2x_0^2 + \frac{1+3\lambda}{2}a^4\right)\\ =& \frac{a^2}{2x_0^2}\left(x_0^2 - a^2\right)\left(\frac{3+\lambda}{2}x_0^2 - \frac{1+3\lambda}{2}a^2\right).\end{aligned}$$

The latter is negative if

$$\text{either } \; a < x_0 < \sqrt{\frac{1+3\lambda}{3+\lambda}}a \;\text{ for }\; \lambda > 1 \;\text{ or }\; \sqrt{\frac{1+3\lambda}{3+\lambda}}a < x_0 < a \;\text{ for }\; \lambda < 1.$$

It can be directly translated to the statements for ρ_{11} and $\partial_\lambda \rho_{11}$. □

In the rest of this part, we discuss a number of properties of the critical potentials. It follows from Definition 5.13 and Theorem 5.10 that

Proposition 5.18. *The potentials V_0, V_c and V^c have the following expressions*

$$\begin{aligned}V_0 := V_0(L_1,L_2,R_1,R_2) &= -\frac{kT}{e}\frac{\rho_{00}(L_1,L_2,R_1,R_2)}{\rho_{01}(L_1,L_2,R_1,R_2)},\\ V_c := V_c(L_1,L_2,R_1,R_2;\lambda) &= -\frac{kT}{e}\frac{\rho_{10}(L_1,L_2,R_1,R_2;\lambda)}{\rho_{11}(L_1,L_2,R_1,R_2;\lambda)},\\ V^c := V^c(L_1,L_2,R_1,R_2;\lambda) &= -\frac{kT}{e}\frac{\rho_{10,\lambda}(L_1,L_2,R_1,R_2;\lambda)}{\rho_{11,\lambda}(L_1,L_2,R_1,R_2;\lambda)}.\end{aligned}$$

Remark 5.19. *The critical potentials V_0, V_c and V^c are independent of the cross-section area $h(x)$ of the channel.* □

When electroneutrality conditions $z_1L_1 = -z_2L_2 = L$ and $z_1R_1 = -z_2R_2 = R$ hold, we write

$$\begin{aligned}V_0(L,R) :=& V_0(L_1,L_2,R_1,R_2),\\ V_c(L,R;\lambda) :=& V_c(L_1,L_2,R_1,R_2;\lambda),\end{aligned}$$

$$V^c(L,R;\lambda) := V^c(L_1,L_2,R_1,R_2;\lambda).$$

Corollary 5.20. *Assume the electroneutrality boundary conditions $z_1L_1 = -z_2L_2 = L$ and $z_1R_1 = -z_2R_2 = R$. Then, we have*

$$\begin{aligned}
V_0(L,R) =& \frac{kT}{e}\frac{(D_1-D_2)}{z_1D_1-z_2D_2}\ln\frac{R}{L},\\
V_c(L,R;\lambda) =& \frac{kT}{e}\frac{\lambda-1}{\lambda z_1-z_2}f\left(\frac{L}{R}\right)-\frac{kT}{e}\frac{D_1-D_2}{z_1D_1-z_2D_2}g\left(\frac{L}{R}\right), \ \textit{if } L\neq R,\\
V^c(L,R;\lambda) =& \frac{kT}{e}\frac{1}{z_1}f\left(\frac{L}{R}\right)-\frac{kT}{e}\frac{D_1-D_2}{z_1D_1-z_2D_2}g\left(\frac{L}{R}\right), \ \textit{if } L\neq R,
\end{aligned}$$

where, for $x>0$,

$$f(x) = \frac{(x-1)\ln x}{(1+x)\ln x-2(x-1)}, \quad g(x) = \frac{(1+x)(\ln x)^2}{(1+x)\ln x-2(x-1)}. \tag{5.4}$$

Proof. The formulas follow directly from Proposition 5.18 and display (5.3). □

Lemma 5.21. *For the functions f and g defined in (5.4), one has*

(i) $f(x) = -f(1/x)$ *and* $g(x) = -g(1/x)$*;*

(ii) $\lim_{x\to1^+} f(x)\ln x = 6$, $\lim_{x\to\infty} f(x) = 1$, *and* $f'(x) < 0$ *for* $x > 1$*;*

(iii) $\lim_{x\to1^+} g(x)\ln x = 12$, $\lim_{x\to\infty}\frac{g(x)}{\ln x} = 1$, *and* $g(x)$ *has a unique positive minimum in* $(1,\infty)$.

Proof. The verifications of these properties are elementary. □

As a direct consequence of Corollary 5.20 and Lemma 5.21, one has

Corollary 5.22. *Assume the electroneutrality boundary conditions $z_1L_1 = -z_2L_2 = L$ and $z_1R_1 = -z_2R_2 = R$. Then,* *(i)* $V_0(L,R) = -V_0(R,L)$, $V_c(L,R;\lambda) = -V_c(R,L;\lambda)$, $V^c(L,R;\lambda) = -V^c(R,L;\lambda)$;

(ii) *for* $L \geq R$, $V_0(L,R)$ *is decreasing (resp. increasing) in* L *if* $D_1 > D_2$ *(resp.* $D_1 < D_2$*), and, for fixed* $R > 0$, $\lim_{L\to R} V_0(L,R) = 0$;

(iii) *for fixed* $R > 0$,

$$\begin{aligned}
&\lim_{L\to R} V_c(L,R;\lambda)(\ln L - \ln R) = \frac{kT}{e}\left(\frac{6(\lambda-1)}{\lambda z_1 - z_2} - \frac{12(D_1-D_2)}{z_1D_1 - z_2D_2}\right), \\
&\lim_{L\to R} V^c(L,R;\lambda)(\ln L - \ln R) = \frac{kT}{e}\frac{6z_1(D_2-D_1)+6(z_1-z_2)D_2}{z_1(z_1D_1-z_2D_2)}, \\
&\lim_{L\to\infty} \frac{V_c(L,R;\lambda)}{\ln L - \ln R} = \lim_{L\to\infty} \frac{V^c(L,R;\lambda)}{\ln L - \ln R} = -\frac{kT}{e}\frac{D_1-D_2}{z_1D_1-z_2D_2};
\end{aligned} \tag{5.5}$$

(iv) $V^c(L,R;\lambda) - V_c(L,R;\lambda) = \dfrac{kT}{e}\dfrac{z_1-z_2}{z_1(\lambda z_1 - z_2)} f\left(\dfrac{L}{R}\right)$, *and hence, for fixed* $R > 0$,

$$\begin{aligned}
&\lim_{L\to R} \left(V^c(L,R;\lambda) - V_c(L,R;\lambda)\right)(\ln L - \ln R) = \frac{kT}{e}\frac{6(z_1-z_2)}{z_1(\lambda z_1 - z_2)}, \\
&\lim_{L\to\infty} \left(V^c(L,R;\lambda) - V_c(L,R;\lambda)\right) = 1.
\end{aligned}$$

Scaling laws

Next result concerns the dependences of I_0, I_1, V_0, V_c and V^c on the boundary concentrations. For this discussion, we include the boundary conditions in the arguments of I_0, I_1, V_0, V_c and V^c; for example, we write I_0 as $I_0(V;L_1,L_2,R_1,R_2)$, etc..

Theorem 5.23. *The following scaling laws hold,*

(i) I_0 *scales* linearly *in boundary concentrations, that is, for any* $s > 0$,

$$I_0(V;sL_1,sL_2,sR_1,sR_2) = sI_0(V;L_1,L_2,R_1,R_2);$$

(ii) $I_1(V; sL_1, sL_2, sR_1, sR_2)$ *scales* quadratically *in boundary concentrations, that is, for any* $s > 0$,

$$I_1(V; sL_1, sL_2, sR_1, sR_2) = s^2 I_1(V; L_1, L_2, R_1, R_2);$$

(iii) V_0, V_c *and* V^c *are* invariant *under scaling in boundary concentrations, that is, for any* $s > 0$,

$$\begin{aligned} V_0(sL_1, sL_2, sR_1, sR_2) =& V_0(L_1, L_2, R_1, R_2), \\ V_c(sL_1, sL_2, sR_1, sR_2) =& V_c(L_1, L_2, R_1, R_2), \\ V^c(sL_1, sL_2, sR_1, sR_2) =& V^c(L_1, L_2, R_1, R_2). \end{aligned}$$

Proof. A direct observation gives

$$\begin{aligned} \rho_{00}(sL_1, sL_2, sR_1, sR_2) =& s\rho_{00}(L_1, L_2, R_1, R_2), \\ \rho_{01}(sL_1, sL_2, sR_1, sR_2) =& s\rho_{01}(L_1, L_2, R_1, R_2), \\ \rho_{10}(sL_1, sL_2, sR_1, sR_2, \lambda) =& s^2\rho_{10}(L_1, L_2, R_1, R_2; \lambda), \\ \rho_{11}(sL_1, sL_2, sR_1, sR_2, \lambda) =& s^2\rho_{11}(L_1, L_2, R_1, R_2; \lambda). \end{aligned}$$

The above scaling laws then follow from Theorem 5.10 and Proposition 5.18. □

Remark 5.24. *(i) Note that* I_0 *and* V_0 *are* not linear *in boundary concentrations, and* I_1, V_c *and* V^c *are* not quadratic *in boundary concentrations.*

(ii) Recall, from (5.1), that the zeroth order in ε *and first order in* d *approximation of the I-V relation* $\mathscr{I}(V; \lambda, \varepsilon, d)$ *is* $I_0 + I_1 d$. *Since* I_0 *and* I_1 *scale differently in boundary concentrations, the approximation* $I_0 + I_1 d$ *does not have a simple scaling law.*

(iii) It follows from the scaling laws for I_0 and I_1 that, at higher ion concentrations, the ion size effect becomes more significant. This is well expected. On the other hand, our scaling law results reveal a concrete way on how the ion size effect is manifested as the concentrations increase.

5.4.2 The flow rate $\mathscr{T}$ of matter

In this part, we briefly discuss ion size effects on the rate $\mathscr{T}$. Recall from (2.30) that The flow rate $\mathscr{T}$ of matter is

$$\mathscr{T}(V;\lambda,\varepsilon,d) = \mathscr{J}_1 + \mathscr{J}_2 = D_1 J_1 + D_2 J_2.$$

We have the following observation. Note that J_1 and J_2 are *independent* of D_1 and D_2. We will indicate the dependence of $\mathscr{T}$ and $\mathscr{I}$ on D_1 and D_2 explicitly and omit their dependences on other variables; that is, we denote the current $\mathscr{I}(V;\lambda,\varepsilon,d)$ in Section 5.4.1 by $\mathscr{I}(D_1,D_2)$, and $\mathscr{T}(V;\lambda,\varepsilon,d)$ by $\mathscr{T}(D_1,D_2)$. Then,

$$\mathscr{T}(D_1,D_2) = D_1 J_1 + D_2 J_2 = z_1 \frac{D_1}{z_1} J_1 + z_2 \frac{D_2}{z_2} J_2 = \mathscr{I}\left(\frac{D_1}{z_1}, \frac{D_2}{z_2}\right). \tag{5.6}$$

Therefore, all results in Section 5.4.1 on the current $\mathscr{I}$ can be translated to results on $\mathscr{T}$ by replacing D_1 and D_2 in Section 5.4.1 with D_1/z_1 and D_2/z_2, respectively. We will thus collect the results related to $\mathscr{T}$ only.

Similar to the expression for $\mathscr{I}$ in Section 5.4.1, we express $\mathscr{T}$ as

$$\mathscr{T}(V;\lambda,\varepsilon,d) = T_0(V;\varepsilon) + T_1(V;\lambda,\varepsilon)d + o(d). \tag{5.7}$$

Theorem 5.25. *In the expression (5.7), one has*

$$
\begin{aligned}
T_0(V;0) =& D_1J_{10}+D_2J_{20} = \sigma_{00}(L_1,L_2,R_1,R_2)+\sigma_{01}(L_1,L_2,R_1,R_2)\frac{e}{kT}V,\\
T_1(V;\lambda,0) =& D_1J_{11}+D_2J_{21} = \sigma_{10}(L_1,L_2,R_1,R_2;\lambda)+\sigma_{11}(L_1,L_2,R_1,R_2;\lambda)\frac{e}{kT}V,
\end{aligned}
$$

where

$$
\begin{aligned}
\sigma_{00} =& \frac{(z_2D_1-z_1D_2)(c_{10}^L-c_{10}^R)}{z_2H(1)}+\frac{z_1(D_1-D_2)(c_{10}^L-c_{10}^R)}{H(1)(\ln c_{10}^L-\ln c_{10}^R)}(\ln(L_1R_2)-\ln(L_2R_1)),\\
\sigma_{01} =& \frac{z_1(D_1-D_2)(c_{10}^L-c_{10}^R)}{H(1)(\ln c_{10}^L-\ln c_{10}^R)},
\end{aligned}
$$

$$
\begin{aligned}
\sigma_{10} =& \frac{z_2D_1-z_1D_2}{z_2H(1)}\left[c_{10}^Lw(L_1,L_2)-c_{10}^Rw(R_1,R_2)+\frac{\lambda z_1-z_2}{z_2}\left((c_{10}^L)^2-(c_{10}^R)^2\right)\right]\\
&-\frac{z_1(D_1-D_2)}{H(1)}\left[\frac{1-\lambda}{z_2}\frac{(c_{10}^L-c_{10}^R)^2}{\ln c_{10}^L-\ln c_{10}^R}-\frac{c_{10}^L-c_{10}^R}{\ln c_{10}^L-\ln c_{10}^R}(\phi_1^L-\phi_1^R)\right]\\
&+\frac{z_1(D_1-D_2)}{(z_1-z_2)H(1)}\frac{c_{10}^Lw(L_1,L_2)-c_{10}^Rw(R_1,R_2)}{\ln c_{10}^L-\ln c_{10}^R}(\ln(L_1R_2)-\ln(L_2R_1))\\
&+\frac{z_1(\lambda z_1-z_2)(D_1-D_2)}{(z_1-z_2)z_2H(1)}\frac{(c_{10}^L)^2-(c_{10}^R)^2}{\ln c_{10}^L-\ln c_{10}^R}(\ln(L_1R_2)-\ln(L_2R_1))\\
&-\frac{z_1(D_1-D_2)}{(z_1-z_2)H(1)}\frac{(c_{10}^L-c_{10}^R)(w(L_1,L_2)-w(R_1,R_2))}{(\ln c_{10}^L-\ln c_{10}^R)^2}(\ln(L_1R_2)-\ln(L_2R_1)),
\end{aligned}
$$

$$
\begin{aligned}
\sigma_{11} =& \frac{z_1(D_1-D_2)}{H(1)}\frac{c_{10}^Lw(L_1,L_2)-c_{10}^Rw(R_1,R_2)}{\ln c_{10}^L-\ln c_{10}^R}\\
&+\frac{z_1(\lambda z_1-z_2)(D_1-D_2)}{z_2H(1)}\frac{(c_{10}^L)^2-(c_{10}^R)^2}{\ln c_{10}^L-\ln c_{10}^R}\\
&-\frac{z_1(D_1-D_2)}{H(1)}\frac{(c_{10}^L-c_{10}^R)(w(L_1,L_2)-w(R_1,R_2))}{(\ln c_{10}^L-\ln c_{10}^R)^2}.
\end{aligned}
$$

Definition 5.26. *Define three potentials $\hat{V}_0$, $\hat{V}_c$ and $\hat{V}^c$ by*

$$T_0(\hat{V}_0;0)=0, \quad T_1(\hat{V}_c;\lambda,0)=0, \quad \frac{d}{d\lambda}T_1(\hat{V}^c;\lambda,0)=0.$$

It follows from the definition that

Proposition 5.27. *The potentials $\hat{V}_0$, $\hat{V}_c$ and $\hat{V}^c$ have the following expressions*

$$\begin{aligned}\hat{V}_0 &= -\frac{kT}{e}\frac{\sigma_{00}(L_1,L_2,R_1,R_2)}{\sigma_{01}(L_1,L_2,R_1,R_2)},\\ \hat{V}_c &= -\frac{kT}{e}\frac{\sigma_{10}(L_1,L_2,R_1,R_2;\lambda)}{\sigma_{11}(L_1,L_2,R_1,R_2;\lambda)},\\ \hat{V}^c &= -\frac{kT}{e}\frac{\sigma_{10,\lambda}(L_1,L_2,R_1,R_2;\lambda)}{\sigma_{11,\lambda}(L_1,L_2,R_1,R_2;\lambda)}.\end{aligned}$$

We have the following *scaling laws*:

Theorem 5.28. *For any $s>0$,*

$$\begin{aligned}\sigma_{00}(sL_1,sL_2,sR_1,sR_2) =& s\sigma_{00}(L_1,L_2,R_1,R_2),\\ \sigma_{01}(sL_1,sL_2,sR_1,sR_2) =& s\sigma_{01}(L_1,L_2,R_1,R_2),\\ \sigma_{10}(sL_1,sL_2,sR_1,sR_2,\lambda) =& s^2\sigma_{10}(L_1,L_2,R_1,R_2;\lambda),\\ \sigma_{11}(sL_1,sL_2,sR_1,sR_2,\lambda) =& s^2\sigma_{11}(L_1,L_2,R_1,R_2;\lambda).\end{aligned}$$

As a consequence, $T_0(V;0)$ scales linearly *in boundary concentrations and $T_1(V;\lambda,0)$ scales* quadratically *in boundary concentrations, and the values $\hat{V}_0$, $\hat{V}_c$ and $\hat{V}^c$ are* invariant *under scaling in boundary concentrations.* □

Theorem 5.29. *Suppose $\partial_V T_1(V;\lambda,0)>0$ (resp. $\partial_V T_1(V;\lambda,0)<0$).*

If $V>\hat{V}_c$ (resp. $V<\hat{V}_c$), then, for small $\varepsilon>0$ and $d>0$, the ion sizes enhance $\mathscr{T}$; that is, $\mathscr{T}(V;\varepsilon,d)>\mathscr{T}(V;\varepsilon,0)$;

If $V < \hat{V}_c$ (resp. $V > \hat{V}_c$), then, for small $\varepsilon > 0$ and $d > 0$, the ion sizes reduce $\mathscr{T}$; that is, $\mathscr{T}(V;\varepsilon,d) < \mathscr{T}(V;\varepsilon,0)$.

Theorem 5.30. *Suppose $\partial^2_{V\lambda}T_1(V;\lambda,0) > 0$ (resp. $\partial^2_{V\lambda}T_1(V;\lambda,0) < 0$).*

If $V > \hat{V}^c$ (resp. $V < \hat{V}^c$), then, for small $\varepsilon > 0$ and $d > 0$, the larger the negatively charged ion the larger $\mathscr{T}$; that is, $\mathscr{T}$ increases λ;

If $V < \hat{V}^c$ (resp. $V > \hat{V}^c$), then, for small $\varepsilon > 0$ and $d > 0$, the smaller the negatively charged ion the larger $\mathscr{T}$; that is, $\mathscr{T}$ decreases λ.

Corollary 5.31. *Assume the electroneutrality conditions $z_1L_1 = -z_2L_2 = L$ and $z_1R_1 = -z_2R_2 = R$, and $L \neq R$. Then*

$$\begin{aligned}
T_0(V;0) =& \frac{(z_2D_1 - z_1D_2)(L-R)}{z_1z_2H(1)} + \frac{(D_1-D_2)(L-R)}{H(1)(\ln L - \ln R)}\frac{e}{kT}V,\\
T_1(V;\lambda,0) =& \frac{(\lambda z_1 - z_2)(z_2D_2 - z_1D_1)(L^2-R^2)}{z_1^2z_2^2H(1)} - \frac{(1-\lambda)(D_1-D_2)(L-R)^2}{z_1z_2H(1)(\ln L - \ln R)}\\
&- \frac{(\lambda z_1 - z_2)(D_1-D_2)(L-R)^2}{z_1z_2H(1)(\ln L - \ln R)^2}\left(\frac{(L+R)(\ln L - \ln R)}{L-R} - 2\right)\frac{e}{kT}V.
\end{aligned}$$

and hence,

$$\begin{aligned}
\hat{V}_0 =& \frac{kT}{e}\frac{(z_2D_1 - z_1D_2)(\ln R - \ln L)}{z_1z_2(D_1-D_2)},\\
\hat{V}_c =& \frac{kT}{e}\frac{(\lambda-1)(\ln L - \ln R)(L-R)}{(\lambda z_1 - z_2)[(\ln L - \ln R)(L+R) - 2(L-R)]}\\
&- \frac{kT}{e}\frac{(z_2D_1 - z_1D_2)(\ln L - \ln R)^2(L+R)}{z_1z_2(D_1-D_2)[(\ln L - \ln R)(L+R) - 2(L-R)]},\\
\hat{V}^c =& \frac{kT}{e}\frac{(\ln L - \ln R)(L-R)}{z_1[(\ln L - \ln R)(L+R) - 2(L-R)]}\\
&- \frac{kT}{e}\frac{(z_2D_1 - z_1D_2)(\ln L - \ln R)^2(L+R)}{z_1z_2(D_1-D_2)[(\ln L - \ln R)(L+R) - 2(L-R)]}.
\end{aligned}$$

Note also that, under electroneutrality conditions,

$$
\begin{aligned}
\partial_V T_1(V;\lambda,0) &= -\frac{e(\lambda z_1 - z_2)(D_1 - D_2)(L-R)^2}{z_1 z_2 kTH(1)(\ln L - \ln R)^2}\left(\frac{(L+R)(\ln L - \ln R)}{L-R} - 2\right)\\
\partial_{V\lambda} T_1(V;\lambda,0) &= -\frac{(D_1 - D_2)(L-R)^2}{z_2 H(1)(\ln L - \ln R)^2}\left(\frac{(L+R)(\ln L - \ln R)}{L-R} - 2\right)\frac{e}{kT}.
\end{aligned}
$$

Proposition 5.32. *Assume electroneutrality conditions $z_1L_1 = -z_2L_2 = L$ and $z_1R_1 = -z_2R_2 = R$, and $L \neq R$. If $D_1 > D_2$, then*

$$\partial_V T_1(V;\lambda,0) > 0 \ \text{ and } \ \partial^2_{V\lambda} T_1(V;\lambda,0) > 0;$$

if $D_1 < D_2$, then

$$\partial_V T_1(V;\lambda,0) < 0 \ \text{ and } \ \partial^2_{V\lambda} T_1(V;\lambda,0) < 0.$$

In either case, as $R \to L$,

$$\partial_V T_1(V;\lambda,0) \to 0 \ \text{ and } \ \partial^2_{V\lambda} T_1(V;\lambda,0) = O((L-R)^2).$$

Proof. It can be checked directly or follows from Theorem 5.16 and the relation (5.6) between T_1 and I_1. □

In general, $\partial_V T_1(V;\lambda,0)$ and $\partial^2_{V\lambda} T_1(V;\lambda,0)$ can be negative (resp. positive) for $D_1 > D_2$ (resp. $D_1 < D_2$). In particular, we have

Proposition 5.33. *For $z_1 = -z_2 = 1$ and for any $L > 0$, $R_1^* > 0$ and $R_2^* > 0$ with $R_1^*R_2^* = L^2$, as $(R_1,R_2) \to (R_1^*,R_2^*)$,*

$$\partial_V T_1(V;\lambda,0) \to \frac{(D_1 - D_2)L}{4H(1)R_1^*}(R_1^* - L)\left((3+\lambda)R_1^* - (1+3\lambda)L\right). \qquad (5.8)$$

For $D_1 > D_2$ (resp. $D_1 < D_2$), the limit is negative (resp. positive) if

$$\text{either } L < R_1^* < \frac{1+3\lambda}{3+\lambda}L \text{ for } \lambda > 1 \text{ or } \frac{1+3\lambda}{3+\lambda}L < R_1^* < L \text{ for } \lambda < 1.$$

As $(R_1, R_2) \to (R_1^*, R_2^*)$,

$$\partial_{V\lambda} T_1(V;\lambda,0) \to \frac{(D_1-D_2)L}{4H(1)R_1^*}\left(R_1^*-L\right)\left(R_1^*-3L\right).$$

For $D_1 > D_2$ (resp. $D_1 < D_2$), the limit is negative (resp. positive) if $L < R_1^* < 3L$.

Proof. It follows from Theorem 5.17 and the relation (5.6) between T_1 and I_1. $\square$

Chapter 6

Summary

There are two parts in this chapter. In the first part we briefly summarize the results of the last three chapters. In the second part, a brief discussion of our future work is provided.

6.1 Summary of results

As a basic electrodiffusion equations modeling, the Poisson-Nernst-Planck system has been studied to a great extent both analytically and numerically. In particular, in [24, 46, 57, 58, 60, 61, 62], under the framework of *geometric singular perturbation theory*, some interesting and new phenomenon have been investigated both numerically and analytically, in particular, the ion size effect on the I-V relations is studied and some important critical potential values are investigated and numerically detected.

In this dissertation, first in Chapter 3, we analyzed a one dimensional steady-state cPNP system by applying the method of *Matched Asymptotic Expansion*. Our main interest is to study the I-V relation of a single channel, in particular, we focus on the *cubic-like* feature of the I-V relation for a *single* channel. Our results turn out that, up to the third order in ε, a singular parameter, the I-V relation is indeed a cubic function in the potential V. Moreover, if the initial concentrations applied at the two ends of the channel is not equal, the I-V relation has *three distinct* real roots, which corresponds to the bi-stable structure in the FitzHugh-Nagumo simplification of the Hodgkin-Huxley model. However, for the fourth order system, the I-V relation is *quintic* instead of being cubic. Numerical simulations are performed, and the numerical results are consistent with the analytical ones.

In Chapter 4, we numerically studied a one-dimensional steady-state PNP model including the ion size effect modeled by a *non-local* hard-sphere potential from *density functional theory*. The work is motivated by [46], where, for the same setup, the PNP system is studied analytically. The main purpose here is to detect two *critical potentials* first observed in [46]. To achieve this goal, two numerical tasks are conducted respectively. The first one is a numerical approach of solving the PNP system and obtaining I-V curves, while the second task is to numerically detect two critical potential values V^c and V_c for two cases respectively, one is for the case with zero permanent charge, exactly the same setup as in [46], the other case involves a nonzero piecewise constant permanent charge function. Based on the defining properties of these two critical potentials and by using the numerical I-V curves directly, for the setting in [46], our numerical results agree well with the analytical predictions.

In Chapter 5, a one-dimensional steady-state PNP model including the ion size effect modeled by a *local* hard-sphere potential that depends pointwise on ion concentrations is analyzed with totally different mathematical treatment from the one used in [46]. Based on the geometric singular perturbation theory, in particular, on specific structures of this concrete model, the existence of solutions to the boundary value problem for small ion sizes is established and, treating the ion sizes as small parameters, an approximation of the I-V relation is derived and two critical potentials for ion size effects are identified. Important scaling laws of I-V relations and critical potentials in boundary concentrations are obtained. Under electroneutrality conditions, up to the first order in d, our results are consistent with the ones in [46]. Moreover, without the electroneutrality conditions, partial results about the ion size effect are also obtained. As a byproduct, the ion size effects on the flow of matter are also discussed.

6.2 Future work

Basically speaking, there are three directions for our future work. In one direction, we will focus on the multiplicity and stability of the solutions to classical Poisson-Nernst-planck (cPNP) systems, that is, we ignore the ion-to-ion interaction and treat them as point charged. The existence of multiple solutions has already been investigated, even for a oversimplified case with only two different ion species involved (see [24]). In one of our projects in process, for a very simple case involving two different ion species and with nonzero permanent charges, an important characterization of ion channels, triple solutions are numerically detected. Moreover, the numerical simulation shows that multiple stable solutions are possible for some cases. A systematic study of the stability problem will be one of our near future projects and we believe it will be very interesting, but definitely very challenging.

The other direction is to study the cPNP system involving more ion species (at least 3). The reason is that some biological phenomena of importance do not appear until three or more ion species are involved. For example, the crucial finding for voltage activated Na channels (which make the action potential) is that a third ion (it must be Ca in the case considered) cannot be ignored in addition to Na and Cl and biological conditions, such as magnitudes of concentrations at both ends, have to be within a specific range for the channel to work (for more information, see [58]). New phenomenon has been investigated when three or more different ion species are involved. More precisely, it is possible to have spatially oscillating solutions when three or more ion species are involved, moreover, the spatially oscillating solutions and the spatially non-oscillating solutions can co-exist. An oversimplified example studied in [58] has shown this interesting phenomenon. A systematic investigation for more general case is expected to reveal more interesting behaviors. Also, the co-existence of spatially oscillating solutions and spatially non-oscillating solutions give another form of multiple solutions. A natural question arising here is which solution is more stable?

Finally, we consider the PNP systems including the hard-sphere potential component (modeled either *locally* or *nonlocally*), that is, we study the ion size effects on the topics that we are interested in, such as the I-V relations, critical potentials, multiplicity and stability of solutions. This direction is much more challenging, but definitely more interesting.

Bibliography

[1] N. Abaid, R. S. Eisenberg, and W. Liu, Asymptotic expansions of I-V relations via a Poisson-Nernst-Planck system. *SIAM J. Appl. Dyn. Syst.* **7** (2008), 1507-1526. Cited on 5, 7, 26, 27, 28, 31, 32, 35, 42, 44, 45

[2] S. Aboud, D. Marreiro, M. Saraniti, and R. S. Eisenberg, A Poisson P3M Force Field Scheme for Particle-Based Simulations of Ionic Liquids. *J. Comput. Electronics* **3** (2004), 117-133. Cited on 3

[3] M. Z. Bazant, M. S. Kilic, B. D. Storey, and A. Ajdari, Towards an understanding of induced-charge electrokinetics at large applied voltages in concentrated solutions. *Adv. Colloid Interface Sci.* **152** (2009), 48-88. Cited on 9

[4] V. Barcilon, Ion flow through narrow membrane channels: Part I. *SIAM J. Appl. Math.* **52** (1992), 1391-1404. Cited on 2, 3, 64

[5] V. Barcilon, D.-P. Chen, and R. S. Eisenberg, Ion flow through narrow membrane channels: Part II. *SIAM J. Appl. Math.* **52** (1992), 1405-1425. Cited on 2, 7, 64

[6] V. Barcilon, D.-P. Chen, R. S. Eisenberg, and J. W. Jerome, Qualitative properties of steady-state Poisson-Nernst-Planck systems: Perturbation and simulation study. *SIAM J. Appl. Math.* **57** (1997), 631-648. Cited on 2, 7, 27

[7] J. J. Bikerman, Structure and capacity of the electrical double layer. *Philos. Mag.* **33** (1942), 384. Cited on 9

[8] D. Boda, D. Gillespie, W. Nonner, D. Henderson, and B. Eisenberg, Computing induced charges in inhomogeneous dielectric media: application in a Monte Carlo simulation of complex ionic systems. *Phys. Rev. E* **69** (2004), 046702 (1-10). Cited on 3

[9] D. Boda, D. Busath, B. Eisenberg, D. Henderson, and W. Nonner, Monte Carlo simulations of ion selectivity in a biological Na+ channel: charge-space competition. *Phys. Chem. Chem. Phys.* **4** (2002), 5154-5160. Cited on 3, 9, 64

[10] M. Burger, R. S. Eisenberg, and H. W. Engl, Inverse problems related to ion channel selectivity. *SIAM J. Appl. Math.* **67** (2007), 960-989. Cited on 7

[11] A. E. Cardenas, R. D. Coalson, and M. G. Kurnikova, Three-Dimensional Poisson-Nernst-Planck Theory Studies: Influence of Membrane Electrostatics on Gramicidin A Channel Conductance. *Biophys. J.* **79** (2000), 80-93. Cited on 7

[12] D. P. Chen and R. S. Eisenberg, Charges, currents and potentials in ionic channels of one conformation. *Biophys. J.* **64** (1993), 1405-1421. Cited on 7

[13] S. Chung and S. Kuyucak, Predicting channel function from channel structure using Brownian dynamics simulations. *Clin. Exp. Pharmacol Physiol.* **28** (2001), 89-94. Cited on 3

[14] R. D. Coalson, Poisson-Nernst-Planck theory approach to the calculation of current through biological ion channels. *IEEE Trans Nanobioscience* **4** (2005), 81-93. Cited on 7

[15] R. D. Coalson, Discrete-state model of coupled ion permeation and fast gating in ClC chloride channels. *J. Phys. A* **41** (2009), 115001. Cited on

[16] R. Coalson and M. Kurnikova, Poisson-Nernst-Planck theory approach to the calculation of current through biological ion channels. *IEEE Transaction on NanoBioscience* **4** (2005), 81-93. Cited on 7

[17] Eckhaus, W. *Asymptotic Analysis of Singular Perturbations.* Studies in Mathematics and its Applications, **9**. North-Holland Publishing Co., Amsterdam-New York, 1979. Cited on 16

[18] Eckhaus, W. Fundamental concepts of matching. *SIAM Rev.* **36** (1994), 431–439. Cited on 16

[19] B. Eisenberg, Ion Channels as Devices. *J. Comp. Electro.* **2** (2003), 245-249. Cited on 5

[20] B. Eisenberg, Proteins, Channels, and Crowded Ions. *Biophys. Chem.* **100** (2003), 507 - 517. Cited on 5

[21] R. S. Eisenberg, Channels as enzymes. *J. Memb. Biol.* **115** (1990), 1-12. Cited on 5

[22] R. S. Eisenberg, From Structure to Function in Open Ionic Channels. *J. Memb. Biol.* **171** (1999), 1-24. Cited on

[23] B. Eisenberg, Y. Hyon, and C. Liu, Energy variational analysis of ions in water and channels: Field theory for primitive models of complex ionic fluids. *J. Chem. Phys.* **133** (2010), 104104 (1-23). Cited on 3, 5

[24] B. Eisenberg and W. Liu, Poisson-Nernst-Planck systems for ion channels with permanent charges. *SIAM J. Math. Anal.* **38** (2007), 1932-1966. Cited on 2, 5, 7, 25, 27, 64, 80, 93, 98, 99, 109, 129, 131

[25] R. Evans, The nature of the liquid-vapour interface and other topics in the statistical mechanics of non-uniform, classical fluids. *Adv. Phys.* **28** (1979), 143-200. Cited on 9

[26] R. Evans, Density functionals in the theory of nonuniform fluids, in *Fundamentals of of inhomogeneous fluids*, ed. D. Henderson (New York: Dekker), 85-176, (1992). Cited on 9

[27] Fenichel, N. Persistence and Smoothness of Invariant Manifolds for Flows. *Ind. Univ. Math. J.* **21** (1971), pp. 193-225. Cited on 19

[28] Fenichel, N. Geometric singular perturbation theory for ordinary differential equations. *J. Differential Equations.***31** (1979), pp.53-98. Cited on 5

[29] J. Fischer and U. Heinbuch, Relationship between free energy density functional, Born-Green-Yvon, and potential distribution approaches for inhomogeneous fluids. *J. Chem. Phys.* **88** (1988), 1909-1913. Cited on 9, 10, 65

[30] D. Gillespie, A singular perturbation analysis of the Poisson-Nernst-Planck system: Applications to Ionic Channels. *Ph.D Dissertation*, Rush University at Chicago, 1999. Cited on 1, 2, 5, 7, 25, 27, 64

[31] D. Gillespie, W. Nonner, and R. S. Eisenberg, Coupling Poisson-Nernst-Planck and density functional theory to calculate ion flux. *J. Phys.: Condens. Matter* **14** (2002), 12129-12145. Cited on 3, 6, 7, 9, 64

[32] D. Gillespie, W. Nonner, and R. S. Eisenberg, Density functional theory of charged, hard-sphere fluids. *Phys. Rev. E* **68** (2003), 0313503 (1-10). Cited on 9, 64

[33] D. Gillespie, W. Nonner, and R. S. Eisenberg, Crowded Charge in Biological Ion Channels. *Nanotech.* **3** (2003), 435-438. Cited on 6, 9, 64

[34] P. Graf, M. G. Kurnikova, R. D. Coalson, and A. Nitzan, Comparison of Dynamic Lattice Monte-Carlo Simulations and Dielectric Self Energy Poisson-Nernst-Planck Continuum Theory for Model Ion Channels. *J. Phys. Chem. B* **108** (2004), 2006-2015. Cited on 7

[35] Morris W. Hirsch, Charles C. Pugh, and Michael Shub, Invariant manifolds. *Springer Lecture Notes in Mathematics***583** (1977). Cited on 19

[36] U. Hollerbach, D.-P. Chen, and R. S. Eisenberg, Two- and Three-Dimensional Poisson-Nernst-Planck Simulations of Current Flow through Gramicidin-A. *J. Comp. Science* **16** (2002), 373-409. Cited on 7

[37] U. Hollerbach, D. Chen, W. Nonner, and B. Eisenberg, Three-dimensional Poisson-Nernst-Planck Theory of Open Channels. *Biophys. J.* **76** (1999), p. A205. Cited on 5, 7

[38] Y. Hyon, B. Eisenberg, and C. Liu, A mathematical model for the hard sphere repulsion in ionic solutions. *Commun. Math. Sci.* **9** (2010), 459-475. Cited on 3

[39] Y. Hyon, J. Fonseca, B. Eisenberg, and C. Liu, A new Poisson-Nernst-Planck equation (PNP-FS-IF) for charge inversion near walls. *Biophys. J.* **100** (2011), 578a. Cited on 3, 5

[40] Y. Hyon, J. Fonseca, B. Eisenberg, and C. Liu, Energy variational approach to study charge inversion (layering) near charged walls. *Discrete Contin. Dyn. Syst. Ser. B* **17** (2012), 2725-2743. Cited on 3

[41] Y. Hyon, C. Liu, and B. Eisenberg, PNP equations with steric effects: a model of ion flow through channels. *J. Phys. Chem. B* **116** (2012), 11422-11441. Cited on 3, 5

[42] W. Im, D. Beglov, and B. Roux, Continuum solvation model: Electrostatic forces from numerical solutions to the Poisson-Bolztmann equation. *Comp. Phys. Comm.* **111** (1998), 59-75. Cited on 3

[43] W. Im and B. Roux, Ion permeation and selectivity of OmpF porin: a theoretical study based on molecular dynamics, Brownian dynamics, and continuum electrodiffusion theory. *J. Mol. Biol.* **322** (2002), 851-869. Cited on 3, 7, 64

[44] J. W. Jerome, *Mathematical Theory and Approximation of Semiconductor Models.* Springer-Verlag, New York, 1995. Cited on 7, 64

[45] J. W. Jerome and T. Kerkhoven, A finite element approximation theory for the drift-diffusion semiconductor model. *SIAM J. Numer. Anal.* **28** (1991), 403-422. Cited on 7

[46] S. Ji and W. Liu, Poisson-Nernst-Planck Systems for Ion Flow with Density Functional Theory for Hard-Sphere Potential: I-V relations and Critical Potentials. Part I: Analysis. *J. Dyn. Diff. Equat.* **24** (2012), 955-983. Cited on iv, v, 3, 5, 10, 27, 63, 64, 65, 66, 67, 68, 69, 71, 72, 73, 74, 76, 77, 78, 85, 86, 87, 89, 115, 116, 129, 130

[47] C. Jones, Geometric singular perturbation theory. *Dynamical systems (Montecatini Terme, 1994)*, pp. 44-118. Lect. Notes in Math. **1609**, Springer, Berlin, 1995. Cited on 5, 20, 92, 109, 110

[48] C. Jones, T. Kaper, and N. Kopell, Tracking invariant manifolds up tp exponentially small errors. *SIAM J. Math. Anal.* **27** (1996), 558-577. Cited on 109, 110

[49] C. Jones and N. Kopell, Tracking invariant manifolds with differential forms in singularly perturbed systems. *J. Differential Equations* **108** (1994), 64-88. Cited on 5, 109, 110

[50] M. S. Kilic, M. Z. Bazant, and A. Ajdari, Steric effects in the dynamics of electrolytes at large applied voltages. II. Modified Poisson-Nernst-Planck equations. *Phys. Rev. E* **75** (2007), 021503 (11 pages). Cited on

[51] M. G. Kurnikova, R. D. Coalson, P. Graf, and A. Nitzan, A Lattice Relaxation Algorithm for 3D Poisson-Nernst-Planck Theory with Application to Ion Transport Through the Gramicidin A Channel. *Biophys. J.* **76** (1999), 642-656. Cited on 7

[52] J. Kierzenka, and L. Shampine, A BVP Solver Based on Residual Control and the Matlab PSE. *ACM Trans. Math. Software* **27** (2001), pp. 299-316. Cited on 20, 22, 72

[53] Lagerstrom, P. A. *Matched Asymptotic Expansions.* Springer-Verlag, New York, 1988. Cited on 16

[54] Liu, W. Geometric singular perturbation approach to steady-state Poisson-Nernst-Planck systems. *SIAM J. Appl. Math.* **65** (2005), 754-766. Cited on 27

[55] B. Li, Minimizations of electrostatic free energy and the Poisson-Boltzmann equation for molecular solvation with implicit solvent. *SIAM J. Math. Anal.* **40** (2009), 2536-2566. Cited on 3

[56] B. Li, Continuum electrostatics for ionic solutions with non-uniform ionic sizes. *Nonlinearity* **22** (2009), 811-833. Cited on 3

[57] W. Liu, Geometric singular perturbation approach to steady-state Poisson-Nernst-Planck systems. *SIAM J. Appl. Math.* **65** (2005), 754-766. Cited on 5, 7, 93, 98, 99, 107, 109, 129

[58] W. Liu, One-dimensional steady-state Poisson-Nernst-Planck systems for ion channels with multiple ion species. *J. Differential Equations* **246** (2009), 428-451. Cited on 5, 7, 25, 27, 31, 64, 80, 93, 98, 99, 109, 129, 131, 132

[59] Liu, W. Exchange lemmas for singular perturbations with certain turning points. *J. Differential Equations* **167** (2000), pp. 134-180. Cited on 5, 20

[60] G. Lin, W. Liu, Y.Yi, and M. Zhang, Poisson-Nernst-Plank systems for ion flow with density functional theory for local hard sphere potential. *SIAM J. on Applied Dynamical Systems* Accepted. Cited on 129

[61] W. Liu, X. Tu, and M. Zhang, Poisson-Nernst-Planck Systems for Ion Flow with Density Functional Theory for Hard-Sphere Potential: I-V relations and Critical Potentials. Part II: Numerics. *J. Dyn. Diff. Equat.* **24** (2012), 985-1004. Cited on 5, 27, 86, 129

[62] W. Liu and B. Wang, Poisson-Nernst-Planck systems for narrow tubular-like membrane channels. *J. Dyn. Diff. Equat.* **22** (2010), 413-437. Cited on 5, 7, 129

[63] M. S. Mock, An example of nonuniqueness of stationary solutions in device models. *COMPEL* **1** (1982), 165-174. Cited on 7, 25

[64] B. Nadler, Z. Schuss, A. Singer, and B. Eisenberg, Diffusion through protein channels: from molecular description to continuum equations. *Nanotech.* **3** (2003), 439-442. Cited on 3

[65] W. Nonner and R. S. Eisenberg, Ion permeation and glutamate residues linked by Poisson-Nernst-Planck theory in L-type Calcium channels. *Biophys. J.* **75** (1998), 1287-1305. Cited on 2, 5, 7

[66] S. Y. Noskov, S. Berneche, and B. Roux, Control of ion selectivity in potassium channels by electrostatic and dynamic properties of carbonyl ligands. *Nature* **431** (2004), 830-834. Cited on

[67] S. Y. Noskov, W. Im, and B. Roux, Ion Permeation through the z_1-Hemolysin Channel: Theoretical Studies Based on Brownian Dynamics and Poisson-Nernst-Planck Electrodiffusion Theory. *Biophys. J.* **87** (2004), 2299-2309. Cited on 3

[68] S. Y. Noskov and B. Roux, Ion selectivity in potassium channels. *Biophys. Chem.* **124** (2006), 279-291. Cited on

[69] J.-K. Park and J. W. Jerome, Qualitative properties of steady-state Poisson-Nernst-Planck systems: Mathematical study. *SIAM J. Appl. Math.* **57** (1997), 609-630. Cited on 7

[70] Lawrence Perko, Differential Equations and Dynamical Systems (Texts in Applied Mathematics), 3rd edition. Cited on 5, 12, 13

[71] J. K. Percus, Equilibrium state of a classical fluid of hard rods in an external field. *J. Stat. Phys.* **15** (1976), 505-511. Cited on 10, 65

[72] J. K. Percus, Model grand potential for a nonuniform classical fluid. *J. Chem. Phys.* **75** (1981), 1316-1319. Cited on 10, 65

[73] A. Robledo and C. Varea, On the relationship between the density functional formalism and the potential distribution theory for nonuniform fluids. *J. Stat. Phys.* **26** (1981), 513-525. Cited on 10, 65

[74] Y. Rosenfeld, Free-Energy Model for the Inhomogeneous Hard-Sphere Fluid Mixture and Density-Functional Theory of Freezing. *Phys. Rev. Lett.* **63** (1989), 980-983. Cited on 9, 10, 65

[75] Y. Rosenfeld, Free energy model for the inhomogeneous fluid mixtures: Yukawa-charged hard spheres, general interactions, and plasmas. *J. Chem. Phys.* **98** (1993), 8126-8148. Cited on 9, 10, 65

[76] R. Roth, Fundamental measure theory for hard-sphere mixtures: a review. *J. Phys.: Condens. Matter* **22** (2010), 063102 (1-18). Cited on 9, 10

[77] B. Roux, T. W. Allen, S. Berneche, and W. Im, Theoretical and computational models of biological ion channels. *Quat. Rev. Biophys.* **37** (2004), 15-103. Cited on 3

[78] B. Roux, Theory of Transport in Ion Channels: From Molecular Dynamics Simulations to Experiments, in *Comp. Simul. In Molecular Biology*, J. Goodefellow ed., VCH Weinheim, Ch. 6, 133-169 (1995). Cited on 3

[79] B. Roux and S. Crouzy, Theoretical studies of activated processes in biological ion channels, in *Classical and quantum dynamics in condensed phase simulations*, B.J. Berne, G. Ciccotti and D.F. Coker Eds, World Scientific Ltd., 445-462 (1998). Cited on

[80] I. Rubinstein, Multiple steady states in one-dimensional electrodiffusion with local electroneutrality. *SIAM J. Appl. Math.* **47** (1987), 1076-1093. Cited on 7, 25

[81] I. Rubinstein, *Electro-Diffusion of Ions.* SIAM Studies in Applied Mathematics, SIAM, Philadelphia, PA, 1990. Cited on 2, 7, 25

[82] M. Saraniti, S. Aboud, and R. Eisenberg, The Simulation of Ionic Charge Transport in Biological Ion Channels: an Introduction to Numerical Methods. *Rev. Comp. Chem.* **22** (2005), 229-294. Cited on 7

[83] M. Schmidt, H. Löwen, J. M. Brader, and R. Evans, Density Functional for a Model Colloid-Polymer Mixture. *Phys. Rev. Lett.* **85** (2000), 1934-1937. Cited on

[84] M. Schmidt, H. Löwen, J. M. Brader, and R. Evans, Density Functional Theory for a Model Colloid-Polymer Mixture: Bulk Fluid Phases. *J. Phys.: Condens. Matter* **14** (2002), 9353-9382. Cited on 9

[85] Z. Schuss, B. Nadler, and R. S. Eisenberg, Derivation of Poisson and Nernst-Planck equations in a bath and channel from a molecular model. *Phys. Rev. E* **64** (2001), 1-14. Cited on 3, 5

[86] A. Singer and J. Norbury, A Poisson-Nernst-Planck model for biological ion channels–an asymptotic analysis in a three-dimensional narrow funnel. *SIAM J. Appl. Math.* **70** (2009), 949-968. Cited on 7

[87] A. Singer, D. Gillespie, J. Norbury, and R. S. Eisenberg, Singular perturbation analysis of the steady-state Poisson-Nernst-Planck system: applications to ion channels. *European J. Appl. Math.* **19** (2008), 541-560. Cited on 5, 7

[88] H. Steinrück, Asymptotic analysis of the current-voltage curve of a *pnpn* semiconductor device. *IMA J. Appl. Math.* **43** (1989), 243–259. Cited on 7, 25

[89] H. Steinrück, A bifurcation analysis of the one-dimensional steady-state semiconductor device equations. *SIAM J. Appl. Math.* **49** (1989), 1102–1121. Cited on 7, 25

[90] T. A. van der Straaten, G. Kathawala, R. S. Eisenberg, and U. Ravaioli, BioMOCA - a Boltzmann transport Monte Carlo model for ion channel simulation. *Molecular Simulation* **31** (2004), 151-171. Cited on 3

[91] P. Tarazona and Y. Rosenfeld, From zero-dimension cavities to free-energy functionals for hard disks and hard spheres. *Phys. Rev. E* **55** (1997), R4873-R4876. Cited on 9

[92] P. Tarazona and Y. Rosenfeld, Free energy density functional from 0D cavities; in *New Approaches to Problems in Liquid State Theory*, edited by C. Caccamo, J.P. Hansen, and G. Stell (Kluwer Academic, Doordrecht, 1999), 293-302. Cited on 9

[93] S.-K. Tin, N. Kopell, and C. Jones, Invariant manifolds and singularly perturbed boundary value problems. *SIAM J. Numer. Anal.* **31** (1994), 1558-1576. Cited on 5, 109, 110

[94] M. Zhang, Asymptotic expansions and numerical simulations of I-V relations via a steady-state Poisson-Nernst-Planck system. *Submitted.* Cited on 5, 7

[95] Q. Zheng, D. Chen, and W. Wei, Second-order Poisson-Nernst-Planck solver for ion transport. *J. Comput. Phys.* **230** (2011), 52395262. Cited on 7

[96] Q. Zheng and W. Wei, Poisson-Boltzmann-Nernst-Planck model. *J. Chem. Phys.* **134** (2011), 194101 (1-17). Cited on 7